

INSIGHTS INTO THE REGULATION OF aPKC POLARITY
THROUGH PROTEIN-PROTEIN INTERACTIONS

by

Elizabeth Vargas

A dissertation accepted and approved in partial fulfillment of the

requirements for the degree of

Doctor of Philosophy

in Biology

Dissertation Committee:

Dr. Bradley Nolen, Chair

Dr. Kenneth Prehoda, Advisor

Dr. Christopher Doe, Core Member

Dr. Bruce Bowerman, Core Member

Dr. Carrie McCurdy, Institutional Representative

University of Oregon

Fall 2023

© 2023 Elizabeth Vargas

DISSERTATION ABSTRACT

Elizabeth Vargas

Doctor of Philosophy in Biology

Title: Insights into the Regulation of aPKC Polarity through Protein-Protein Interactions

Cell polarity is a crucial factor in enabling a cell to carry out its specialized functions during animal development and homeostasis. It involves the organized distribution of cellular components into distinct regions, playing a critical role in various processes like asymmetric cell division, cell migration, and epithelial morphogenesis. One critical regulator of animal cell polarity is the protein atypical Protein Kinase C (aPKC), whose catalytic activity is essential for directing the localization of downstream polarity proteins. Consequently, precise regulation of aPKC becomes imperative for the proper control of cell polarity.

The regulation of aPKC's polarization and activity involves interactions with several proteins, including Par-6, Cdc42, and Par-3. However, the mechanisms through which these proteins exert their regulatory influence on aPKC have remained a subject of confusion within the cell polarity field. This dissertation investigates the intricate intermolecular interactions responsible for regulating aPKC to establish proper cell polarity.

In the first part of this work, we focus on regulation of aPKC by Par-6. Existing models suggest contradictory roles for Par-6 in either activating aPKC or relieving its autoinhibition while keeping it catalytically inactive. To address this ambiguity, we conducted structure/function analyses and *in vitro* binding assays and found that Par-6 may inhibit aPKC's catalytic activity through a novel interaction involving Par-6's C-terminus. More studies need to be done to address how this new interaction may be regulating aPKC's kinase domain.

We then turn our focus onto how Par-3 interacts with aPKC and Par-6, which together form the Par complex. Previous studies have reported multiple interactions through various biochemical assays. To gain some clarity, we utilized qualitative and quantitative binding assays to understand (1) which domains within Par-3 contribute to its interaction with the Par complex and (2) the overall binding energy contributed by these interactions. Our results indicate that Par-3 PDZ2 and PDZ3 domains bind to the aPKC Kinase domain-PBM region.

Lastly, we set out to determine the mechanism behind the transition of the Par complex between its two regulators, Par-3 and Cdc42, to form two distinct complexes. While one biochemical study suggested simultaneous interaction of Par-3 and Cdc42 with the Par complex, *in vivo* data suggested the formation of separate complexes. Our qualitative binding assays show that Par-3 and Cdc42 negatively cooperate for binding to the Par complex. Questions remain on the detailed mechanism of competition.

In summary, this dissertation elucidates the intricacies of aPKC regulation and provides valuable insights into the mechanisms by which Par-6, Cdc42, and Par-3 contribute to the control of aPKC's localization and activity.

This work contains both unpublished and published co-authored materials.

CURRICULUM VITAE

NAME OF AUTHOR: Elizabeth Vargas

GRADUATE AND UNDERGRADUATE SCHOOLS ATTENDED:

University of Oregon
University of California, Davis

DEGREES AWARDED:

Doctor of Philosophy, Biology, 2023, University of Oregon
Bachelor of Science, Genetics and Genomics, 2015, University of California, Davis

AREAS OF SPECIAL INTEREST:

Molecular Biology
Biochemistry
Cell Biology

PROFESSIONAL EXPERIENCE:

Lead Intern, Thermo Fisher Scientific, Eugene, OR, 2023

Graduate Teaching Assistant, Department of Biology, University of Oregon,
Eugene, OR, 2018-2019

Junior Specialist, Department of Molecular and Cellular Biology, University of
California, Davis, CA, 2015-2018

Undergraduate Research Assistant, Department of Molecular and Cellular Biology,
University of California, Davis, CA, 2014-2015

GRANTS, AWARDS, AND HONORS:

Pete von Hippel Graduate Scholar Award, University of Oregon, 2023

NIH F31 Diversity - Predoctoral Fellowship, Elucidating the Mechanism of Cell Type
Specific Regulation of the Par Complex, University of Oregon, 2023

U.S. Underrepresented Minorities Travel Grant, American Society for Cell Biology, 2022

Carl Storm Underrepresented Minority Fellowship, Gordon Research Conference, 2022

Community for Minorities in STEM Travel Award, University of Oregon, 2022

NIH T32 - Developmental Biology Training Grant, University of Oregon, 2019-2021

Promising Scholar Award, University of Oregon, 2018

NSF California Alliance for Minority Participation Scholar, University of California, Davis, 2014

PUBLICATIONS:

Vargas, E. and Prehoda, K.E. (2023). Negative cooperativity underlies dynamic assembly of the Par complex regulators Cdc42 and Par-3. *J Biol Chem.* 299(1), 102749. *J Biol Chem.* Editors' Pick.

Penkert R.R., Vargas E., Prehoda K.E. (2022). Energetic determinants of animal cell polarity regulator Par-3 interaction with the Par complex. *J Biol Chem.* 298(8), 102223.

Danlasky B.M., Panzica M.T., McNally K.P., Vargas E., Bailey C., Li W., Gong T., Fishman E.S., Jiang X., McNally F.J. (2020). Evidence for anaphase pulling forces during *C. elegans* meiosis. *J Cell Biol.* 219(12), e202005179.

Vargas E., McNally K.P., Cortes D.B., Panzica M.T., Danlasky B.M., Li Q., Maddox A.S., McNally F.J. (2019). Spherical spindle shape promotes perpendicular cortical orientation by preventing isometric cortical pulling on both spindle poles during *C. elegans* female meiosis. *Development.* 1146(2), dev178863.

Vargas E., McNally K., Friedman J.A., Cortes D.B., Wang D.Y., Korf I.F., McNally F.J. (2017). Autosomal trisomy and triploidy are corrected during female meiosis in *Caenorhabditis elegans*. *Genetics.* 207(3):911-922.

ACKNOWLEDGMENTS

I begin by expressing my gratitude to my advisor, Dr. Ken Prehoda, for his invaluable mentorship and support, which were pivotal in shaping my graduate education. He continually challenged me to think critically, guided me through all of the experimental problems that I ran into, and made me step out of my comfort zone to try new things. I am especially indebted to him for making me a better scientist and for the numerous milestones achieved during my training. I would also like to thank my committee: Dr. Brad Nolen, Dr. Bruce Bowerman, Dr. Chris Doe, and Dr. Carrie McCurdy for all of their advice.

Furthermore, I would like to thank the members of the Prehoda Lab, both past and present, whose technical expertise and constructive feedback greatly enriched my research journey. I wish to acknowledge Dr. Rhiannon Penkert, Dr. Bryce LaFoya, Dr. Ryan Holly, and Dr. Krystal Oon for their contributions to my growth as a scientist.

In addition, I am grateful to the friends I found within my graduate cohort – Jordan, Zac, Kona, Ethan, Rachel, and Michael. We navigated the challenges of graduate school together, always supporting one another and trying to make the best of it.

I extend my heartfelt gratitude to my friends and mentors from UC Davis, Dr. Frank McNally, Dr. Karen McNally, and Dr. Michelle Panzica. Frank's unwavering belief in my abilities, even when I struggled to find my place in the lab, had a profound impact on my journey. His influence played a crucial role in shaping me into the scientist I am today and in paving my path to graduate school. You and Karen were my parents away from home, and I remain eternally thankful for the invaluable training provided in their lab. I also thank Michelle for her friendship and guidance, and for being an inspiration for me to go to graduate school.

I am extremely grateful for my parents, Jazmin and Francisco, who always valued my

education and made sacrifices to support me and my aspirations. Your strong work ethic and drive to succeed has always inspired me to persevere and try my absolute best. Gladys and Panchi, thank you for always sticking by my side and supporting me. I could not have pursued a doctorate without any of you.

A special thanks go to my sweet baby angel, Chabella, whose companionship always comforted me after long days in lab. Thank you for your constant love and affection, your silliness, and for helping me spend more time outdoors. You bring me so much joy.

Lastly, my deepest appreciation goes to Andony, who, despite having no background in science, eagerly listened to my practice talks. His reassurance and support during the toughest moments of my graduate training helped me keep moving forward. You stayed by my side even though I decided to relocate over 500 miles away. Thank you for always believing in me and for visiting me in Oregon more often than I visited you in California. I love you forever.

To Andony, Chabella, and my family,
whose love and support
paved the way for this achievement.

TABLE OF CONTENTS

Chapter	Page
I. REGULATION OF aPKC LOCALIZATION AND ACTIVITY IN ANIMAL CELL POLARITY	17
Introduction.....	17
Animal Cell Polarity	17
Regulation of Animal Cell Polarity	18
Asymmetric Cell Division	18
Epithelial Cell Organization	20
aPKC: The Key Mediator of Cell Polarity.....	21
Mechanisms of aPKC Regulation in Cell Polarity	22
Autoinhibition.....	22
Role of Par-6 in aPKC Regulation.....	23
Role of Cdc42 in aPKC Regulation.....	25
Role of Par-3 in aPKC Regulation.....	26
Overall Model and Outstanding Questions.....	27
Bridge to Chapter II	29
II. PAR-6 ALLEVIATES aPKC SELF-INHIBITION THROUGH A NOVEL INTERACTION.....	30
Introduction.....	30
Results.....	32
Multiple interactions exist between Par-6 and aPKC	32
The Par-6 PDZ domain binds to aPKC kinase domain.....	34

Chapter	Page
Par-6 CRIB-PDZ relieves aPKC autoinhibition by displacement of the PB1-C1 module from the kinase domain.....	35
Cdc42 and Par-6 ligands prevent Par-6 CRIB-PDZ from interacting with aPKC's kinase domain.....	37
Discussion.....	38
Experimental Procedures	41
Protein Expression	41
Protein Purification.....	42
Qualitative Binding Assay	43
Bridge to Chapter III.....	47
 III. ENERGETIC DETERMINANTS OF ANIMAL CELL POLARITY	
REGULATOR PAR-3 INTERACTION WITH THE PAR COMPLEX.....	48
Introduction.....	48
Results.....	51
Multiple interactions contribute to Par-3–Par complex interaction energy	51
The aPKC kinase domain and PBM form the Par complex binding surface for Par-3	54
A conserved basic region NH ₂ -terminal to Par-3 PDZ2 contributes to Par complex binding.....	55
The Par-3 PDZ3 domain binds the aPKC kinase domain and PBM.....	56
Par-3 BR-PDZ2-3 binding to aPKC KD-PBM recapitulates the overall interaction energy.....	57
Discussion.....	59
Experimental Procedures	62
Cloning.....	62

Chapter	Page
Expression.....	62
Purification.....	63
Quantitative Binding Assay	64
Qualitative Binding Assays.....	67
Bridge to Chapter IV.....	71
 IV. NEGATIVE COOPERATIVITY UNDERLIES DYNAMIC ASSEMBLY OF THE PAR COMPLEX REGULATORS CDC42 AND PAR-3	
	73
Introduction.....	73
Results.....	76
Par-3 and Cdc42 bind with negative cooperativity to the Par complex.....	76
Par-3 may bind the Par complex with higher affinity than Cdc42	80
The Par-3 PDZ2–aPKC Kinase-PBM interaction mediates the displacement of Cdc42 from the Par complex	81
Par-3 BR-PDZ2 and PDZ3 displace Cdc42 from the Par complex	84
Discussion.....	85
Experimental Procedures	88
Protein Expression	88
Bacterial Cells.....	88
Mammalian Cells.....	89
Protein Purification.....	89
Bacterial Cells.....	89
Mammalian Cells.....	90
Qualitative Binding Assay (Affinity Chromatography)	91

Chapter	Page
Quantitative Binding Assay (Supernatant Depletion).....	91
Bridge to Chapter V	97
V. SUMMARY AND DISCUSSION.....	99
Summary	99
Discussion.....	102
Closing Remarks.....	104
APPENDICES	106
A. SUPPLEMENTAL MATERIALS FOR CHAPTER III.....	106
B. SUPPLEMENTAL MATERIALS FOR CHAPTER IV.....	108
REFERENCES CITED.....	109

LIST OF FIGURES

Figure	Page
1. Diverse cell types exhibit cell polarity.....	19
2. aPKC polarized substrates through phosphorylation.....	22
3. The PKC family is autoinhibited	23
4. Regulation of aPKC through interactions with Par-6, Cdc42, and Par-3	24
5. Par-6 CRIB-PDZ interacts with aPKC KD-PBM.....	31
6. Nature of the interaction between Par-6 CRIB-PDZ and aPKC KD-PBM	33
7. Regulation of aPKC regulatory module interaction with aPKC KD-PBM by Par-6 CRIB-PDZ.....	36
8. Cdc42 and Par-6 PDZ ligands Crumbs and Stardust displace aPKC KD-PBM from Par-6 CRIB-PDZ.....	37
9. Model for regulation of aPKC by Par-6, Cdc42, and Par-6 PDZ ligands.....	40
10. Energetic composition of the Par-3 interaction with the Par complex.	50
11. The aPKC kinase domain and PDZ binding motif form the Par complex binding site for Par-3.....	52
12. Energetic contributions to the Par-3/Par complex interaction from the Par-3 PDZ domains.....	53
13. A conserved basic region (BR) contributes binding energy to the Par-3 PDZ2 interaction with the Par complex	55
14. Par-3 PDZ3 binds the aPKC kinase domain and PDZ Binding Motif.....	58
15. Par-3 BR-PDZ2-3 binding to the aPKC kinase domain-PBM fully recapitulates the Par-3 interaction with the Par complex.....	60
16. Par-3 and Cdc42 bind to the Par complex with strong negative cooperativity.....	75
17. Par-3 binds to the Par complex with a greater affinity than Cdc42 in a supernatant depletion assay.....	78

Figure	Page
18. The Par-3 PDZ2 interaction with the aPKC PBM is required to displace Cdc42 from the Par complex.....	79
19. Par-3 PDZ2 and PDZ3 are sufficient for displacement of Cdc42 from the Par complex.....	82
20. Model for transition from Par-3- to Cdc42-bound Par complex.....	85

LIST OF TABLES

Table	Page
1. Key Resources Table 1	43
2. Key Resources Table 2	67
3. Key Resources Table 3	93

CHAPTER I
REGULATION OF aPKC LOCALIZATION AND ACTIVITY IN ANIMAL CELL
POLARITY

Chapter I contains unpublished material by me.

Chapter II contains unpublished co-authored material by me and Dr. Kenneth Prehoda.

Chapter III contains published co-authored material by me, Dr. Rhiannon Penkert and Dr. Kenneth Prehoda.

Chapter IV contains published co-authored material by me and Dr. Kenneth Prehoda.

INTRODUCTION

Animal Cell Polarity

The unequal distribution of cellular components such as proteins, lipids, organelles, and cytoplasm to specific regions of the cell is critical for a cell to undergo its specialized function (Nelson, 2003). This process, also known as cell polarity, contributes to a stem cells ability to asymmetrically divide into two distinct cells, a migratory cells ability to move from one part of the body to another, or a neuron's ability to transmit signals to another neuron (Campanale et al., 2017; Nelson, 2003) (Fig. 1). As nearly every type of cell displays some form of polarity, studying this process is essential for a comprehensive understanding of biological processes, with implications for medicine, development, and basic biology. Below I focus on the role and importance of protein complexes in cell polarity.

Regulation of Animal Cell Polarity

Polarity proteins are critical for various signaling pathways necessary for the cell to undergo its function (Mazel, 2017). Depending on the context, different proteins are involved in the polarization process. However, one key aspect is that the localization and activity of these polarity proteins is essential to their function. What do we know about these polarity protein complexes? A key molecular player involved in animal cell polarity is the kinase, atypical Protein Kinase C (aPKC) (Hong, 2018). aPKC is responsible for the targeted phosphorylation of its various downstream substrates to regulate their localization, making it a main driver of cell polarity (Drummond and Prehoda, 2016). Thus, understanding how its activity and localization are regulated is crucial to understanding how cells polarize. Before I focus on aPKC regulation, I will introduce the role of aPKC in specific cell contexts such as asymmetric cell division and epithelial cell organization, emphasizing its critical function in phosphorylating substrates.

Asymmetric Cell Division

Asymmetric cell division (ACD) promotes the generation of diverse cell types by specifying distinct fates for the daughter cells. It is a very intricate process that not only requires multiple cellular cues to specify the polarity axis, but also mutually antagonistic protein complexes that dictate one another's localization and activity (Lang and Munro, 2017; Sunchu and Cabernard, 2020). Additionally, polarity complexes ensure that the mitotic spindle is aligned with the polarity axis so that the cell can divide asymmetrically (Loyer and Januschke, 2020; Sunchu and Cabernard, 2020). The cell polarity cycle coincides with the mitotic division, with polarity establishment occurring throughout prophase and polarity maintenance occurring during metaphase (Lang and Munro, 2017; Loyer and Januschke, 2020). Two well studied examples of

ACD include the *Drosophila melanogaster* neural stem cell (NSC) and the *C. elegans* one-celled embryo. The *Drosophila* NSC divides asymmetrically to produce two daughter cells, one that will retain the stem cell fate and another that will differentiate and eventually become a neuron or glial cell (Chia et al., 2008). The stem cell will continue to proliferate throughout brain development and generate the central nervous system of the adult fly (Chia et al., 2008). The NSC's ability to divide and generate daughter cells with different fates is dependent on the polarization of a highly conserved network of proteins (polarity proteins) to the apical or basal cortex (Prehoda, 2009). aPKC is one of many proteins that needs to localize to the apical membrane. Before the cell enters mitosis, aPKC is cytoplasmic (Oon and Prehoda, 2019). However, once the cell enters mitosis, aPKC is asymmetrically recruited to the apical membrane and activated through various protein regulators (Oon and Prehoda, 2019). Now polarized and

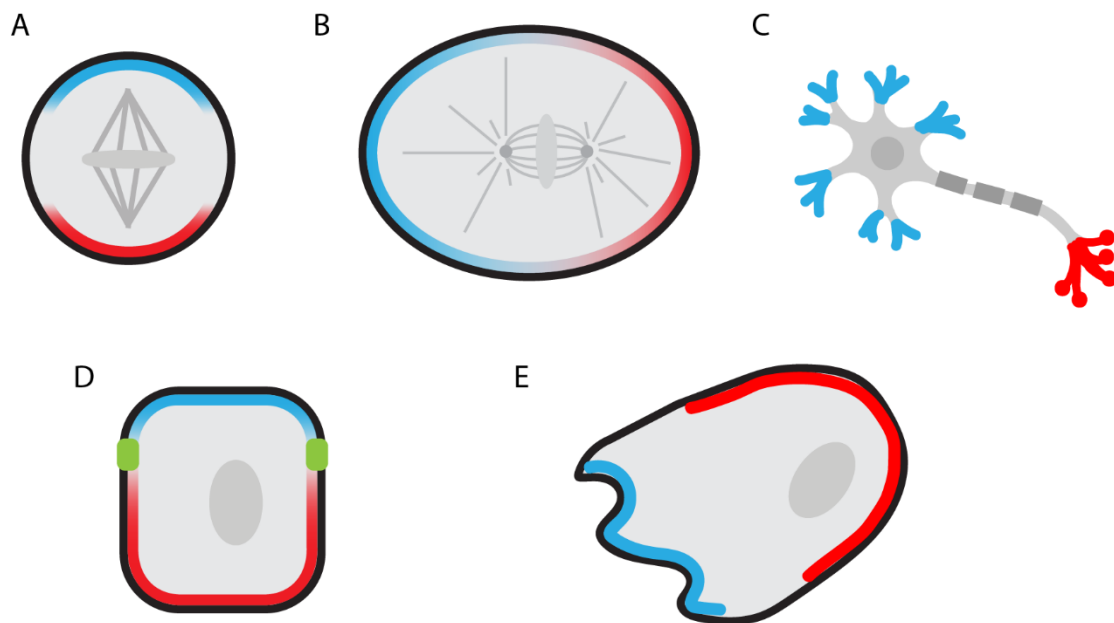


Figure 1. Diverse cell types exhibit cell polarity. Animal cells asymmetrically recruit specific cellular components (red = apical/anterior, blue = basal/ posterior) to different regions of the cell for a broad range of functions. A, *Drosophila* neural stem cell. B, *C. elegans* one-celled embryo. C, Neuron. D, Epithelial cell. E, Migratory cell.

active, aPKC can phosphorylate substrates such as Miranda at specific residues within membrane binding motifs and restrict their localization to the basal domain (Atwood and Prehoda, 2009; Bailey and Prehoda, 2015). Through this mechanism, the cell will divide and maintain aPKC in the cell that retains the stem cell fate and the substrates, many of which are fate determinants, will go into the other cell and program cell differentiation (Hong, 2018; Wodarz et al., 2000). Similarly, the *C. elegans* one-cell embryo will undergo a round of ACD to produce two daughter cells with distinct fates (Goldstein and Macara, 2007). These cells will continue to proliferate, ultimately forming a newly hatched larva that will become an adult worm (Goldstein and Macara, 2007). While the embryo also polarizes in two cortical domains, these domains are termed the anterior and posterior instead of apical and basal. Throughout this mitotic cell division, aPKC is recruited to the anterior membrane, where it will phosphorylate and exclude proteins such as Par-1 or Par-2 from this region and into the posterior domain (Lang and Munro, 2017). The cell will then divide into two cells with different fates, forming the anterior AB cell, which goes on to form neurons and other cells, and the posterior P1 cell, which goes divides to form the germline and other cells (Sulston et al., 1983). In both of these ACD examples, aPKC's localization and activity is regulated in a spatially and temporally defined manner. Polarization of aPKC in these cell types is ultimately required for the generation of diverse cells, with defects resulting in the improper localization of cell fate determinants, leading to problems such as tissue and organ malformation and cancer development (Garg et al., 2014).

Epithelial Cell Organization

Epithelial cells make up the epithelial tissue that lines the organism's internal and external surfaces and various organs. It serves many functions, including forming sheets or

layers of cells to make tissue, lining organs and forming protective barriers, and secreting or absorbing substances. The organization of epithelial cells and the formation of barriers between them is dependent on cell polarity (Buckley and St Johnston, 2022). When epithelial cells undergo polarization, they form discrete domains where the apical membrane borders the external environment, lateral membranes seal the intercellular spaces, basal membranes attach to extracellular matrices, and junctions separate the apical and basal membranes (Buckley and St Johnston, 2022; Martin et al., 2021). Polarization at the apical/basal axis is tightly controlled by proper localization and activity of polarity protein complexes, each playing a precise role establishing and maintaining cell polarity. Like the *Drosophila* NSC, aPKC is recruited from the cytoplasm to the apical membrane where it is activated. Its activation allows for the phosphorylation of proteins such as Lgl or Par-3 to restrict their localization to the basal membrane and junctions, respectively (Buckley and St Johnston, 2022; Martin et al., 2021). aPKC is crucial for apical/basal polarity in epithelial cells, with improper regulation resulting in barrier function impairment and tissue morphology defects, among other abnormalities (Garg et al., 2014).

aPKC: The Key Mediator of Cell Polarity

As aPKC is one of the main drivers of cell polarity, its dysregulation can result in a variety of defects such as overproliferation, tissue morphology abnormalities, and tumorigenesis (Garg et al., 2014). Its activity needs to be spatially and temporally controlled, so understanding not only how aPKC itself is localized but also how its catalytic domain is regulated is important.

MECHANISMS OF aPKC REGULATION IN CELL POLARITY

In this section, I will describe the current models in the field that explain aPKC regulation through intramolecular interactions (autoinhibition) and intermolecular interactions with the evolutionarily conserved apical polarity proteins Par-6, Cdc42, and Par-3.

Autoinhibition

aPKC is a member of the Serine/Threonine Protein Kinase C (PKC) family, which also includes novel (nPKC) and conventional (cPKC) PKC's. Each member of the PKC family is essential for controlling various signaling pathways by catalyzing the phosphorylation of a substrate utilizing ATP, ultimately influencing the substrate's function and subcellular localization (Rosse et al., 2010). While the C-terminal end of these kinases is highly conserved, the N-terminal region contains divergent regulatory domains (Fig. 3). aPKC is the most unique member of the PKC family as it contains only one C1 domain and has a PB1 domain instead of a C2 domain (Rosse et al., 2010). Additionally, it is the only one whose kinase activation and membrane recruitment is not regulated by DAG nor Ca^{2+} (Lipp and Reither, 2011). Despite these differences, all members of the PKC family exhibit a form of allosteric inhibition where their N-terminal domains regulate the catalytic domain (Leroux and Biondi, 2020; Rosse et al.,

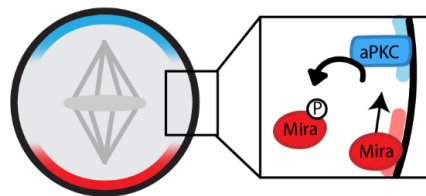


Figure 2. aPKC polarizes substrates through phosphorylation. Example of a polarized *Drosophila* neural stem cell. Apically polarized and active aPKC phosphorylates substrates, such as Miranda (Mira), to displace them from the apical membrane and restrict them to the basal membrane.

2010). More specifically, the pseudosubstrate (PS) region of each PKC, which contains a basic amino acid sequence that resembles that of a substrate except contains an Ala instead of a Ser, is known to occupy the substrate binding pocket of the kinase domain (Graybill et al., 2012; House and Kemp, 1987; Newton, 2018). As the active site is inaccessible due to the PS, the PKC is maintained in a catalytically inactive state. In addition, the C1 domains have also been implicated in PKC inhibition, with some findings suggesting that the C1 helps the PS in this process (Graybill et al., 2012; Lopez-Garcia et al., 2011; Sommese et al., 2017). Not only do these domains regulate activity, but they are also involved in membrane recruitment. The PS was observed to directly interact with the membrane through the phosphoinositides PI4P and PIP2 (Dong et al., 2020). Recently, it was shown that aPKC's C1 domain could interact with phospholipids to recruit aPKC to the membrane in *Drosophila* NSCs (Jones et al., 2023). All of these observations suggest that the PS and C1 inhibit the kinase domain from phosphorylating substrates and the kinase domain inhibits the regulatory domains from interacting with the membrane. Through this mechanism, aPKC activity is strongly coupled to localization.

Role of Par-6 in aPKC Regulation

Partitioning defective 6, or Par-6, was first identified in a *C. elegans* genetic screen which showed that Par-6 acts with other par polarity proteins to polarize the cell (Watts et al., 1996).

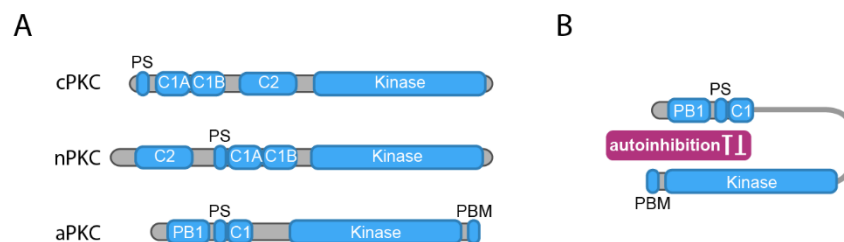


Figure 3. The PKC family is autoinhibited. A, Domain architecture of nPKC, cPKC, and aPKC. B, C-terminal kinase domain regulation by N-terminal domains of aPKC.

Par-6 is an adaptor protein that contains a PB1 domain, a CRIB motif that is coupled to the adjacent PDZ domain, and a PBM (PDZ binding motif) (Hung and Kemphues, 1999; Joberty et al., 2000; Lin et al., 2000; Renschler et al., 2018) (Fig. 4) Soon after its discovery, Par-6 was found to not only colocalize with aPKC but also interact with aPKC through PB1-PB1 heterodimerization to regulate aPKC localization and activity (Hirano et al., 2005; Noda et al., 2003). Binding of Par-6 and aPKC forms the Par complex, which is required for recruitment of aPKC to the membrane (I will refer to the Par-6/aPKC complex as the Par complex in the next sections). Par-6 and aPKC polarization is interdependent, with their interaction being vital for their localization and activity (Lang and Munro, 2017).

As Par-6 is required for aPKC membrane localization, it brings up the question of whether it also regulates aPKC activity. An early study using Co-IPs found that Par-6 was an inhibitor of aPKC activity. Their observation that the activity of the Par complex (full-length Par-6/aPKC) was lower than that of the Par complex Δ Par-6 CRIB-PDZ suggested that the CRIB-PDZ domains of Par-6 are necessary for inhibiting aPKC (Yamanaka et al., 2001). Two more studies went on to show through *in vitro* kinase assays with purified mammalian proteins and *in vivo* cell based assays that Par-6 indeed inhibits aPKC activity (Atwood et al., 2007; Dong

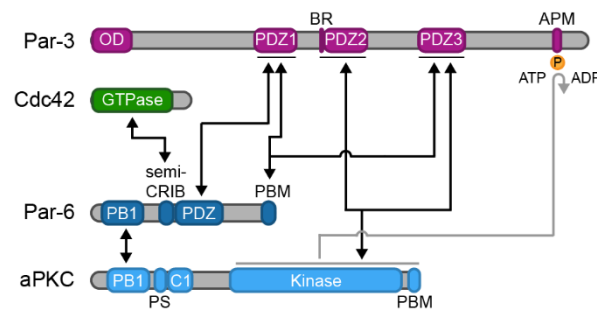


Figure 4. Regulation of aPKC through interactions with Par-6, Cdc42, and Par-3. Domain architecture of Par-3, Cdc42, Par-6, and aPKC with arrows indicating reported interactions.

et al., 2020). Despite these findings, Par-6 has also been referred to as an activator of aPKC. This study used purified proteins from mammalian cells and cell-based assays to conclude that Par-6 binding to aPKC displaces the PS from the substrate binding pocket, activating aPKC (Graybill et al., 2012). They instead observed that the Par complex was more active than Par complex Δ Par-6 CRIB-PDZ and suggested that the CRIB-PDZ domains assist in activating aPKC (Graybill et al., 2012). These conflicting observations have made it difficult to understand how exactly Par-6 regulates activity. However, it is clear that Par-6 is required for aPKC's membrane localization and activation mechanism.

Role of Cdc42 in aPKC Regulation

The small Rho GTPase, Cdc42, was known to be involved in yeast polarity, however, its role in Par-mediated polarity was not established until several studies found that Cdc42 colocalizes and interacts with Par-6 (Joberty et al., 2000; Lin et al., 2000; Noda et al., 2001; Qiu et al., 2000) (Fig. 4). For this interaction to occur, Cdc42 needs to be in the active, GTP-bound form. Through further assessment, it was found that Cdc42 requires both the CRIB and PDZ domains for its interaction with Par-6 because the CRIB-PDZ domains are coupled to one another (Garrard et al., 2003; Joberty et al., 2000; Lin et al., 2000). It was also shown through *in vitro* studies that binding of Cdc42 induces a conformational change in the PDZ domain, resulting in an increased binding affinity for Par-6's PDZ ligands, although this appears to be dependent on the exact PDZ ligand (Peterson et al., 2004; Whitney et al., 2016, 2011).

Cdc42 plays a critical role in Par-mediated polarity by recruiting the Par complex to the membrane in a polarized manner. Prenylation of Cdc42 is required for its own membrane localization, thus is necessary for Par complex membrane localization (Zhou et al., 2013). Aside

from membrane recruitment, Cdc42 is proposed to be an activator of aPKC's catalytic activity through its association with Par-6. An *in vitro* analysis using mammalian cells reported that Cdc42 activated aPKC because the Par complex was less active in its absence (Yamanaka et al., 2001). Additionally, an *in vitro* kinase assay showed that aPKC activity was increased in the presence of Cdc42 (Atwood et al., 2007). However, Cdc42 has also been found to have no effect on activity. An *in vitro* analysis using *Drosophila* embryos reported that aPKC could still phosphorylate Lgl when using a Par-6 mutant that could not bind to Cdc42 (Hutterer et al., 2004). Another study concluded that Cdc42 did not have an effect on aPKC membrane recruitment nor activation (Dong et al., 2020). Although this could be due to the various factors such as types of assays, cells, or organisms used to study activity, it has further confused the field.

Role of Par-3 in aPKC Regulation

Partitioning defective 3, or Par-3, was first discovered in a screen in *Drosophila* embryos and was found to regulate epithelial cell polarity (Wieschaus et al., 1984). Par-3 is a large scaffold protein that contains an oligomerization domain, three PDZ domains, and an aPKC phosphorylation motif (Thompson, 2021). While its oligomerization domain is required for its membrane localization and accumulation into cortical clusters, the PDZ domains play a key role in recruiting other proteins to the membrane (Chang and Dickinson, 2022; Dickinson et al., 2017). Through the PDZ domains, Par-3 can interact with the Par complex to efficiently recruit it to the membrane in a polarized manner. The following interactions have been reported: Par-3 PDZ1—Par-6 PDZ, Par-3 PDZ2-3—aPKC, Par-3 PDZ1 or PDZ3—Par-6 PBM, Par-3 APM—aPKC KD, Par-3 PDZ2—aPKC PBM (Holly et al., 2020; Joberty et al., 2000; Lin et al., 2000;

Penkert et al., 2022; Renschler et al., 2018; Wodarz et al., 2000) (Fig. 4). Additionally, Par-3 contains an aPKC phosphorylation motif, which has been shown to interact with aPKC's catalytic domain (Izumi et al., 1998) (Fig. 4).

Although many interactions have been identified, it's unclear how each of these interactions may collectively contribute to Par polarity or if it depends on the cell context. Additionally, do these interactions only contribute to Par complex membrane recruitment or do they also regulate activity? While it is uncertain how these interactions regulate aPKC activity, many studies support an inhibitor role for Par-3. This was due to the finding that aPKC is more active in the absence of Par-3 in *C. elegans*, and an *in vitro* analysis showed that the Par-3 APM bound to aPKC's catalytic domain to inhibit other substrates from phosphorylation (Rodriguez et al., 2017; Soriano et al., 2016). However, two studies reported that the Par-3 APM did not inhibit aPKC activity and another found that Par-3 actually increases aPKC activity or has no effect (Morais-de-Sá et al., 2010; Wirtz-Peitz et al., 2008). Par-3 is a critical regulator of aPKC, but the mechanism by which it regulates aPKC needs further analysis.

Overall Model and Outstanding Questions

There are many ideas out there for how aPKC polarization and activity is regulated. Here I will walk through the most generally accepted model. aPKC is initially autoinhibited through its PS, but Par-6 binding displaces the PS and “partially activates” aPKC (Graybill et al., 2012). We now have the Par complex. Throughout polarity establishment, oligomerized Par-3 recruits the Par complex to the membrane, and through other polarity cues not discussed in this dissertation, it transports the Par complex to the apical/anterior domain while maintaining it in the inactive state (Dickinson et al., 2017; Rodriguez et al., 2017; Wang et al., 2017). Once

localized at the apical/anterior domain, the Par complex transitions from Par-3 to Cdc42-GTP, which activates the Par complex at the membrane and results in the phosphorylation and polarization of downstream substrates (Rodriguez et al., 2017; Wang et al., 2017). Now properly polarized, the cell can perform its function such as divide asymmetrically or migrate in a directed manner.

Although this model is accepted, it is important to acknowledge the existence of various issues and gaps in our understanding. First of all, while aPKC is mainly reported to be autoinhibited by its PS, the C1 domain has also been implicated to have a larger role in autoinhibition, yet many models overlook its contribution to aPKC regulation (Jones et al., 2023; Lopez-Garcia et al., 2011). Furthermore, very little is known about the association of aPKC and Par-6 before polarity establishment, so it is unclear whether the Par complex forms in the cytoplasm in a temporally defined manner, or whether Par-6 and aPKC are always associated with one another. A study did, however, find that Par-6 was unstable on its own, suggesting that they may always be in a complex (Nunes de Almeida et al., 2019). Also, whether Par-6 is an activator is still in question. Studies suggest that Par-6 is an inhibitor, displacing the PS and allosterically repressing aPKC's catalytic activity with its C-terminal domains (Dong et al., 2020; Yamanaka et al., 2001). In addition, regulation of the Par complex by Par-3 has been difficult to understand because of the numerous reported interactions between Par-3 and the individual Par complex members (Holly et al., 2020; Izumi et al., 1998; Joberty et al., 2000; Lin et al., 2000; Penkert et al., 2022; Renschler et al., 2018; Wodarz et al., 2000). Furthermore, while distinct Par-3-bound and Cdc42-bound Par complexes are proposed through *in vivo* models, *in vitro* data suggests that they can form a quaternary complex, making it unclear how this important transition occurs (Joberty et al., 2000). Finally, while most models agree that Cdc42 is an

activator of the Par complex, other evidence suggests that Cdc42 has no effect on activity (Dong et al., 2020; Hutterer et al., 2004). Many questions remain and it's possible that multiple mechanisms of polarity and aPKC regulation exist depending on the cell type and organism. In the next three chapters, I will discuss new insights into how aPKC is regulated by Par-6, Cdc42, and Par-3.

BRIDGE TO CHAPTER II

In this chapter, I discussed the importance of cell polarity on animal development and homeostasis and the critical role of aPKC, the central regulator of animal cell polarity. I also discussed the current models on aPKC regulation by intermolecular interactions between aPKC and Par-6, Par-3, and Cdc42, proteins implicated in playing central roles in animal cell polarity. In the next chapter, I first focus on understanding how Par-6 binding regulates aPKC. Using qualitative pull-down assays and purified proteins, I found a novel interaction between the C-terminal domains of Par-6 and aPKC and further show that this interaction is regulated by Cdc42, Crumbs, and Stardust. Additionally, I demonstrate that this interaction displaces the regulatory module from the catalytic domain. These findings provide us with new insights into the mechanism by which Par-6 relieves autoinhibition and regulates aPKC activity.

CHAPTER II
PAR-6 ALLEVIATES aPKC SELF-INHIBITION THROUGH A NOVEL
INTERACTION

*This chapter contains unpublished co-authored material.

Author Contributions: E. V. and K. E. P. conceptualization; E. V. and K. E. P. methodology; E. V. investigation; E. V. writing; K. E. P. supervision; K. E. P. project administration; E. V. and K. E. P. funding acquisition.

INTRODUCTION

Cell polarity is a tightly regulated, evolutionarily conserved process across the animal kingdom. While many molecular players are involved in this highly dynamic process, the Par complex is one of the most critical components (Hong, 2018; Lang and Munro, 2017). Composed of the partitioning defective 6 protein (Par-6) and atypical Protein Kinase C (aPKC), the Par complex is recruited to the Par domain, where it becomes catalytically active and displaces substrates through phosphorylation and restrict their localization to the opposite domain (Bailey and Prehoda, 2015). aPKC is initially suggested to be in an autoinhibited state while cytoplasmic, but through its interaction with Par-6, it can be recruited to the membrane through interactions with Par-3 or Cdc42 (Dickinson et al., 2017; Rodriguez et al., 2017; Wang et al., 2017). While both recruit the Par complex to the membrane, they induce different activities from the Par complex. Cdc42 interacts with Par-6 to indirectly activate aPKC, whereas Par-3, which has numerous reported interactions with aPKC and Par-6 that inactivate aPKC

(Garrard et al., 2003; Gotta et al., 2001; Holly et al., 2020; Izumi et al., 1998; Joberty et al., 2000; J. Li et al., 2010; Lin et al., 2000; Noda et al., 2001; Penkert et al., 2022; Qiu et al., 2000; Renschler et al., 2018; Wodarz et al., 2000). While Par-6 is required for the formation of an active, Cdc42-bound Par complex and an inactive, Par-3-bound Par complex, the activity of aPKC when solely bound to Par-6 remains unclear.

Par-6 and aPKC interact through their PB1 (Hirano et al., 2005; Noda et al., 2003) (Fig. 5A). As aPKC is autoinhibited, with its pseudosubstrate binding to the active site in the catalytic domain, heterodimerization of the PB1-PB1 domains is proposed to cause conformational changes within aPKC that alter its catalytic state (Dong et al., 2020; Graybill et al., 2012; Yamanaka et al., 2001). Thus, the current model in the field proposes that Par-6 “partially” activates aPKC, with binding of the PB1 domains displacing the PS from the active site (Graybill et al., 2012). Yet, there is also evidence suggesting that although PB1 heterodimerization displaces the PS from the active site and alleviates autoinhibition, that Par-6’s C-terminal

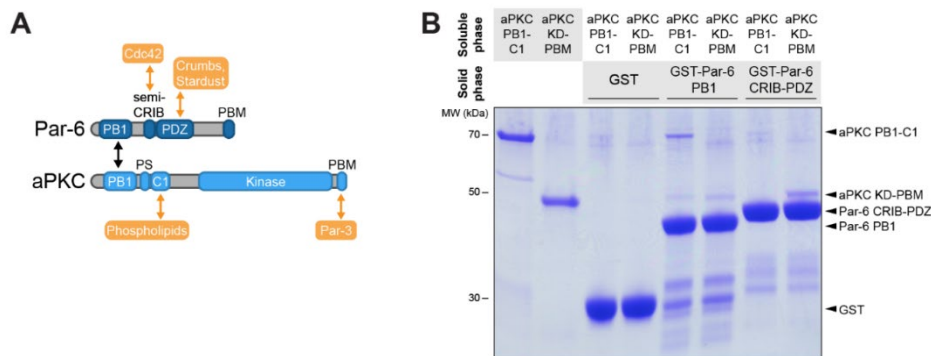


Figure 5. Par-6 CRIB-PDZ interacts with aPKC KD-PBM. A, Domain architecture of Par-6 and aPKC. Black arrow indicates the reported interactions between Par-6 and aPKC; Yellow arrows indicate reported interactions with other proteins. B, Interaction of Par-6 PB1 or Par-6 CRIB-PDZ with aPKC PB1-C1 or aPKC KD-PBM. Solid-phase (glutathione resin)-bound glutathione S-transferase (GST)-fused Par-6 PB1 or Par-6 CRIB-PDZ incubated with aPKC PB1-C1 or aPKC KD-PBM. Shaded regions indicate the fraction applied to the gel (soluble-phase or solid-phase components after mixing with soluble-phase components and washing).

domains now inhibit aPKC's catalytic activity (Dong et al., 2020; Yamanaka et al., 2001). The available data suggesting that Par-6 is an activator or an inhibitor is conflicting and has made it difficult to figure out how Par-6 is altering aPKC to change its catalytic activity. Additionally, the lack of structural information of the full-length proteins and the proteins in a complex have made it challenging to understand exactly how Par-6 regulates aPKC. Here we have used a biochemical reconstitution approach with purified proteins to determine how aPKC is regulated by Par-6. The results provide the mechanistic framework for understanding how Par-6 is regulating aPKC activity and how it allows other proteins such as Par-3 and Cdc42 to bind.

RESULTS

Multiple interactions exist between Par-6 and aPKC

Although Par-6 and aPKC have only been shown to interact through their PB1 domains, a recent study suggested that the C-terminus of Par-6 inhibits the kinase domain (Dong et al., 2020). While this has been proposed previously (Yamanaka et al., 2001), another model suggested that the C-terminus further activated aPKC (Graybill et al., 2012). Inhibition could be due to allosteric changes occurring due to PB1 interactions, where the Par-6 CRIB-PDZ domain blocks access to the kinase active site. To test this model, we examined whether the N- or C-terminus of Par-6 binds to the N- or C-terminus of aPKC using a reconstitution approach. We performed a pull-down assay with purified aPKC PB1-C1 (regulatory module) or aPKC kinase domain-PBM (KD-PBM) on the soluble phase and GST-fused Par-6 PB1 or GST-fused Par-6 CRIB-PDZ on the solid phase. If aPKC PB1-C1 interacts with both Par-6 PB1 and Par-6 CRIB-PDZ, then these Par-6 fragments should pull down aPKC PB1-C1. Alternatively, aPKC PB1-C1 will only be pulled down by Par-6 PB1 and not Par-6 CRIB-PDZ. As expected, aPKC PB1-C1

was pulled down by Par-6 PB1 and no interaction was observed with Par-6 CRIB-PDZ (Fig. 5B). When adding soluble aPKC KD-PBM to either Par-6 PB1 or CRIB-PDZ, if aPKC KD-PBM is pulled down, this would denote an interaction with these domains, respectively. No interaction was observed between Par-6 PB1 and aPKC KD-PBM, but to our surprise, aPKC KD-PBM was pulled down by Par-6 CRIB-PDZ (Fig. 5B). Our results indicate that a direct interaction exists between the C-terminal ends of aPKC and Par-6.

The available biochemical evidence suggested that Par-6 and aPKC solely interact through PB1 heterodimerization, yet we have identified a novel interaction between aPKC KD-PBM and Par-6 CRIB-PDZ utilizing purified components. Why has no one previously observed an interaction between the C-terminal ends of aPKC and Par-6? It has been difficult to develop most of the reagents, with bacterial expression resulting in highly aggregated proteins or little to no expression. As our proteins were purified and used in a controlled system, other cellular factors could potentially have prevented this interaction. Additionally, the low affinity of Par-6 CRIB-PDZ for aPKC KD-PBM (K_d of $\sim 20 \mu\text{M}$, data not shown) could have made it difficult to

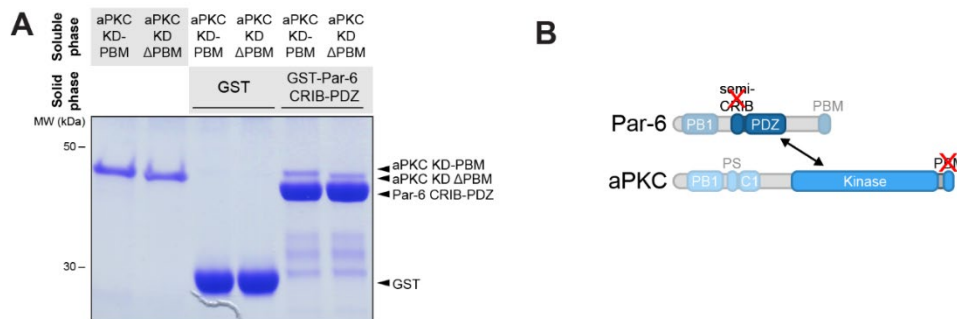


Figure 6. Nature of the interaction between Par-6 CRIB-PDZ and aPKC KD-PBM. A, Interaction of Par-6 CRIB-PDZ with aPKC KD-PBM or aPKC KD Δ PBM. Solid-phase (glutathione resin)-bound glutathione S-transferase (GST)-fused Par-6 PB1 or Par-6 CRIB-PDZ incubated with aPKC KD-PBM or aPKC KD Δ PBM. Shaded regions indicate the fraction applied to the gel (soluble-phase or solid-phase components after mixing with soluble-phase components and washing). B, Domain architecture of Par-6 and aPKC showing the novel interaction between aPKC and Par-6 with a black arrow. Red X's mark domains that are not necessary for the interaction.

detect this interaction. Furthermore, in the context of full-length aPKC, which possesses a strong intramolecular interaction between its regulatory module and the KD-PBM, Par-6 would have to have a stronger affinity to sufficiently displace the regulatory module on its own. In terms of understanding how Par-6 regulates aPKC, our results indicate that the Par-6 and aPKC interact at two regions, with the heterodimerization of the N-terminal PB1 domains and binding at the C-terminal Par-6 CRIB-PDZ—aPKC KD-PBM domains.

The Par-6 PDZ domain binds to aPKC kinase domain

The CRIB motif and PDZ domain of Par-6 are structurally coupled to one another, with Cdc42 requiring both domains for its interaction with Par-6 (Garrard et al., 2003; Joberty et al., 2000; Lin et al., 2000). To investigate the nature of the Par-6 CRIB-PDZ—aPKC KD-PBM interaction, we truncated these proteins further and tested which components are required. If aPKC KD-PBM interacts with Par-6 in a similar manner as Cdc42 interacts with Par-6, then no interaction would be observed with either the CRIB motif or PDZ domain. Alternatively, aPKC KD-PBM could potentially be a Par-6 PDZ ligand and only requires the PDZ domain for binding. As aPKC KD-PBM contains a PDZ binding motif, and we previously observed an interaction between Par-3 PDZ2 and PDZ3 with aPKC KD-PBM, this interaction is highly likely, and we would expect to observe that the PDZ domain pulls down aPKC KD-PBM. We added soluble aPKC KD-PBM to GST-fused Par-6 CRIB-PDZ, CRIB, or PDZ on the solid phase. We found that Par-6 CRIB-PDZ and PDZ sufficiently pulled down aPKC KD-PBM, whereas Par-6 CRIB could not pull down aPKC KD-PBM (data not shown). Our result suggests that aPKC KD-PBM interacts with the Par-6 PDZ domain and is a Par-6 PDZ ligand.

As our previous result suggests that the aPKC KD-PBM—Par-6 CRIB-PDZ interaction is likely due to the PBM and PDZ domains of aPKC and Par-6, respectively, we wanted to test whether the PBM was required for this interaction or whether the kinase domain alone was sufficient. If Par-6 CRIB-PDZ pulls down aPKC KD Δ PBM to the same extent as aPKC KD-PBM, this would suggest that the interaction is due to the kinase domain and not the PBM. Alternatively, if Par-6 no longer pulls down aPKC KD Δ PBM, this would suggest that Par-6 requires the PBM to bind. It is also possible that Par-6 pulls down less aPKC KD Δ PBM than aPKC KD-PBM, suggesting that Par-6 makes binding contacts with both the kinase domain and the PBM. To probe this interaction, we added soluble aPKC KD-PBM or aPKC KD Δ PBM to GST-fused Par-6 CRIB-PDZ on the solid phase. We did not detect an effect of removing the PBM on Par-6's ability to interact with the kinase domain (Fig. 6A). Our results indicate that the interaction between Par-6 CRIB-PDZ and aPKC KD-PBM occurs through the PDZ and kinase domains within Par-6 and aPKC, respectively (Fig. 6B). However, as we did not test whether Par-6 CRIB-PDZ could interact with aPKC PBM alone, it remains possible that Par-6 CRIB-PDZ also makes binding contacts with the PBM.

Par-6 CRIB-PDZ relieves aPKC autoinhibition by displacement of the PB1-C1 module from the kinase domain

Given the model that Par-6 displaces aPKC's pseudosubstrate (PS) from the active site, we sought to determine whether this was due to Par-6 CRIB-PDZ competing with aPKC PS for binding to KD-PBM. As the C1 domain is also proposed to contribute to KD-PBM binding, we examined whether aPKC's whole regulatory module (PB1-C1), rather than the PS alone, affects Par-6 CRIB-PDZ binding to aPKC KD-PBM. We first formed a complex of Par-6 CRIB-PDZ-

bound aPKC KD-PBM by placing GST-Par-6 CRIB-PDZ on the solid phase and incubating with soluble, purified aPKC KD-PBM. We assessed the effect of aPKC PB1-C1 on the Par-6 CRIB-PDZ-bound aPKC KD-PBM by adding soluble aPKC PB1-C1. If binding of the regulatory module to KD-PBM had no effect on Par-6 CRIB-PDZ binding, or the proteins bound with positive cooperativity, we expected that aPKC PB1-C1 would be pulled down and the amount of aPKC KD-PBM would stay the same or increase. Alternatively, if aPKC PB1-C1 and Par-6 CRIB-PDZ negatively cooperate, either through direct steric occlusion or an allosteric mechanism, little or no aPKC PB1-C1 would be pulled down, and the amount of aPKC KD-PBM pulled down Par-6 CRIB-PDZ would decrease. This would be due to the decreased affinity of aPKC KD-PBM for Par-6 CRIB-PDZ by binding to the regulatory module. We observed that addition of aPKC PB1-C1 reduced the amount of aPKC KD-PBM associated with Par-6 CRIB-PDZ (Fig. 7A). We conclude that Par-6 CRIB-PDZ and aPKC PB1-C1 negatively cooperate for binding to aPKC KD-PBM (Fig. 7B).

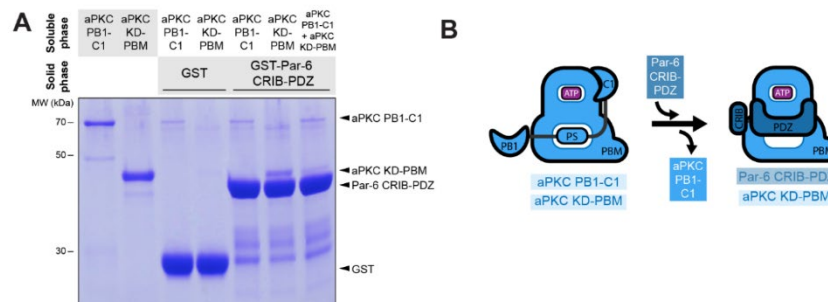


Figure 7. Regulation of aPKC regulatory module interaction with aPKC KD-PBM by Par-6 CRIB-PDZ. A, Effect of aPKC PB1-C1 on the interaction between Par-6 CRIB-PDZ and aPKC KD-PBM. Solid-phase (glutathione resin)-bound glutathione S-transferase (GST)-fused Par-6 CRIB-PDZ incubated with aPKC KD-PBM and/or aPKC PB1-C1. Shaded regions indicate the fraction applied to the gel (soluble-phase or solid-phase components after mixing with soluble-phase components and washing). B, Cartoon summary of Par-6 CRIB-PDZ negatively cooperating with aPKC PB1-C1 for binding to aPKC KD-PBM.

Cdc42 and Par-6 ligands prevent Par-6 CRIB-PDZ from interacting with aPKC's kinase domain

The PDZ domain of Par-6 is regulated by Cdc42, with binding of Cdc42 to the CRIB domain inducing a conformational change in the PDZ domain resulting in an increased affinity for ligands (Peterson et al., 2004). While the effect of Cdc42 binding to Par-6 on PDZ ligand binding depends highly on the PDZ ligand itself, Cdc42 either has no effect on the interaction or increases the affinity between the PDZ ligand and Par-6 PDZ (Penkert et al., 2004; Peterson et al., 2004; Whitney et al., 2016, 2011). Given that aPKC KD-PBM may be a Par-6 PDZ ligand based on our previous results, we investigated whether the Par-6 PDZ ligands could displace aPKC KD-PBM from Par-6 CRIB-PDZ. We assessed the effect of Par-6 PDZ ligands on Par-6 CRIB-PDZ-bound aPKC KD-PBM by adding soluble Crumbs or Stardust. If either PDZ ligand displaced aPKC KD-PBM from Par-6, this would suggest that aPKC KD-PBM and Crumbs or Stardust are negatively cooperating for binding, most likely through a direct mechanism. We

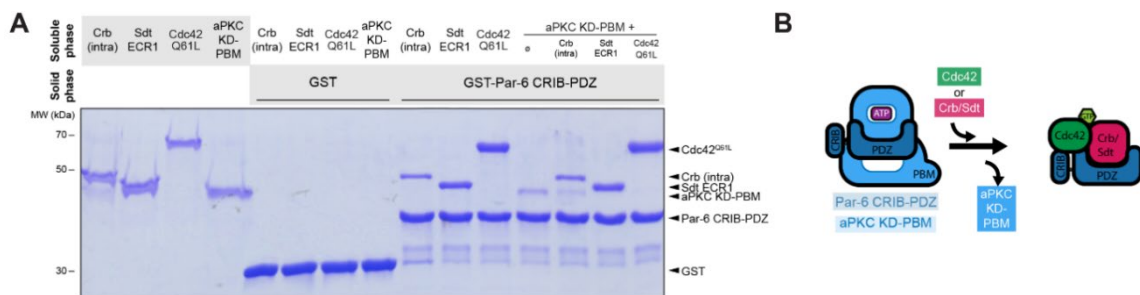


Figure 8. Cdc42 and Par-6 PDZ ligands Crumbs and Stardust displace aPKC KD-PBM from Par-6 CRIB-PDZ. A, Effect of Crumbs (intra), Stardust ECR1, and Cdc42^{Q61L} (constitutively active) on the interaction between Par-6 CRIB-PDZ and aPKC KD-PBM. Solid-phase (glutathione resin)-bound glutathione S-transferase (GST)-fused Par-6 CRIB-PDZ incubated with aPKC KD-PBM and/or Crb (intra), Sdt ECR1, or Cdc42^{Q61L}. Shaded regions indicate the fraction applied to the gel (soluble-phase or solid-phase components after mixing with soluble-phase components and washing). B, Cartoon summary of Crumbs (intra), Stardust ECR1, and Cdc42^{Q61L} negatively cooperating with aPKC KD-PBM for binding to Par-6 CRIB-PDZ.

found that the amount of aPKC KD-PBM pulled down by Par-6 CRIB-PDZ was reduced in the presence of either Crumbs or Stardust (Fig. 8A). Our results indicate that Crumbs and Stardust compete with aPKC KD-PBM for binding to Par-6 CRIB-PDZ (Fig. 8B).

As aPKC KD-PBM is likely a PDZ ligand, and Cdc42 is a regulator of Par-6's PDZ domain, we further investigated the effect of Cdc42 on Par-6's ability to bind aPKC KD-PBM. If we observe an increase in the amount of aPKC KD-PBM pulled down by Par-6 CRIB-PDZ in the presence of Cdc42, then this would suggest that Cdc42 positively cooperates with aPKC KD-PBM for binding to Par-6. Alternatively, if we observe no change in the amount of aPKC KD-PBM pulled down after the addition of Cdc42, this would indicate that Cdc42 does not regulate Par-6's ability to bind aPKC KD-PBM. This would be similar to Par-6's interaction with Stardust, in which Cdc42 has no effect on. Another possibility would be that the addition of Cdc42 would displace aPKC KD-PBM from Par-6 CRIB-PDZ. We first formed a complex by incubating soluble aPKC KD-PBM with GST-fused Par-6 CRIB-PDZ and added Cdc42^{Q61L}, a constitutively active form of Cdc42. A decrease in the amount of aPKC KD-PBM pulled down by Par-6 CRIB-PDZ in the presence of Cdc42 was observed (Fig. 8A). Our results suggest that Cdc42 negatively cooperates with aPKC KD-PBM for binding to Par-6 CRIB-PDZ (Fig. 8B).

DISCUSSION

Par-6 and aPKC work collaboratively to polarize cells, with Par-6 acting as an adaptor protein and aPKC utilizing its kinase activity to phosphorylate and polarize proteins (Lang and Munro, 2017). While aPKC is in the autoinhibited state, intramolecular interactions regulate its ability to be catalytically active and localize to the membrane (Dong et al., 2020; Graybill et al., 2012; House and Kemp, 1987; Jones et al., 2023; Newton, 2018). Par-6's interaction with aPKC

is required for the displacement of pseudosubstrate from the substrate binding pocket and relieving aPKC's autoinhibition (Graybill et al., 2012). Their interaction also mediates the formation of a catalytically active complex with Cdc42 and an inactive complex with Par-3 while also helping recruit aPKC to the membrane through these complexes (Aceto et al., 2006; Atwood et al., 2007; Hutterer et al., 2004; Lang and Munro, 2017; Munro et al., 2004; Rodriguez et al., 2017). While Par-6 binding to aPKC may alleviate autoinhibition, the effect Par-6 has on aPKC activity remains in question. Utilizing a biochemical reconstitution approach to understand the molecular mechanism by which Par-6 regulates aPKC activity, we set out to identify how Par-6 binding may alter aPKC's structural conformation. A previous study suggested that Par-6 activated aPKC, with the PB1 domain being sufficient to displace the PS from the catalytic domain and the CRIB-PDZ domains contributing to aPKC activation (Graybill et al., 2012). However, other models suggested that Par-6 maintains aPKC in an inactive state, with the PB1 displacing the PS and the CRIB-PDZ domains inhibiting the kinase domain through an allosteric mechanism (Dong et al., 2020; Yamanaka et al., 2001). Using purified components, we found that Par-6 relieves aPKC autoinhibition through a novel interaction (Fig. 9 A, B). Here we discuss the implications of our findings and any outstanding questions that remain in understanding the mechanism of aPKC regulation by Par-6.

An interaction between Par-6's and aPKC's C-terminal domains was not previously observed, and yet, we found that Par-6 CRIB-PDZ and aPKC KD-PBM interact. How can these findings be reconciled? Firstly, this could be due to a difference in assays or cell types. Additionally, we found that the interaction between Par-6 CRIB-PDZ and aPKC KD-PBM is not that strong. The interaction may not have been detected because of the low affinity. Lastly the strong interaction between aPKC and Par-6's PB1 domains could have made the interaction

undetectable, especially in the context of full-length aPKC and truncated Par-6 CRIB-PDZ, which would have to compete with aPKC PB1-C1. The lack of structural information has also made it difficult to understand exactly how Par-6 and aPKC interact. While the structures of individual domains have been reported, nothing is known about the structure of the full-length proteins and how binding of aPKC to Par-6 results in conformational changes.

Here we examined the nature of the Par-6 and aPKC interaction and found that Par-6 and aPKC bind at two locations: through their PB1 domains and through their C-terminal ends. We show that Par-6 CRIB-PDZ interacts with aPKC KD-PBM and that this interaction is regulated by Cdc42 and Par-6 PDZ ligands, Crumbs and Stardust. While the interaction appears to only require Par-6's PDZ domain, it's currently unclear whether aPKC's PBM is necessary for this interaction. Our results are in a way consistent with the model that Par-6 CRIB-PDZ inhibits

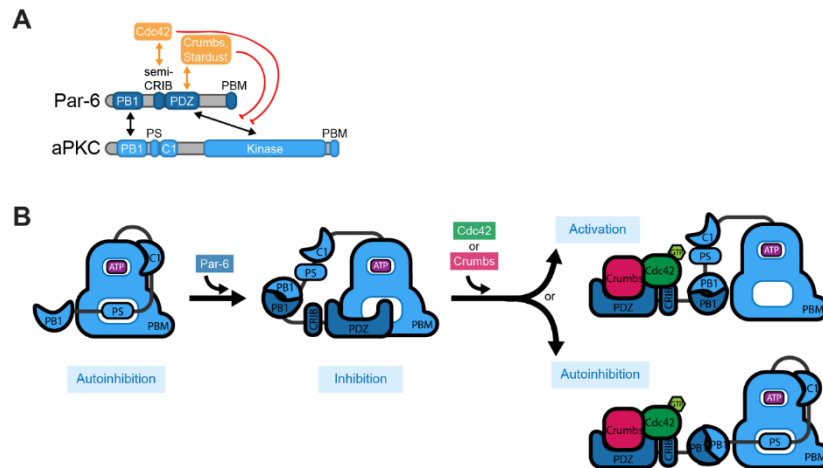


Figure 9. Model for regulation of aPKC by Par-6, Cdc42, and Par-6 PDZ ligands. A, Domain architecture demonstrating the interactions between aPKC and Par-6., Cdc42, and the Par complex that are sufficient for regulating the transition between a Par-3- and Cdc42-bound Par complex. B, Model for regulation of aPKC. aPKC is found in the autoinhibited state, with its pseudosubstrate (PS) binding the active site. Par-6 PB1 interacts with aPKC PB1 and Par-6 CRIB-PDZ interacts with aPKC KD-PBM. These interactions relieve autoinhibition but maintain aPKC in the inactive state. In the presence of Par-6 regulators, such as Cdc42, Crumbs, or Stardust, Par-6 CRIB-PDZ no longer interacts with aPKC KD-PBM. This results in either activation or releases the catalytic domain for the PS to bind again.

aPKC kinase activity (Dong et al., 2020). However, as we did not test activity or access to the substrate binding site, we cannot conclude that Par-6 CRIB-PDZ represses aPKC activity. On the other hand, our finding that Par-6 CRIB-PDZ negatively cooperates with aPKC PB1-C1 for binding to aPKC KD-PBM suggests that Par-6 CRIB-PDZ displaces the regulatory module and alleviates autoinhibition.

While our results suggest that Par-6 CRIB-PDZ relieves autoinhibition and potentially continues to inhibit aPKC, it remains unclear how binding of Cdc42, Crumbs, or Stardust to Par-6 affects aPKC in the context of the Par complex. If Par-6 PDZ ligands and Cdc42 negatively cooperate and displace aPKC KD-PBM from Par-6 CRIB-PDZ, it could be indicative of an activation mechanism because the kinase domain is no longer occupied. In support of this, Cdc42 has long been proposed to be an activator of the Par complex (Atwood et al., 2007; Qiu et al., 2000; Yamanaka et al., 2001). One study reported that Cdc42 could not activate the Par complex by relieving Par-6 inhibition of aPKC, yet they found that Crumbs was able to alleviate inhibition and activate aPKC (Dong et al., 2020). Alternatively, it remains possible that removal of the CRIB-PDZ from the kinase domain by Par-6 regulators allows aPKC's PS access to the catalytic domain. Further examination of these interactions in the presence of an aPKC substrate is required to better assess the mechanism of aPKC regulation by Par-6.

EXPERIMENTAL PROCEDURES

Protein Expression

Plasmids were transformed into BL21-DE3 cells, aliquoted onto LB + AMP plates, and grown at 37°C overnight. 100 mL LB + AMP starter cultures were inoculated with transformants and grown at 37°C for 2-3 hours until an OD600 of 0.4-1.0 was reached. Starter cultures were

then added into 2 L LB + AMP and depending on the protein, grown at either 18°C or 37°C. Once an OD600 of 0.8-1.0 was reached, cultures were induced with 500 μM IPTG for 3 hours and then then centrifuged at 5,000 RPM for 15-20 minutes. Pellets were subsequently resuspended in nickel lysis buffer (50 mM NaH₃PO₄, 300 mM NaCl, 10 mM Imidazole, pH 8.0), GST lysis buffer (IX PBS, 1 mM DTT, pH 7.5), or maltose lysis buffer (20 mM Tris, 200 mM NaCl, 1 mM EDTA, 1 mM DTT, pH 7.5), frozen in liquid N₂, and then stored at -80°C.

Protein Purification

Frozen, resuspended pellets were thawed, lysed by probe sonication (70% amplitude, 0.3 seconds/0.7 seconds on/off pulse rate, 3x 1 minute), and subsequently centrifuged at 15,000 RPM for 20 minutes. Lysates for GST-tagged proteins were aliquoted, frozen in liquid N₂ and stored at -80°C. For all other proteins (His- or MBP-fused), lysates were incubated with either cobalt/nickel resin (His) or amylose resin (MBP) and incubated for 30-60 minutes at 4°C with mixing. Protein-labeled resin was washed 3x with nickel lysis buffer (50 mM NaH₃PO₄, 300 mM NaCl, 10 mM Imidazole, pH 8.0) or maltose lysis buffer (20 mM Tris, 200 mM NaCl, 1 mM EDTA, 1 mM DTT, pH 7.5) and eluted in 0.5-2 mL fractions with nickel elution buffer (50 mM NH₃PO₄, 300 mM NaCl, 300 mM Imidazole, pH 8.0) or maltose elution buffer (maltose lysis buffer, 10 mM Maltose). Fractions containing protein of interest were pooled together and buffer exchanged into 20 mM HEPES, pH 7.5, 100 mM NaCl, and 1 mM DTT using a PD10 desalting column. Afterwards, protein was concentrated using a Vivaspin 20 centrifugal concentrator, aliquoted, frozen in liquid N₂, and stored at -80°C.

Note that aPKC KD-PBM was His-purified partially under denaturing conditions due to solubility issues. After sonication and centrifugation, the insoluble pellet was resuspended in

nickel lysis buffer (50 mM NaH₃PO₄, 300 mM NaCl, 10 mM Imidazole, pH 8.0) and 8 M Urea, and then centrifuged again under the same conditions as noted above. The supernatant was incubated with either cobalt/nickel resin (His) for 30-60 minutes at 4°C with mixing, washed with nickel lysis buffer, eluted, concentrated, aliquoted, and frozen as noted above.

Qualitative Binding Assay

Bacterial lysates were incubated with glutathione resin for 30 minutes at 4°C. After incubation, protein-labeled resin was washed 3x with binding buffer (20 mM HEPES pH 7.5, 100 mM NaCl, 5 mM MgCl₂, 0.5% Tween-20, 1 mM DTT, 200 μM ATP). Soluble proteins were then added to protein-labeled resin and incubated for 60 minutes at room temperature with rotational mixing. Resin was quickly washed 3x with binding buffer and proteins were eluted with 4X LDS sample buffer. Samples were then run on a 12% Bis-Tris gel and stained with Coomassie Brilliant Blue R-250.

Key Resources Table 1

Reagent or Resource type	Reagent or Resource	Source	Identifier	Additional Information
Recombinant Protein	MBP-aPKC PB1-C1	This paper		Cloned by Gibson Assembly; expressed in BL21 cells from pMAL aPKC 1-225-His; His-purified; <i>Drosophila melanogaster</i> protein
Recombinant protein	His-aPKC KD-PBM	PMID: 35787373		Cloned using traditional methods; expressed in BL21 cells from pBH aPKC 259-606; his-purified under denaturing

				conditions; <i>Drosophila melanogaster</i> protein
Recombinant Protein	His-aPKC KD- Δ PBM	This paper		Cloned by Q5 site-directed mutagenesis; expressed in BL21 cells from pBH aPKC 259-600; his-purified under denaturing conditions; <i>Drosophila melanogaster</i> protein
Recombinant Protein	MBP-Cdc42 ^{Q61L}	This paper		Cloned by Gibson assembly; expressed in BL21 cells from pMal Cdc42 1-191 Q61L; amylose-purified; <i>Drosophila melanogaster</i> protein
Recombinant Protein	MBP-Crumbs (intra)	This paper		Cloned by traditional methods; expressed in BL21 cells from pMal Crumbs 2217-2253; amylose-purified; <i>Drosophila melanogaster</i> protein
Recombinant Protein	MBP-Stardust ECR1	This paper		Cloned by Gibson assembly; expressed in BL21 cells from pMal Stardust 3-34; amylose-purified; <i>Drosophila melanogaster</i> protein
Recombinant Protein	GST-Par-6 PB1	This paper		Cloned by Gibson assembly; expressed in BL21 cells from pGEX Par-6 1-102; <i>Drosophila melanogaster</i> protein
Recombinant Protein	GST-Par-6 CRIB-PDZ	PMID: 36436559		Cloned by Gibson assembly; expressed in BL21 cells from pGEX Par-6 130-256;

				<i>Drosophila melanogaster</i> protein
Recombinant Protein	GST-Par-6 CRIB	This paper		Cloned by Gibson assembly; expressed in BL21 cells from pGEX Par-6 130-158; <i>Drosophila melanogaster</i> protein
Recombinant Protein	GST-Par-6 PDZ	This paper		Cloned by Gibson assembly; expressed in BL21 cells from pGEX Par-6 156-255; <i>Drosophila melanogaster</i> protein
Recombinant DNA	pCMV (mammalian expression plasmid)	ThermoFisher	10586014	
Recombinant DNA	pMAL c4X (bacterial expression plasmid)	Addgene	75288	
Recombinant DNA	pGEX 4T1 (bacterial expression plasmid)	Amersham	27458001	
Recombinant DNA	pBH (bacterial expression plasmid)	PMID: 15023337		
Bacterial Strain	TG1			Molecular cloning
Bacterial Strain	BL21-DE3			Protein expression
Chemical	HisPur Cobalt Resin	ThermoFisher	89965	

Chemical	HisPur NiNTA Resin	ThermoFisher	88222	
Chemical	Amylose Resin	NEB	E8021L	
Chemical	Glutathione Resin	GoldBio	G250-100	
Chemical	4X BOLT LDS Sample Buffer	ThermoFisher	B0007	
Chemical	PageRuler Plus Prestained Protein Ladder, 10-250 kDa	ThermoFisher	26619	
Chemical	20X BOLT MES SDS Running Buffer	ThermoFisher	B0002	
Chemical	Coomassie Brilliant Blue R-250	GoldBio	C-461-5	
Chemical	Q5 Site-Directed Mutagenesis Kit	NEB	E0552S	
Chemical	Gibson Assembly Cloning Kit	NEB	E5510S	
Other	Bolt 12% Bis-Tris Gels	ThermoFisher	NW00125 BOX	
Other	PD-10 Desalting Columns	VWR	95017-001	
Other	VivaSpin 20 MWCO 5kDa	Cytiva	28932359	
Other	VivaSpin 20 MWCO 10kDa	Cytiva	28932360	

Other	VivaSpin 20 MWCO 30kDa	Cytiva	28932361	
Software	ImageJ	NIH		https://imagej.nih.gov/ij/
Software	Prism	GraphPad Software		https://www.graphpad.com/
Software	Estimation Statistics BETA	PMID: 31217592		www.estimationstats.com

BRIDGE TO CHAPTER III

In this chapter, we demonstrated that Par-6 and aPKC interact through a novel interaction that potentially regulates aPKC's catalytic activity. Using *in vitro* assays with purified components, we showed that Par-6 CRIB-PDZ displaces aPKC PB1-C1 from KD-PBM, thereby relieving autoinhibition. We also found that the interaction between Par-6 CRIB-PDZ and aPKC KD-PBM is negatively regulated by Cdc42 and Par-6 PDZ ligands. Our findings suggest that aPKC KD-PBM could be exposed in the presence of these Par-6 regulators. In the next chapter, we focus on the regulation of Par-6 and aPKC, together as the Par complex, by Par-3. Utilizing quantitative pull-down assays, we investigate which of the many reported interactions between Par-3 and the Par complex contribute to their overall binding energy. This work provides a better understanding of the interactions that play a role in regulating Par complex localization and activity.

CHAPTER III

ENERGETIC DETERMINANTS OF ANIMAL CELL POLARITY REGULATOR PAR-3 INTERACTION WITH THE PAR COMPLEX

*This chapter contains previously published co-authored material.

Penkert RR, Vargas E, Prehoda KE. (2022). Energetic determinants of animal cell polarity regulator Par-3 interaction with the Par complex. *J Biol Chem.* 102223.

Author Contributions: R. R. P. and K. E. P. conceptualization; R. R. P. and K. E. P. methodology; R. R. P. and E. V. investigation; R. R. P. and E. V. writing–review and editing; K. E. P. writing original draft; K. E. P. supervision; K. E. P. project administration; K. E. P. funding acquisition.

INTRODUCTION

The Par complex polarizes diverse animal cells by forming a specific domain on the plasma membrane. In the Par domain, the Par complex component atypical Protein Kinase C (aPKC) phosphorylates and displaces substrates, thereby restricting them to a complementary membrane domain (Bailey and Prehoda, 2015). In this manner, the cellular pattern formed by Par-mediated polarity is ultimately determined by the mechanisms that target the Par complex to the membrane. Membrane recruitment relies at least in part on interactions with proteins that directly associate with the membrane, including the Rho GTPase Cdc42 and the multi-PDZ protein Par-3. The Par complex's interaction with Cdc42 is via a single well-defined site, the Par

complex component Par-6's semi-CRIB domain (Garrard et al., 2003; Joberty et al., 2000; Lin et al., 2000; Noda et al., 2001; Qiu et al., 2000). However, numerous interactions between Par-3 and the Par complex have been reported (Holly et al., 2020; Izumi et al., 1998; Joberty et al., 2000; Lin et al., 2000; Renschler et al., 2018; Wodarz et al., 2000) and it has been unclear how each contributes to the overall interaction.

The interaction between Par-3 and the Par complex was originally discovered in the context of the interaction between aPKC and its phosphorylation site on Par-3, the aPKC Phosphorylation Motif (APM aka Conserved Region 3–CR3) (Izumi et al., 1998). Subsequently, interactions were reported outside of aPKC's catalytic domain: i) Par-3 PDZ1 and the Par-6 PDZ (Joberty et al., 2000; J. Li et al., 2010; Lin et al., 2000), ii) Par-3 PDZ2-3 acting together and aPKC (Wodarz et al., 2000), iii) Par-3 PDZ1 or PDZ3 binding to the Par-6 PDZ Binding Motif (PBM) (Renschler et al., 2018), and iv) PDZ2 with a PBM in aPKC (Holly et al., 2020) (Fig. 10A). Each of these interactions, except for the interaction of aPKC's kinase domain with its substrate sequence on Par-3, involves one or more of Par-3's three PDZ protein interaction domains.

Several factors have made it difficult to understand how the many interactions identified between Par-3 and the Par complex contribute to the overall interaction. Most interactions have not been examined in the context of the intact Par complex. In this context it is not possible to understand how individual interactions contribute to the overall energetics of Par-3 assembly with the Par complex, or if interactions might cooperate or compete. Furthermore, many of the interactions have not been examined quantitatively so it has not been possible to assess their relative strength. Finally, the presence of multiple potential Par complex binding sites on Par-3 raises the possibility that each Par-3 protein might bind more than one Par complex. Here we

examine the energetics of Par-3 binding to the fully reconstituted Par complex using a quantitative binding assay to address these issues.

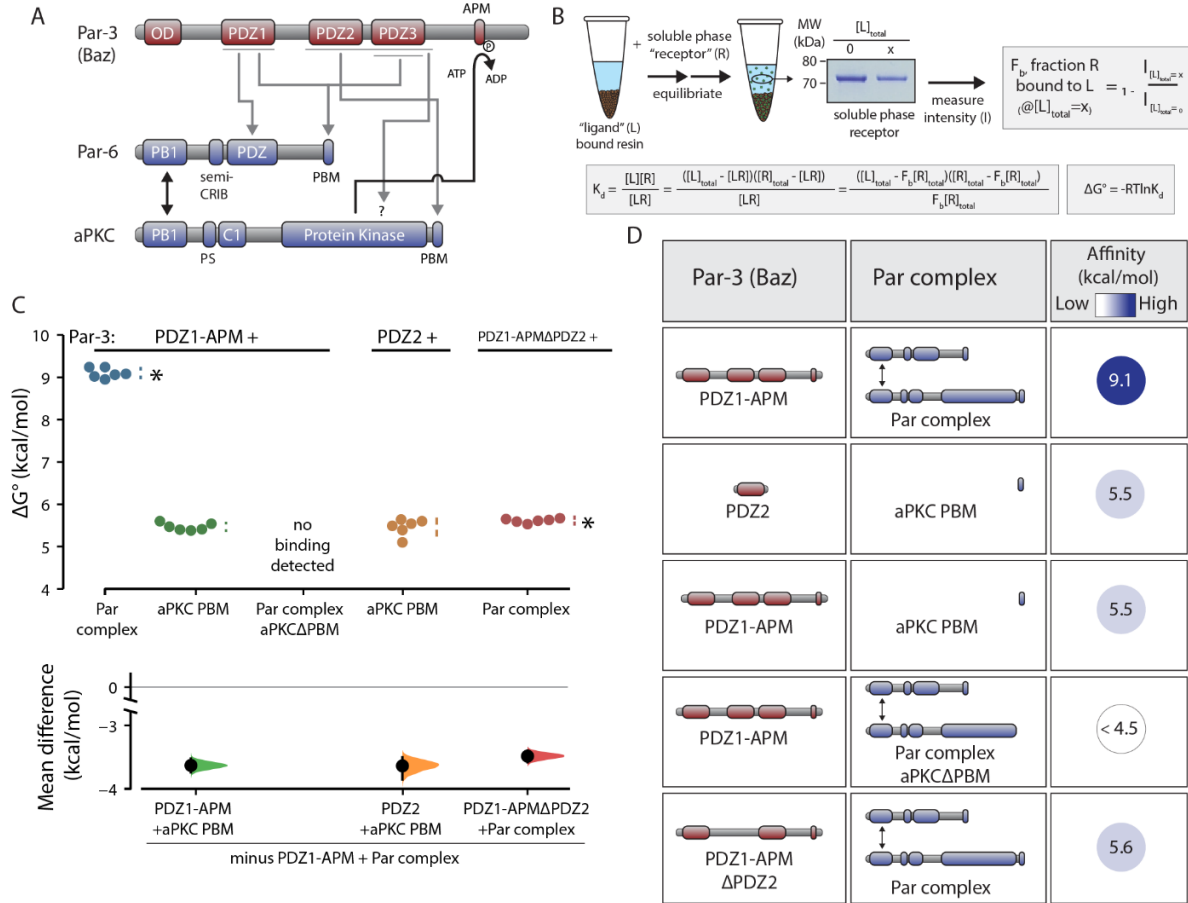


Figure 10. Energetic composition of the Par-3 interaction with the Par complex. *A*, Schematic of reported Par-3 interactions with the Par complex. *B*, Schematic of the supernatant depletion quantitative binding assay and key equations used to calculate the fraction of “R” bound to “L” (F_b), the equilibrium dissociation binding constant (K_d), and ultimately the binding energy (ΔG°). *C*, Cumming estimation plot of Par-3/Par complex interaction energies measured using the supernatant depletion assay. The result of each replicate is shown (filled circles) along with mean and standard deviation (gap and bars adjacent to filled circles) are shown in the top plot. The difference in the means relative to the PDZ1-APM/Par complex mean are shown in the bottom plot (filled circles) along with the 95% confidence intervals (black bar) derived from the bootstrap 95% confidence interval (shaded distribution). Asterisks indicate apparent values that may be the result of multiple binding interactions. *D*, Summary of binding energies for Par-3 and Par complex variants.

RESULTS

Multiple interactions contribute to Par-3–Par complex interaction energy

To investigate the energetic determinants of Par-3's interaction with the Par complex (Par-6 and aPKC), we measured binding energy using a supernatant depletion assay (Fig. 10B), using the *Drosophila* proteins. The supernatant depletion assay uses solid (glutathione or amylose agarose resin) and soluble phases like a typical “pull-down” assay but the amount of protein in the soluble phase (“receptor”) is monitored at equilibrium rather than what remains on the solid phase after washing (Pollard, 2010) (Fig. 10B and S1A). To confirm that the supernatant depletion assay yields similar affinities to another established protein interaction assay, we measured the affinity of the Crumbs intracellular domain for the Par-6 CRIB-PDZ (6.89 ± 0.07 kcal/mole; mean \pm 1 SD, $n = 6$). This result is indistinguishable from measurements made using the fluorescence anisotropy method (6.89 ± 0.06 kcal/mole) (Whitney et al., 2016). For measuring Par complex affinities for Par-3, we used the PDZ1-APM region of Par-3 (Fig. 10A) as a starting point because it contains all domains that have been reported to interact with the Par complex and it can be purified to a level suitable for quantitative analysis (all protein reagents used in this study are shown in Fig. S1B) (Holly et al., 2020). We examined binding of Par-3 PDZ1-APM to the full Par complex to allow the multiple, potentially cooperative interactions to form. As shown in Fig. 10C and D, the binding energy (ΔG°) of Par-3 PDZ1-APM to the Par complex is 9.1 kcal/mole (9.0-9.2 95% CI; all binding energies reported in this study can be found in Supplemental Table 1). Because of the potential for multiple interactions between Par-3 and the Par complex, this energy may be the cumulative effect of individual binding events. For this reason, binding energies for reactions that have stoichiometries that are potentially greater than one are labeled as “apparent”. Below we examine how each of the

potential interactions between Par-3 and the Par complex contributes to the overall binding energy.

We recently discovered an interaction between the second of Par-3's three PDZ domains (PDZ2) and a highly conserved PBM at the COOH-terminus of aPKC (Holly et al., 2020). The Par-3 PDZ2-aPKC PBM interaction is required for the recruitment of the Par complex to the cortex of asymmetrically dividing *Drosophila* neural stem cells. Using the supernatant depletion assay we found that this interaction has an apparent binding energy of 5.5 kcal/mole (5.3-5.7 95% CI) which represents approximately 60% of the full Par-3 PDZ1-APM's binding energy, and indistinguishable from PDZ1-APM binding to the aPKC PBM (Fig. 10C and D). We were

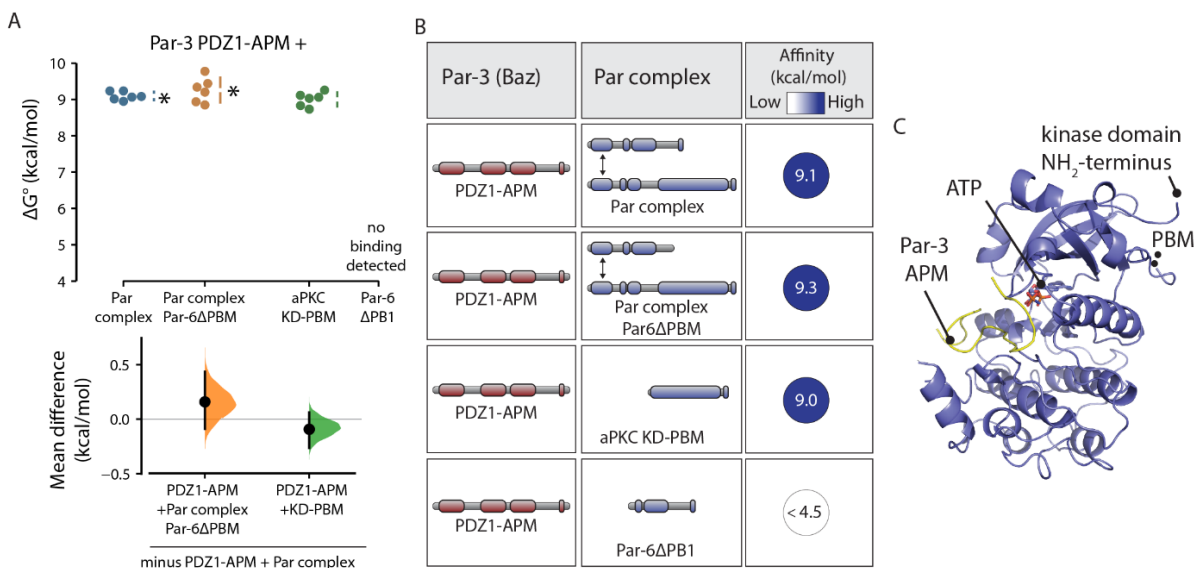


Figure 11. The aPKC kinase domain and PDZ binding motif form the Par complex binding site for Par-3. *A*, Cumming estimation plot of Par-3/Par complex interaction energies measured using the supernatant depletion assay. Note: the data for PDZ1-APM binding to the Par complex is the same as shown in Figure 10. Asterisk indicates apparent value that may be the result of multiple binding interactions. *B*, Summary of binding energies for Par-3 interaction with the aPKC KD-PBM and Par complex lacking the Par-6 PBM. *C*, Structure of the aPKC kinase domain in complex with the Par-3 phosphorylation site (from PDB ID 5LI1; Soriano et al 2016) showing the relative position of the PBM and substrate binding sites. Note that electron density for the residues directly preceding the PBM, but not the PBM itself, are present in this structure.

unable to detect an interaction between PDZ2 and a Par complex lacking aPKC's PBM (the limit of detection of the supernatant depletion assay is approximately 4.5 kcal/mole) consistent with a central role for this motif in the overall interaction. Surprisingly, however, removal of PDZ2 did not abrogate binding as PDZ1-APM Δ PDZ2 bound the Par complex with approximately the same binding energy as that for Par-3 PDZ2-aPKC PBM (Fig. 10C and D; 5.6 kcal/mole; 5.6-5.7 95% CI). We conclude that while Par-3 PDZ2-aPKC PBM represents a significant fraction of the Par-3 interaction with the Par complex, interactions outside of the PDZ2 (but also potentially involving the aPKC PBM) make a significant contribution. Furthermore, individual interactions appear to be non-additive (i.e. cooperative).

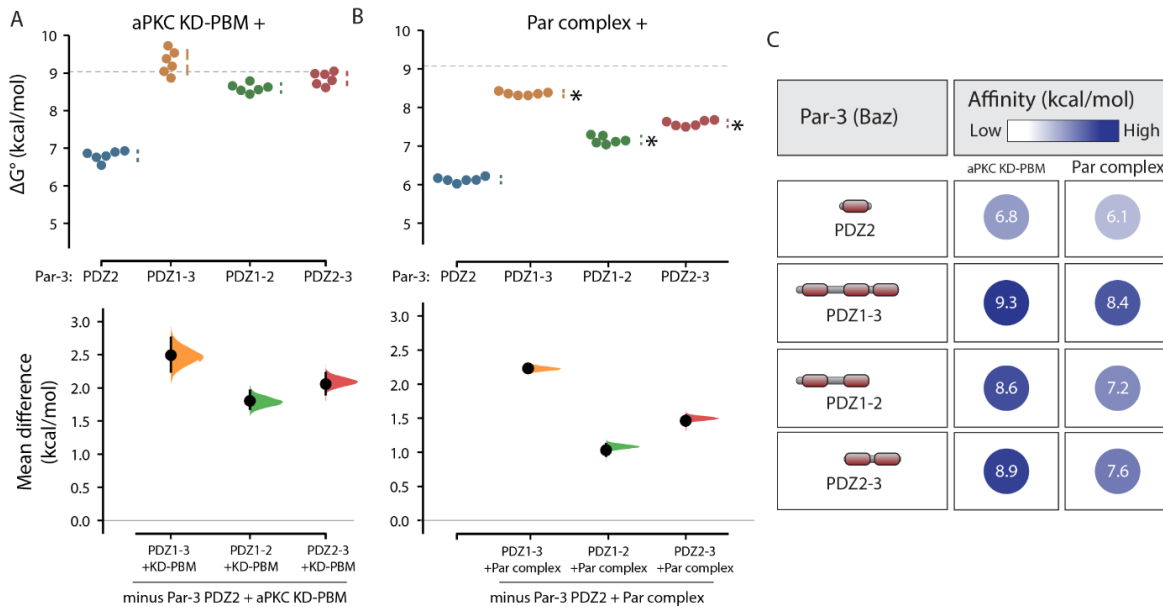


Figure 12. Energetic contributions to the Par-3/Par complex interaction from the Par-3 PDZ domains. *A, B*, Cumming estimation plots of Par-3/Par complex interaction energies measured using the supernatant depletion assay. The dashed lines indicate the binding energy of PDZ1-APM binding to the Par complex. Asterisks indicate apparent values that may be the result of multiple binding interactions. *C*, Summary of binding energies for Par-3 interaction with the aPKC KD-PBM and Par complex.

The aPKC kinase domain and PBM form the Par complex binding surface for Par-3

We sought to determine which interaction domains or motifs from the Par complex collaborate with the aPKC PBM to contribute binding energy for Par-3. Par-6 has been reported to contain a PBM that interacts with Par-3 PDZ1 or PDZ3 (Renschler et al., 2018). When examining the effect of removing Par-6's PBM on the overall interaction energetics, we were unable to detect a difference in binding of Par-3 to the Par complex lacking the Par-6 PBM (Fig. 11A and B; 9.3 kcal/mole; 8.9-9.6 95% CI). Given that our implementation the supernatant depletion assay reliably detects binding energy differences on the order of 0.2 kcal/mole (Fig. 10C), and that we were unable to detect an interaction between Par-3 PDZ1-APM and Par-6 Δ PB1 (Fig. 11A and B), we conclude that Par-3 interactions with the Par-6 PBM do not play a significant role in stabilizing Par-3 binding to the Par complex in the context of these purified components.

Given that the Par-6 PBM is not responsible for the additional interaction energy with Par-3, we sought to determine which Par complex interaction domains or motifs might contribute the additional binding energy beyond the aPKC PBM. We found that the aPKC kinase domain along with the adjacent PBM (KD-PBM; Fig. 11C) fully recapitulated the interaction energy of the Par complex with Par-3 (Fig. 11A and B; 9.0 kcal/mole; 8.8-9.2). Thus, in the context of these purified components, we do not find that the Par-3 PDZ1 interaction with the Par-6 PDZ, or the PDZ1 and 3 interactions with the Par-6 PBM substantially contribute to the overall Par-3 and Par complex binding energy.

A conserved basic region NH₂-terminal to Par-3 PDZ2 contributes to Par complex binding

We used both the Par complex and the isolated aPKC KD-PBM to identify which regions of Par-3 outside of PDZ2 contribute to the overall interaction energy. We found that a Par-3 fragment containing its three PDZ domains has similar binding energy as PDZ1-APM (Fig. 12A-C; 9.3 kcal/mole; 9.0-9.6 95% CI). This result indicates that Par-3's phosphorylation site (APM) and the linker region connecting it to PDZ3 do not contribute significantly to the interaction. Note that ATP was present in our binding assay so that any interaction of the aPKC kinase domain with the APM was likely transient (and the interaction with the phosphorylated APM is

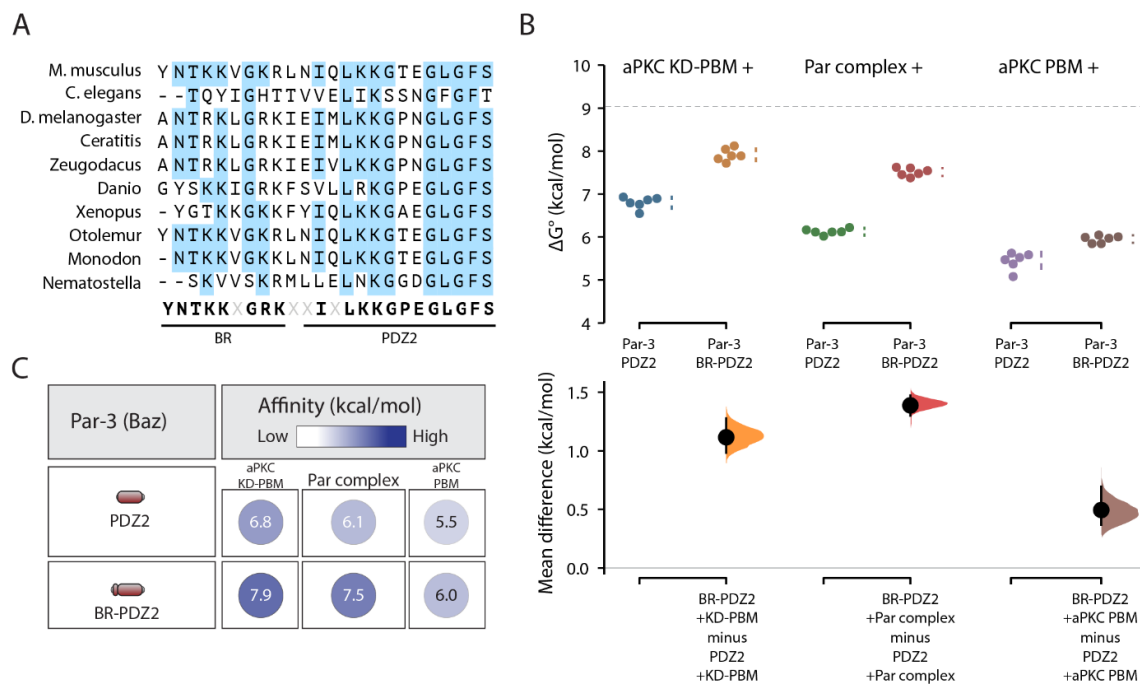


Figure 13. A conserved basic region (BR) contributes binding energy to the Par-3 PDZ2 interaction with the Par complex. *A*, Sequence alignment of the region NH₂-terminal to the Par-3 PDZ2 from the Par-3 sequence from diverse animal species. *B*, Cumming estimation plot of Par-3/Par complex interaction energies measured using the supernatant depletion assay. The dashed lines indicate the binding energy of PDZ1-APM binding to the Par complex. *C*, Summary of binding energies for Par-3 PDZ2 and BR-PDZ2 interaction with the aPKC KD-PBM, Par complex, and aPKC PBM.

weak) (Holly et al., 2020; Holly and Prehoda, 2019). We did not detect any difference in binding energy of Par-3 PDZ1-3 to the Par complex when ATP was replaced with ADP (Fig. S2A).

When examining the three Par-3 PDZ domains, we found that either PDZ1-2 or PDZ2-3 bound with binding energies similar to PDZ1-APM although PDZ1-2's was somewhat lower than PDZ2-3's, an effect that was larger in the context of the full Par complex relative to the KD-PBM alone (Fig. 12). We noticed that an approximately 30 residue sequence directly NH₂-terminal to the PDZ2 domain is enriched in basic amino acids and highly conserved in Par-3's from diverse animal species (Fig. 13A). We termed this motif the Basic Region (BR) and found that including it with Par-3 PDZ2 (BR-PDZ2) significantly increased the binding energy of the interaction with the aPKC kinase domain and the full Par complex (Fig. 13B and C). We conclude that the higher binding energy of PDZ1-2 compared to PDZ2 alone is contributed by the conserved BR motif.

The Par-3 PDZ3 domain binds the aPKC kinase domain and PBM

Like PDZ1-2, the combination of PDZ2 and 3 (Par-3 PDZ2-3) also bound aPKC KD-PBM and full Par complex with higher affinity than PDZ2 alone (Fig. 14A-D). In this case, the higher binding energy originates from PDZ3 as we discovered that it binds the aPKC KD-PBM with similar energy to PDZ2 and somewhat less energy to the full Par complex (Fig. 14A-D). We also found that PDZ3 binds the aPKC PBM with a similar energy as PDZ2. Like PDZ2, the binding energy of PDZ3 was higher for aPKC KD-PBM compared to the PBM alone.

Our results indicate that Par-3 PDZ2 and PDZ3 use a similar binding mode and therefore may compete for binding to aPKC KD-PBM. To test this hypothesis, we performed a competition experiment, first assembling a complex of the aPKC KD-PBM with PDZ2 and then

adding PDZ3. We found that the presence of PDZ3 caused a significant decrease in the amount of aPKC bound to PDZ2 (Fig 14E). Soluble PDZ2 was also able to displace PDZ3 from aPKC KD-PBM (Fig. 14E). The competitive binding for the two PDZ domains suggests that PDZ2 and PDZ3 each binds a distinct Par complex. Furthermore, the increased binding affinity when both PDZ2 and 3 are present (e.g. PDZ2-3) relative to the individual domains likely arises from an avidity effect in which more than one Par complex is participating in the interaction.

Par-3 BR-PDZ2-3 binding to aPKC KD-PBM recapitulates the overall interaction energy

Taken together, our results suggest that the binding energy of the Par-3 interaction with the Par complex arises from separate interactions of the BR-PDZ2 and PDZ3 with the aPKC KD-PBM. As shown in Fig. 15A and B, Par-3 BR-PDZ2-3 nearly completely recapitulates the binding energy of PDZ1-APM. To determine if distinct Par complexes can bind to PDZ2 and PDZ3, we asked whether the Par-3 PDZ1-APM adsorbed to the solid phase via the aPKC PBM, could recruit the Par complex. We found that the Par complex was specifically adsorbed to GST-aPKC PBM in the presence of Par-3 PDZ1-APM (Fig. 15C). We conclude that distinct interactions of BR-PDZ2 and PDZ3 with aPKC KD-PBM form the basis of the Par-3 interaction with the Par complex (Fig. 15D). In the context of these purified proteins, we do not detect a significant contribution from the interaction of PDZ1 or PDZ3 with the Par-6 PBM, the interaction of PDZ1 with the Par-6 PDZ, or the interaction of the aPKC kinase domain with its phosphorylation site.

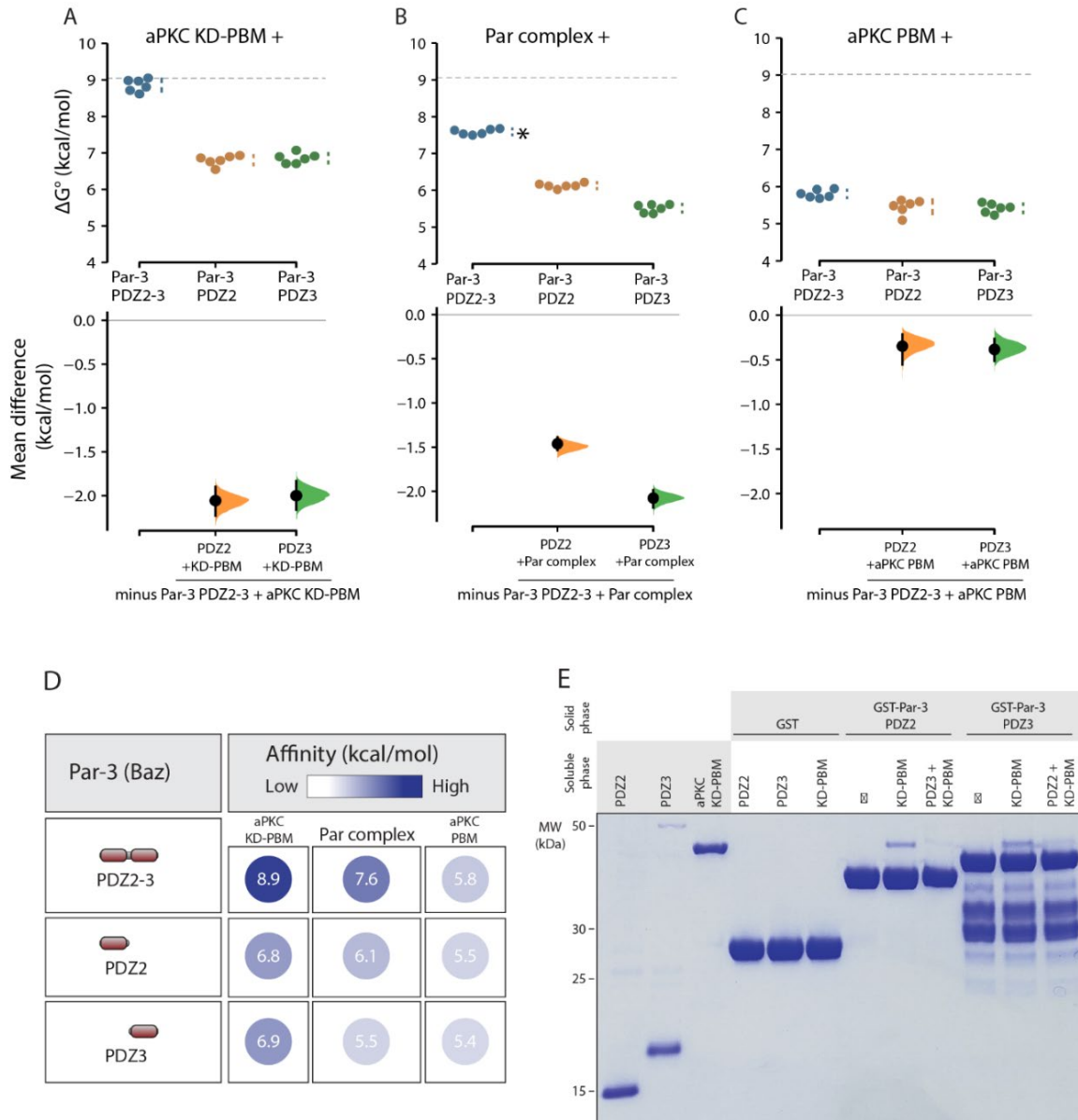


Figure 14. Par-3 PDZ3 binds the aPKC kinase domain and PDZ Binding Motif. *A-C*, Cumming estimation plots of Par-3 PDZ2 and PDZ3 interaction energies with the aPKC kinase domain–PBM (*A*), full Par complex (*B*) and aPKC PBM (*C*) measured using the supernatant depletion assay. Dashed lines represent the interaction energy of PDZ1-APM to the Par complex. Asterisk indicates apparent value that may be the result of multiple binding interactions. *D*, Summary of binding energies for Par-3 PDZ2 and PDZ3 interaction with the aPKC kinase domain-PBM, Par complex, and aPKC PBM. *E*, Competition between Par-3 PDZ2 and PDZ3 for binding to aPKC KD-PBM. Solid phase (glutathione resin) bound Glutathione-S-Transferase (GST) fused Par-3 PDZ2 or PDZ3 incubated with aPKC KD-PBM (arrowhead) and the indicated competing PDZ domain. Shaded regions of legend indicate the fraction applied to the gel (soluble-phase or solid-phase components after mixing with soluble-phase components and washing).

DISCUSSION

The nature of the Par-3 interaction with the Par complex has been enigmatic (Lang and Munro, 2017; Martin et al., 2021; Riga et al., 2020; Thompson, 2021; Wu et al., 2020). In this study, we used a quantitative biochemical approach with purified, full-length Par complex and a region of Par-3 that contains all known binding motifs to address the challenge of understanding this complicated interaction. We found that Par-3 PDZ2 and PDZ3 binding to the aPKC KD-PBM nearly fully recapitulates the binding energy of the overall interaction between Par-3 and the Par complex. We note that these interactions most closely resemble the previously identified interaction of Par-3 PDZ2-3 with full-length aPKC using a yeast two-hybrid assay (Wodarz et al., 2000). We used the *Drosophila* versions of these proteins and, while the Par complex is highly conserved, it is possible that the proteins from other organisms behave differently. Here we examine the implications of our quantitative findings on Par-3's role in Par-mediated polarity.

We used binding energy to evaluate the relative contribution of each of the identified Par-3 interactions with the Par complex. The binding energies of several of the interactions in the context of isolated Par complex fragments have been previously reported. The interaction of the aPKC kinase domain with the Par-3 APM has been reported to be very high (8.6 kcal/mole) (Soriano et al., 2016). However, this interaction was measured in the absence of ATP, conditions which prevent substrate turnover and are consequently not physiologically relevant (Holly et al., 2020; Holly and Prehoda, 2019). We did not detect any contribution to the overall interaction between Par-3 and the Par complex from the Par-3 APM when ATP was present. The interactions of Par-3 PDZ1 and PDZ3 with the Par-6 PBM were measured using NMR and were found to be weak (5.0 and 5.8 kcal/mole, respectively). While these affinities are low, they are

above the limit of detection of the supernatant depletion assay. However, we did not detect any significant contribution from the Par-6 PBM in the context of Par complex binding to Par-3; we did not detect an interaction of Par-3 with Par-6/aPKC Δ PBM, nor did we detect a change in affinity when the Par-6 PBM was removed (i.e. Par-6 Δ PBM/aPKC).

An analysis of the Par-3 domains required for polarity in the *C. elegans* zygote found that PDZ1 and 3 were dispensable but the oligomerization domain and PDZ2 were necessary (B. Li et al., 2010). A similar analysis found that the interaction of the Par-6 PDZ domain with Par-3

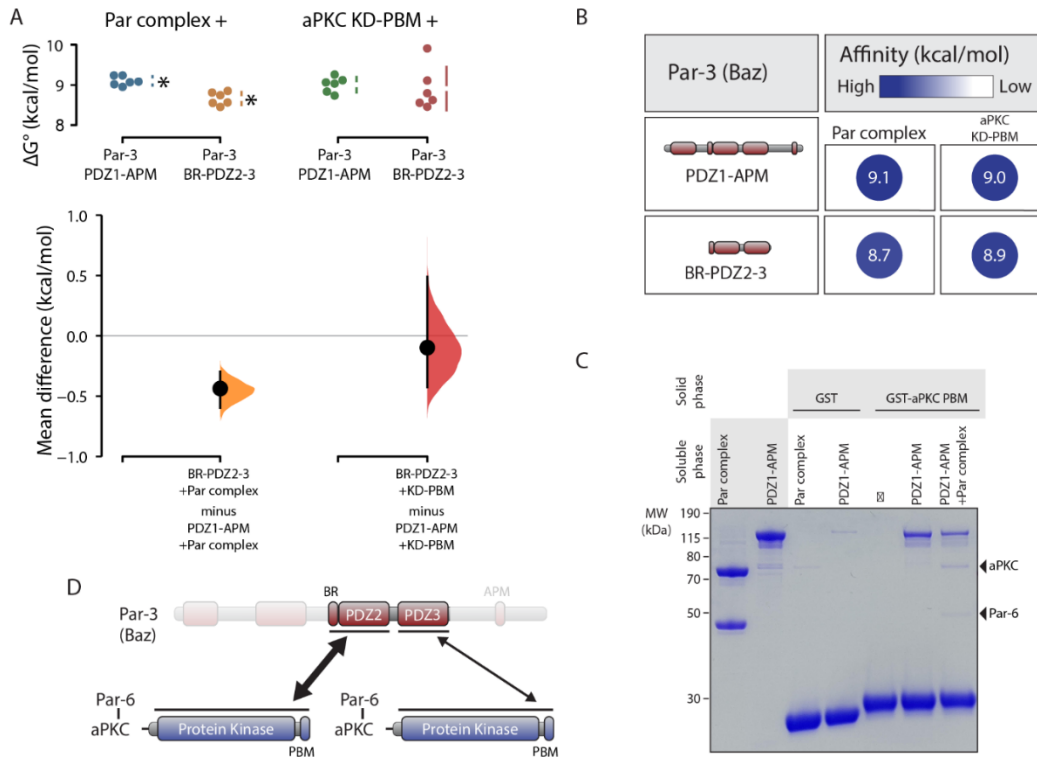


Figure 15. Par-3 BR-PDZ2-3 binding to the aPKC kinase domain-PBM fully recapitulates the Par-3 interaction with the Par complex. *A*, Cumming estimation plot of Par-3 BR-PDZ2-3 interaction energies with the full Par complex and aPKC KD-PBM measured using the supernatant depletion assay. Asterisks indicate apparent values that may be the result of multiple binding interactions. *B*, Summary of binding energies for BR-PDZ2-3 interaction with the full Par complex and aPKC KD-PBM. *C*, Par-3 PDZ1-APM can bind the Par complex while binding to the aPKC PBM. *D*, Model for interaction of Par-3 with the Par complex.

was also dispensable for Par complex function (J. Li et al., 2010). An examination of the Par-6 PBM found that it is not required for viability in *Drosophila* and its removal did not have a measurable effect on Par-6 recruitment to the cortex of the embryonic epithelium except when the Par-6 PDZ was also removed (Renschler et al., 2018). In a study of aPKC PBM function, aPKC Δ PBM was not polarized to the apical membrane during the asymmetric division of *Drosophila* larval neural stem cells (Holly et al., 2020). These functional results are consistent with the primacy of the aPKC PBM in binding to Par-3. They also suggest that the biochemical redundancy between Par-3 PDZ2 and PDZ3 does not translate to *in vivo* function, either because of the lower affinity of PDZ3 or because PDZ2 participates in other essential functions besides binding to the Par complex.

Our results indicate that the aPKC kinase domain participates in the interaction with Par-3 PDZ2 and PDZ3. The nature of this interaction is not known but the proximity of the aPKC PBM to the kinase domain is suggestive (Fig. 11C) (Soriano et al., 2016). Binding to the PBM would bring PDZ surfaces outside of the PBM pocket near the kinase domain and could lead to so-called “docking” interactions that occur between protein kinase substrates and regions away from the kinase domain active site (Reményi et al., 2006). Another interesting feature of the binding energetics results is the higher binding energy of the Par-3 PDZ domains to the aPKC KD-PBM compared to the full Par complex (Fig. 14A vs 14B). The lower binding affinity to the full Par complex suggests that autoregulation may be present in the system. Future efforts will be directed at exploring the nature of these interactions and any role they may have in regulating aPKC activity.

EXPERIMENTAL PROCEDURES

Cloning

GST-, MBP- and his-tagged Par-3 constructs, GST aPKC PBM and his aPKC kinase domain-PBM (residues 259-606) were cloned as previously described (Holly et al., 2020) using Gibson cloning (New England BioLabs), Q5 mutagenesis (New England BioLabs) or traditional methods. In addition to an N-terminal MBP tag, the Par-3 PDZ1-APM (residues 309-987) construct also contained a C-terminal his-tag. Par complex components (aPKC and his-Par-6) were cloned into pCMV as previously described (Graybill et al., 2012; Holly et al., 2020). Please see the Key Resources table for additional information on specific constructs.

Expression

All proteins, except for Par complex constructs, were expressed in *E. coli* (strain BL21 DE3). Constructs were transformed into BL21 cells, grown overnight at 37°C on LB + ampicillin (Amp; 100 µg/mL). Resulting colonies were selected and used to inoculate 100mL LB+Amp starter cultures. Cultures were grown at 37°C to an OD₆₀₀ of 0.6-1.0 and then diluted into 2L LB+Amp cultures. At an OD₆₀₀ of 0.8-1.0 expression was induced with 0.5 mM IPTG for 2-3 hours. Cultures were centrifuged at 4,400g for 15 minutes to pellet cells. Media was removed and pellets were resuspended in nickel lysis buffer [50mM NaH₂PO₄, 300 mM NaCl, 10 mM Imidazole, pH 8.0], GST lysis buffer [1XPBS, 1 mM DTT, pH 7.5] or Maltose lysis buffer [20 mM Tris, 200 mM NaCl, 1 mM EDTA, 1 mM DTT, pH 7.5], as appropriate. Resuspended pellets were frozen in liquid N₂ and stored at -80°C.

Par complex constructs were expressed in HEK 293F cells (Thermofisher), as previously described (Graybill et al., 2012; Holly et al., 2020). Briefly, cells were grown in FreeStyle 293 expression media (Thermofisher) in shaker flasks at 37°C with 8% CO₂. Cells were transfected with 293fectin (Thermofisher) or ExpiFectamine (Thermofisher) according to the manufacture's protocol. After 48 hours, cells were collected by centrifugation (500g for 5 min). Cell pellets were resuspended in nickel lysis buffer, frozen in liquid N₂ and stored at -80°C.

Purification

Resuspended *E.coli* pellets were thawed and cells were lysed by probe sonication using a Sonicator Dismembrator (Model 500, Fisher Scientific; 70% amplitude, 0.3/0.7s on/off pulse, 3x1 min). 293F cell pellets were lysed similarly using a microtip probe (70% amplitude, 0.3/0.7s on/off pulse, 4x1 min). Lysates were centrifuged at 27,000g for 20 min to pellet cellular debris. GST- and MBP-tagged protein lysates were aliquoted, frozen in liquid N₂ and stored at -80°C.

His-tagged protein lysates, except for aPKC KD-PBM, were incubated with HisPur Ni-NTA (Thermofisher) or HisPur Cobalt (Thermofisher) resin for 30 min at 4°C and then washed 3x with nickel lysis buffer. For 293F lysates, 100µM ATP and 5mM MgCl₂ were added to the first and second washes. Proteins were eluted in 0.5-1.5mL fractions with nickel elution buffer (50 mM NaH₂PO₄, 300 mM NaCl, 300 mM Imidazole, pH 8.0). For all proteins, aside from Par complex, fractions containing protein were pooled, buffered exchanged into 20mM HEPES pH 7.5, 100 mM NaCl and 1 mM DTT using a PD10 desalting column (Cytiva), concentrated using a Vivaspın20 protein concentrator spin column (Cytiva), aliquoted, frozen in liquid N₂ and stored at -80°C. For Par complex, proteins were further purified using anion exchange chromatography on an AKTA FPLC protein purification system (Amersham Biosciences). Following his-

purification fractions were pooled and buffered exchanged into 20mM HEPES pH 7.5, 100 mM NaCl, 1 mM DTT, 100 μ M ATP and 5 mM MgCl₂ using a PD10 desalting column (Cytiva). Buffer-shifted protein was injected onto a Source Q (Cytiva) column and eluted over a salt gradient of 100-550mM NaCl. Fractions containing Par complex were pooled, buffered exchanged into 20 mM HEPES pH 7.5, 100 mM NaCl, 1 mM DTT, 100 μ M ATP, and 5 mM MgCl₂ using a PD10 desalting column (Cytiva), concentrated using a Vivaspin20 protein concentrator spin column (Cytiva), aliquoted, frozen in liquid N₂ and stored at -80°C.

Due to solubility issues, aPKC KD-PBM was expressed in *E. coli* and his-purified partially under denaturing conditions. Following sonication and centrifugation (described above), the soluble fraction was discarded and the insoluble pellet was resuspended in 50mM NaH₂PO₄, 300 mM NaCl, 10 mM Imidazole, 8M Urea pH 8.0. Centrifugation was repeated (27,000g for 20 min) and the resulting soluble phase was incubated with HisPur Ni-NTA resin (ThermoFisher) for 30 min at 4°C. Resin was washed and eluted as described above. Purified protein was aliquoted, frozen in liquid N₂ and stored at -80°C.

Quantitative Binding Assay

For all solid phase proteins, except Par-3 PDZ1-APM and PDZ1-APM Δ PDZ2, GST lysates were incubated with glutathione agarose resin (GoldBio; 50 μ L resin per 0.5-1.5 mL of lysate) for 30 min at 4°C and then washed 6x (3x quick washes, followed by 3x 5min washes at room temp) with binding buffer (10 mM HEPES pH 7.5, 100 mM NaCl, 1 mM DTT 200 μ M ATP, 5 mM MgCl₂ and 0.1% Tween-20). After washing, resin was resuspended in 50 μ L binding buffer to create a 50% slurry. Par-3 PDZ1-APM and PDZ1-APM Δ PDZ2 were double tagged (N-terminal MBP-tag and C-terminal his-tag). Par-3 PDZ1-APM and PDZ1-APM Δ PDZ2 were first

his-purified (described above) prior to incubation with amylose resin (NEB). Amylose-bound Par-3 was then washed and resuspended in binding buffer as described for GST proteins.

Separately, unlabeled resin (amylose or glutathione resin, as appropriate) was washed 3x and resuspended in a 50% slurry with binding buffer. GST- or MBP-labeled resin was then serially diluted 1:1 (30 μ L of 50% slurry) with unlabeled resin to create a gradient of the GST/MBP-tagged protein. Unlabeled resin was used as a negative control for binding. Soluble protein (“receptor”) was added to the solid phase protein (“ligand”) and incubated for one hour at 20°C with rotational mixing (see Supplemental Table 1 for the solid phase-soluble phase combination for each experiment), except for MBP-Par-3 constructs. Due to high levels of leaching into the supernatant from amylose bound MBP-tagged proteins, MBP-Par-3 assays were incubated for ten minutes (we confirmed that GST-Par-3 PDZ1-3 incubated for one hour produced indistinguishable results to MBP-Par-3 PDZ1-3 incubated for ten minutes; Figure S2B).

Following incubation, a sample of the supernatant was removed from each tube and combined with 4X LDS sample buffer (ThermoFisher). Samples were run on a Bis-Tris gel, stained with Coomassie Brilliant Blue R-250 (GolBio) and band intensity was quantified using ImageJ (v1.53a). The fraction of R (soluble phase) bound to L (solid phase) at a specific concentration of L ($[L] = x$) was determined using the following equation:

$$\textit{Fraction bound } ([L] = x) = 1 - \frac{I_{[L]=x}}{I_{[L]=0}}$$

where $I_{[L]=x}$ represents the intensity of the receptor (soluble phase) band at ligand (solid phase) concentration “x” following equilibration, and $I_{[L]=0}$ is the receptor band intensity without any ligand present. The dilution of the solid phase that resulted in 30-60% depletion ($F_b = 0.3-0.6$)

was determined using a ligand titration, and the assay was repeated in sextuplicate at this dilution. The solid phase concentration ([L]) was determined by gel analysis using a standard protein of known concentration.

The binding equilibrium dissociation constant (K_d) was evaluated from the fraction bound (F_b) using the single site binding equation derived below:

$$K_d = \frac{[L][R]}{[LR]}$$

[L],[R] concentration of free ligand (solid phase) and receptor (soluble phase) at equilibrium

[LR] concentration of complex at equilibrium

$$K_d = \frac{([L]_{total} - [LR])([R]_{total} - [LR])}{[LR]}$$

$$K_d = \frac{([L]_{total} - F_b[R]_{total})([R]_{total} - F_b[R]_{total})}{F_b[R]_{total}}$$

The binding energy was calculated using the equation for the standard Gibbs free energy change:

$$\Delta G^\circ = -RT \ln [K_d]$$

Binding results from experiments using Par-3 variants that could potentially bind more than one Par complex are labeled as “apparent” to emphasize that the binding energy could arise from multiple interactions.

The data was visualized and analyzed using Excel (v16.53), GraphPad Prism (v9.2) and the DABEST (Ho et al., 2019) software packages. Confidence intervals were estimated using the bootstrap method as implemented in DABEST.

Qualitative Binding Assays

For GST pulldown assays, GST lysates were incubated with glutathione agarose resin (GoldBio) for 30 min at 4°C and then washed 6x (3x quick washes, followed by 3x 5 min washes at room temp) with binding buffer (10 mM HEPES pH 7.5, 100 mM NaCl, 1 mM DTT 200 μM ATP, 5 mM MgCl₂ and 0.1% Tween-20). Soluble proteins were added to GST-bound proteins, as indicated, and incubated at room temperature with rotational agitation for 30-60 min. Resin was then washed 3x with binding buffer and protein was eluted with 4X LDS sample buffer (ThermoFisher). Samples were run on a Bis-Tris gel and stained with Coomassie Brilliant Blue R-250 (GolBio).

Key Resources Table 2

Reagent type (species) or resource	Designation	Source or reference	Identifiers	Additional information
Recombinant protein	Par complex (his-Par-6, aPKC)	PMID: 32084408		expressed in 293F cells from pCMV his-Par-6 1-351 and pCMV aPKC 1-606
Recombinant protein	Par complex aPKCΔPBM	PMID: 32084408		expressed in 293F cells from pCMV his-Par-6 1-351 and pCMV aPKC 1-600
Recombinant protein	Par complex Par-6ΔPBM	PMID: 32084408		expressed in 293F cells from pCMV his-Par-6 1-343 and pCMV aPKC 1-606
Recombinant protein	GST-aPKC PBM	PMID: 32084408		expressed in BL21 cells from pGEX aPKC 583-606
Recombinant protein	GST-Par-3 PDZ2-3	This paper		Cloned by Q5 mutagenesis; expressed in BL21 cells from pGEX Par-3 444-741

Recombinant protein	GST-Par-3 PDZ1-2	This paper		Gibson cloning; expressed in BL21 cells from pGEX Par-3 309-533
Recombinant protein	GST-Par-3 PDZ1-3	This paper		Gibson cloning; expressed in BL21 cells from pGEX Par-3 309-741
Recombinant protein	GST-Par-3 BR-PDZ2	This paper		Gibson cloning; expressed in BL21 cells from pGEX Par-3 426-533
Recombinant protein	GST-Par-3 PDZ2	This paper		Gibson cloning; expressed in BL21 cells from pGEX Par-3 444-533
Recombinant protein	GST-Par-3 BR-PDZ2-3	This paper		Gibson cloning; expressed in BL21 cells from pGEX Par-3 426-741
Recombinant protein	GST-Par-3 PDZ3	This paper		Gibson cloning; expressed in BL21 cells from pGEX Par-3 616-741
Recombinant protein	aPKC KD-PBM	This paper		Cloned using traditional methods; expressed in BL21 cells from pBH aPKC 259-606; his-purified under denaturing conditions
Recombinant protein	Par-3 PDZ2	This paper		Gibson cloning; expressed in BL21 cells from pET19 Par-3 444-533; his-purified
Recombinant protein	Par-3 BR-PDZ2	This paper		Gibson cloning; expressed in BL21 cells from pET19 Par-3 426-533; his-purified
Recombinant protein	Par-3 PDZ2-3	This paper		Cloned by Q5 mutagenesis; expressed in BL21 cells from pET19 Par-3 444-741; his-purified
Recombinant protein	Par-3 PDZ3	This paper		Gibson cloning; expressed in BL21 cells

				from pET19 Par-3 616-741; his-purified
Recombinant protein	MBP-Par-3 PDZ1-APM	PMID: 32084408		expressed in BL21 cells from pMAL Par-3 309-987-his; C-terminal his-tag; his-purified prior to use in binding assay
Recombinant protein	MBP-Par-3 PDZ1-APM Δ PDZ2	PMID: 32084408		expressed in BL21 cells from pMAL Par-3 309-987 Δ 437-533-his; C-terminal his-tag; his-purified prior to use in binding assay
Recombinant DNA reagent	pCMV (mammalian expression plasmid)	ThermoFisher	10586014	
Recombinant DNA reagent	pMal C4X (bacterial expression plasmid)	Addgene	75288	
Recombinant DNA reagent	pGEX 4Ti (bacterial expression plasmid)	Amersham	27458001	
Recombinant DNA reagent	pBH (bacterial expression plasmid)	PMID: 15023337		
Recombinant DNA reagent	pET19 (bacterial expression plasmid)	Millipore Sigma (Novagen)	69677	
Bacterial strain	BL21-DE3			used for recombinant protein expression
Bacterial strain	TG1			used for DNA cloning
Cell line (human)	FreeStyle 293-F	ThermoFisher	R79007	
Chemical	IPTG	GoldBio	I2481C100	used at 0.5mM
Chemical	293fectin	ThermoFisher	12347019	

Chemical	ExpiFectamine 293 Transfection Kit	ThermoFisher	A14524	
Chemical	Freestyle 293 expression Medium	ThermoFisher	12338018	
Chemical	Opti-Mem	ThermoFisher	3198588	
Chemical	HisPur cobalt resin	ThermoFisher	89965	
Chemical	HisPur NiNTA resin	ThermoFisher	88222	
Chemical	Amylose Resin	NEB	E8021L	
Chemical	Glutathione Resin	GoldBio	G250-100	
Chemical	Source Q anion exchange resin	GE Healthcare	17-1275-01	
Chemical	LB Broth, Miller	Millipore Sigma	71753-6	
Chemical	4X BOLT LDS sample buffer	ThermoFisher	B0007	
Chemical	20X BOLT MES SDS running buffer	ThermoFisher	B0002	
Chemical	Coomassie Brilliant Blue R-250	GoldBio	C-461-5	
Commercial kit	Q5® Site-Directed Mutagenesis Kit	NEB	E0552S	
Commercial kit	Gibson Assembly Cloning Kit	NEB	E5510S	
Other	Bolt 12% Bis-Tris Gels	ThermoFisher	NW00125B OX	
Other	PD10 Desalting columns		95017-001	

Other	VivaSpin 20 sample concentrators MWCO 30kD	Cytiva	28932361	
Other	VivaSpin 20 sample concentrators MWCO 10kD	Cytiva	28932360	
Other	VivaSpin 20 sample concentrators MWCO 5kD	Cytiva	28932359	
Other	Shaker Flasks – 125mL	VWR	89095-258	
Other	Shaker Flasks – 250mL	VWR	89095-266	
software	ImageJ	NIH		v1.53a; https://imagej.nih.gov/ij/
software	GraphPad Prism	GraphPad Software		v.9.2
software	Estimation Statistics BETA	PMID: 31217592		www.estimatestats.com

BRIDGE TO CHAPTER IV

In this chapter, we discussed the confusion in the cell polarity field regarding how Par-3 and the Par complex interact. Utilizing quantitative binding assays and purified components, we first determined the affinity between the Par complex and Par-3 PDZ1-APM. Through further analysis, we found that Par-3 PDZ2 and PDZ3 binding to aPKC KD-PBM almost completely recapitulates the affinity between Par-3 and the Par complex. Our findings suggest that Par-3 may be able to interact with two Par complexes at a time, allowing for efficient polarization of the Par complex. In the following chapter, we focus on understanding the formation of Par-3- and Cdc42-bound Par complexes as each are suggested to have distinct activities. Thus, using

qualitative pull-down assays with purified proteins, we investigate how the Par complex transitions from a Par-3 to Cdc42-bound complex. This work provides the mechanistic framework for understanding regulation of Par complex by Par-3 and Cdc42 and will help us further understand the process of cell polarity.

CHAPTER IV

**NEGATIVE COOPERATIVITY UNDERLIES DYNAMIC ASSEMBLY OF THE
PAR COMPLEX REGULATORS CDC42 AND PAR-3**

*This chapter contains previously published co-authored material.

Vargas E & Prehoda KE. (2023). Negative cooperativity underlies dynamic assembly of the Par complex regulators Cdc42 and Par-3. *J Biol Chem.* 299(1), 102749. *J Biol Chem.* Editors' Pick.

Author Contributions: E. V. and K. E. P. conceptualization; E. V. and K. E. P. methodology; E. V. investigation; E. V. and K. E. P. writing original draft; E. V. and K. E. P. writing–review & editing; K. E. P. supervision; K. E. P. project administration; K. E. P. funding acquisition.

INTRODUCTION

The polarization of animal cells by the Par complex is a highly dynamic, multi-step process, that begins when actomyosin-generated cortical flows transport membrane-bound Par complex from cellular regions where it is catalytically inactive to a single cortical domain where it becomes activated (Aceto et al., 2006; Atwood et al., 2007; Hutterer et al., 2004; Lang and Munro, 2017; Munro et al., 2004; Oon and Prehoda, 2021, 2019; Rodriguez et al., 2017). The transition from an inactive to active complex is mediated by the formation of two distinct complexes: one bound to the multi-PDZ protein Par-3 (Bazooka; Baz in *Drosophila*) and a Rho

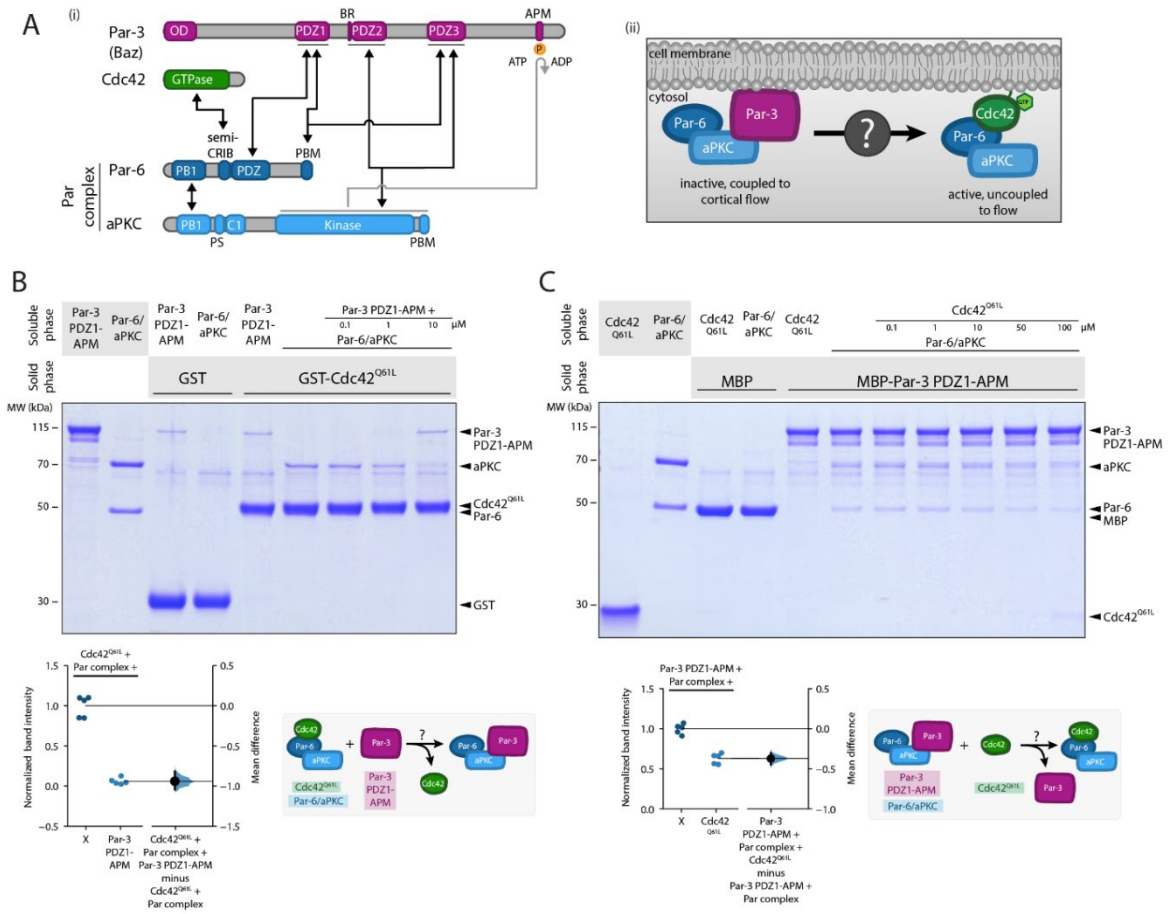
GTPase Cdc42-bound complex. Par-3 has many reported interactions with both Par complex components, atypical Protein Kinase C (aPKC) and Par-6, whereas Cdc42 has one well-defined binding site on Par-6 (Fig. 16A) (Garrard et al., 2003; Holly et al., 2020; Izumi et al., 1998; Joberty et al., 2000; J. Li et al., 2010; Lin et al., 2000; Noda et al., 2001; Penkert et al., 2022; Qiu et al., 2000; Renschler et al., 2018; Wodarz et al., 2000). The transition between these two regulators precisely controls Par complex polarization and activity, with Par-3 coupling the Par complex to cortical flow while inhibiting aPKC activity and GTP-bound Cdc42 maintaining the Par complex at the cell cortex while stimulating aPKC activity (Dickinson et al., 2017; Rodriguez et al., 2017; Wang et al., 2017). Despite the critical importance of the transition from Par-3 to Cdc42 in the mechanism of Par-mediated polarity, very little is known about how it occurs.

While *in vivo* evidence indicates the Par complex switches from Par-3 to Cdc42-bound states, biochemical evidence suggests that Par-3 and Cdc42 can bind the Par complex simultaneously to form a quaternary complex. A co-immunoprecipitation experiment using cell extracts found that Cdc42-bound Par complexes also contain Par-3 (Joberty et al., 2000). However, *in vivo* evidence indicate that there are two distinct cortical pools of Par complex, colocalizing with either Par-3 or Cdc42, and loss of Cdc42 increases the amount of Par-3-bound complex (Aceto et al., 2006; Beers, 2006; Rodriguez et al., 2017; Wang et al., 2017). The reported ability of Cdc42 and Par-3 to bind simultaneously to the Par complex has influenced models for how the transition between the regulators could occur *in vivo*. In one model, Cdc42 briefly docks onto Par-3-bound Par complex and activates aPKC, resulting in the phosphorylation and release of Par-3 from the complex (Morais-de-Sá et al., 2010; Soriano et al., 2016; Walther and Pichaud, 2010). However, recent studies show that phosphorylation of Par-3

by aPKC does not dissociate Par-3 from the Par complex (Holly et al., 2020; Holly and Prehoda, 2019). In another proposed model, actomyosin contractility mechanically dissociates Par-3 clusters and facilitates the Par complex transition to Cdc42 (Dickinson et al., 2017; Rodriguez et al., 2017; Wang et al., 2017).

Because the available biochemical data suggests that Par-3 and Cdc42 can bind simultaneously to the Par complex, models for the transition between the two regulators necessarily include other mechanisms (e.g. phosphorylation) or cellular components (e.g. actomyosin contractility). However, the limited in vitro evidence is based on results from cell extracts or experiments using truncated proteins. Additionally, the numerous reported interactions between Par-3 and the Par complex have made it challenging to understand how the Par-3-bound Par complex is regulated. Finally, very little structural information is known about the Par complex and whether the Par-3 and Cdc42 binding sites are in close proximity to one

Figure 16 (next page) . Par-3 and Cdc42 bind to the Par complex with strong negative cooperativity. A, (i) Domain architecture of Par-3, Cdc42, and the Par complex with reported interactions between Par-3, Cdc42, and the Par complex. Black arrows indicate reported interactions, and the grey arrow indicates phosphorylation. (ii) Schematic for the Par complex transition from Par-3 to Cdc42. B, Effect of Par-3 PDZ1-APM on the interaction between Cdc42 and the Par complex. Solid-phase (glutathione resin)-bound glutathione S-transferase (GST)-fused Cdc42Q61L (constitutively active Cdc42) incubated with Par complex and/or increasing concentrations of Par-3 PDZ1-APM. Shaded regions indicate the fraction applied to the gel (soluble-phase or solid-phase components after mixing with soluble-phase components and washing). Gardner-Altman estimation plot of normalized Cdc42-bound Par complex (Par-6 or aPKC) band intensity in the absence and presence of Par-3. The results of each replicate (filled circles) are plotted on the left and the mean difference is plotted on the right as a bootstrap sampling distribution (shaded region) with a 95% confidence interval (black error bar). C, Effect of Cdc42 on the interaction between Par-3 and the Par complex. Solid-phase (amylose resin)-bound maltose-bound protein (MBP)-fused Par-3 PDZ1-APM incubated with Par complex and/or increasing concentrations of Cdc42Q61L. Labeling as described in (B). Gardner-Altman estimation plot of normalized Par-3-bound Par complex (Par-6 or aPKC) band intensity in the absence and presence of Cdc42Q61L. The results of each replicate (filled circles) are plotted on the left and the mean difference is plotted on the right as a bootstrap sampling distribution (shaded region) with a 95% confidence interval (black error bar).



another to regulate the formation of these complexes. Here we have used a biochemical reconstitution approach with purified components to determine the elements sufficient for Par complex switching between Par-3 and Cdc42. The results provide the mechanistic framework for understanding how the Par complex transitions from Par-3 to Cdc42 to form two distinct complexes.

RESULTS

Par-3 and Cdc42 bind with negative cooperativity to the Par complex

Although Par-3 and Cdc42 are thought to form mutually exclusive complexes with the Par complex in vivo, they have been shown to bind simultaneously in a co-immunoprecipitation

experiment using cell extracts (Joberty et al., 2000). We examined whether Par-3 and Cdc42 influence one another's binding to the Par complex using a reconstitution system. We performed a qualitative affinity chromatography (pull-down) assay with purified Par complex and Par-3 PDZ1-APM (a fragment containing all known interaction motifs between Par-3 and Par-6/aPKC) and GST-fused Cdc42Q61L (constitutively active). The binding buffer included ATP to ensure that the aPKC kinase domain did not form a stalled complex with its phosphorylation site on Par-3.

We formed a complex of Cdc42-bound Par-6/aPKC by placing GST-Cdc42Q61L on the solid phase and incubating with soluble, purified Par complex. We assessed the effect of Par-3 on the Cdc42-bound Par complex by adding increasing concentrations of Par-3 PDZ1-APM. If Par-3 binding to the Par complex had no effect on Cdc42 binding, or the proteins bound with positive cooperativity, we expected that Par-3 would become part of the solid phase complex and the amount of Par complex adhered to the solid phase would stay the same or increase. Alternately, if the Cdc42 and Par-3 binding sites exhibited negative cooperativity, either via direct steric occlusion or an allosteric mechanism, little or no Par-3 would be part of the Cdc42-bound solid phase complex, and the amount of Par complex on the solid phase would decrease (as the affinity of the Par complex for Cdc42 was reduced by binding to Par-3). We observed that addition of Par-3 significantly reduced the amount of Par complex associated with solid phase Cdc42Q61L (Fig. 16B). Furthermore, little or no additional Par-3 appeared in the solid phase relative to a GST control. Our results indicate that in the context of these four proteins, Cdc42 and Par-3 bind with negative cooperativity to Par-6/aPKC.

In a system with two distinct binding sites coupled to one another via negative cooperativity, each protein should reduce the affinity of the Par complex for the other. However, the effect of Cdc42 on Par-3 binding to the Par complex is complicated by the many potential Par-3 binding sites on the Par complex (Fig. 16A). In principle, not all Par-3 binding sites could be coupled to Cdc42 binding, a scenario in which addition of Cdc42 to solid phase Par-3-bound Par complex might not significantly alter the amount of solid phase Par complex. To determine if Cdc42 influences Par-3-bound Par complex, we adsorbed Par complex bound to MBP-Par-3 PDZ1-APM to the solid phase and examined the effect of increasing concentrations of Cdc42Q61L. We observed that addition of Cdc42 reduced the amount of Par complex associated with solid phase Par-3 and Cdc42 was not significantly incorporated into the solid phase (Fig.

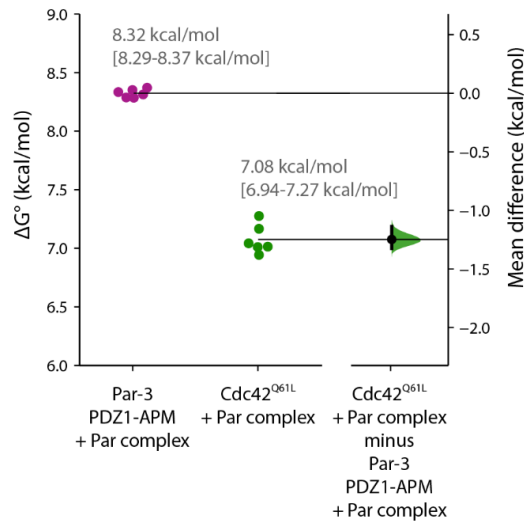
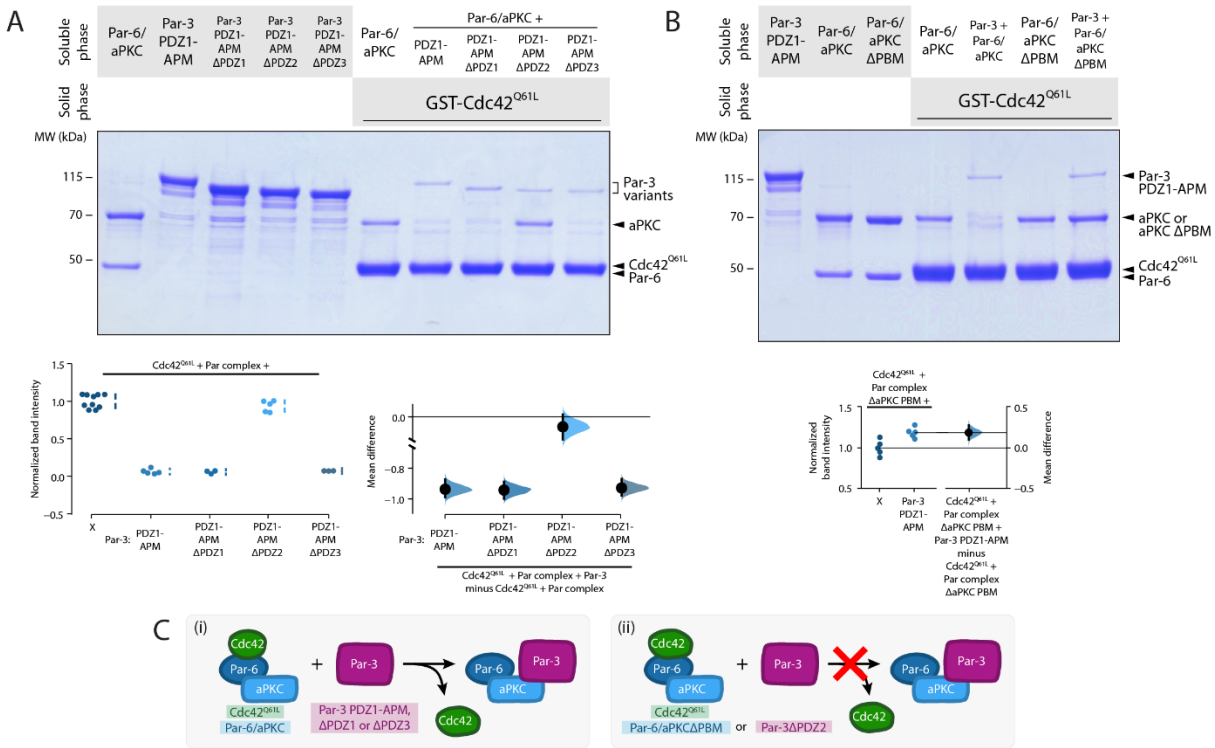


Figure 17. Par-3 binds to the Par complex with a greater affinity than Cdc42 in a supernatant depletion assay. Gardner-Altman estimation plot of Par-3 PDZ1-APM/Par complex and Cdc42Q61L/Par complex binding affinities measured using a supernatant depletion assay. The results of each replicate (filled circles) are plotted on the left and the mean difference is plotted on the right as a bootstrap sampling distribution (shaded region) with a 95% confidence interval (black error bar).

16C). Displacement of Par complex from Par-3 required a significantly higher concentration of Cdc42 than we observed for Par-3 displacement of Cdc42-bound complex.

Our results indicate that Par-3 and Cdc42 compete for binding to the Par complex (i.e. negative cooperativity) and that a quaternary complex does not form at levels detectable in our assay. Our results may differ from previous studies using cell extracts because aPKC's kinase domain is known to form stalled complexes with substrates like Par-3 when ATP is not available to complete the catalytic cycle (forming a persistent interaction rather than a transient interaction) (Holly et al., 2020; Holly and Prehoda, 2019). Additionally, other cellular factors could potentially allow Par-3 and Cdc42 to bind to the Par complex simultaneously. In terms of understanding how the Par complex might transition from Par-3 to Cdc42, our results demonstrate that no other proteins are required—Par-3 and Cdc42 alone are sufficient to form mutually exclusive complexes with the Par complex.

Figure 18 (next page). The Par-3 PDZ2 interaction with the aPKC PBM is required to displace Cdc42 from the Par complex. A, Effect of removing individual Par-3 PDZ domains in the context of PDZ1-APM on the displacement of Cdc42 from the Par complex. Solid-phase (glutathione resin)-bound glutathione S-transferase (GST)-fused Cdc42Q61L incubated with Par complex and/or Par-3 PDZ1-APM, Δ PDZ1, Δ PDZ2, or Δ PDZ3. Shaded regions indicate the fraction applied to the gel (soluble-phase or solid-phase components after mixing with soluble-phase components and washing). Cumming estimation plot of normalized Cdc42-bound Par complex (Par-6 or aPKC) band intensity in the absence and presence of Par-3 variants. The result of each replicate (filled circles) along with the mean and standard deviation (gap and bars next to circles) are plotted on the left and the mean differences are plotted on the right as a bootstrap sampling distribution (shaded region) with a 95% confidence interval (black error bar). Replicates not included in the plot (<5 circles) had a band intensity that was not detectable. B, Effect of removing the aPKC PBM in the context of the intact Par complex on Par-3's ability to displace Cdc42 from the Par complex. GST-fused Cdc42Q61L incubated with Par complex or Par complex Δ aPKC PBM and/or Par-3 PDZ1-APM. Labeling as described in (A). Gardner-Altman estimation plot of normalized Cdc42-bound Par complex Δ aPKC PBM (Par-6 or aPKC) band intensity in the absence and presence of Par-3. The results of each replicate (filled circles) are plotted on the left and the mean difference is plotted on the right as a bootstrap sampling distribution (shaded region) with a 95% confidence interval (black error bar). C, Summary of Cdc42, Par-3, Par-6/aPKC elements that are necessary for negative cooperativity between Par-3 and Cdc42 for the Par complex.



Par-3 may bind the Par complex with higher affinity than Cdc42

Our results indicate that Par-3 is more effective at displacing Cdc42 from the Par complex than Par-3 is at displacing Cdc42. The asymmetry in Par complex displacement could be explained by a higher affinity of Par-3 for the Par complex compared to Cdc42. The affinity of Par-3 PDZ1-APM for the Par complex is known (Penkert et al., 2022), but while Cdc42's affinity for the Par-6 CRIB-PDZ fragment has been reported (Garrard et al., 2003), its affinity for the full Par complex has been unknown. To understand why Par-3 is more effective at displacing Cdc42 from the Par complex, we measured binding affinities for the Par complex using a supernatant depletion assay (Pollard, 2010). Similar to a previous report using the same assay (Penkert et al., 2022), we found that Par-3 PDZ1-APM binds the Par complex with high affinity (Fig. 17; Kd of 0.6 μ M or ΔG° of 8.3 kcal/mol). We measured a substantially weaker affinity of

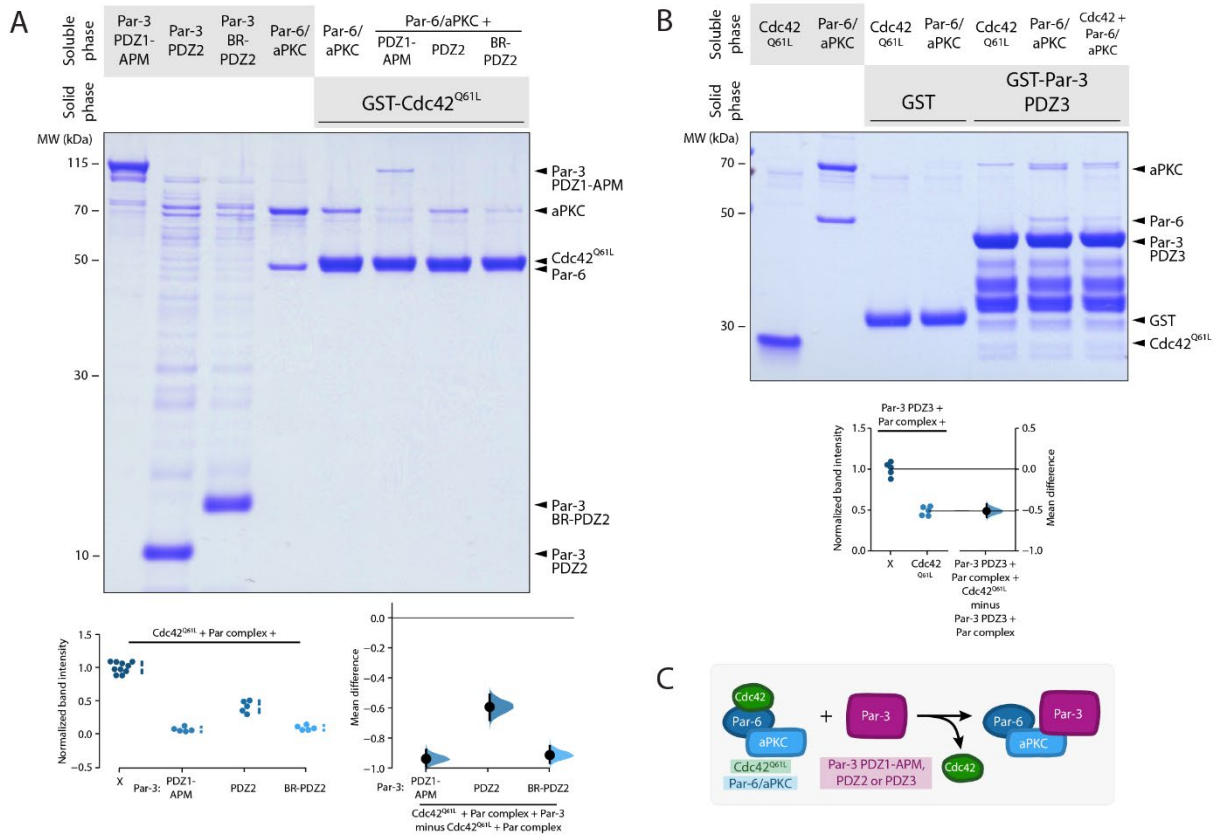
Cdc42 (using the Q61L constitutively active variant) for the Par complex (Fig. 17; K_d of 5.4 μM or ΔG° of 7.1 kcal/mol). This affinity is significantly lower than a previous report of 0.05 μM for Cdc42 binding to the Par-6 CRIB-PDZ fragment using a FRET-based assay (Garrard et al., 2003). To determine if the source of the difference is Cdc42 binding to a Par-6 fragment versus the full Par complex, we measured the Cdc42 interaction with Par-6 CRIB-PDZ with the supernatant depletion (Fig. S1). While the resulting affinity of 2.3 μM is slightly higher than that for the full Par complex, it remains substantially weaker than the FRET-based value (which is a higher affinity than the Par-3 interaction with the Par complex). We are unsure of the source of this discrepancy and, while our results suggest that Par-3 displaces Cdc42 from the Par complex more efficiently because of an intrinsic difference in affinity, it is possible that there is another source for this phenomenon.

The Par-3 PDZ2–aPKC Kinase-PBM interaction mediates the displacement of Cdc42 from the Par complex

Given that Par-3 and Cdc42 bind with negative cooperativity to Par-6/aPKC, we sought to identify the binding sites on the Par complex that are coupled. While the interaction between Cdc42 and Par-6 semi-CRIB is well established, several interactions between Par-3 and the Par complex have been identified (Fig. 16A) (Garrard et al., 2003; Holly et al., 2020; Izumi et al., 1998; Joberty et al., 2000; J. Li et al., 2010; Lin et al., 2000; Noda et al., 2001; Penkert et al., 2022; Qiu et al., 2000; Renschler et al., 2018; Wodarz et al., 2000). We excluded the interaction of the aPKC kinase domain with its phosphorylation site on Par-3 (i.e. the Par-3 APM) because the interaction is transient in the presence of ATP, as expected for an enzyme-substrate interaction (Holly et al., 2020; Holly and Prehoda, 2019). Given that each Par-3 PDZ domain

reportedly interacts with either Par-6 or aPKC, more than one interaction between Par-3 and the Par complex could be involved in displacement of Cdc42 from the Par complex. However, if only one of the interactions between Par-3 and the Par complex displaces Cdc42 from the Par complex, deletion of the required Par-3 element would eliminate Par-3's negative cooperativity with Cdc42 for the Par complex. Alternately, removal of more than one Par-3 element might be necessary to eliminate displacement of Cdc42 from the Par complex by Par-3. To distinguish between these possibilities, we generated deletions of individual Par-3 PDZ domains in the context of the PDZ1-APM fragment and tested which Par-3 elements are involved in displacing Cdc42 from the Par complex. We examined the effect of Par-3 PDZ1-APM, Δ PDZ1, Δ PDZ2, or Δ PDZ3 on Cdc42-bound Par complex. We did not detect an effect of removing PDZ1 or PDZ3 on Par-3's ability to displace Cdc42 from the Par complex (Fig. 18A). In contrast, deletion of Par-3 PDZ2 eliminated displacement of Cdc42 such that the amount of Par complex associated with solid phase Cdc42 did not change upon addition of Par-3 PDZ1-APM Δ PDZ2 (Fig. 18A).

Figure 19 (next page). Par-3 PDZ2 and PDZ3 are sufficient for displacement of Cdc42 from the Par complex. A, Effect of Par-3 elements on the interaction between Cdc42 and the Par complex. Solid-phase (glutathione resin)-bound glutathione S-transferase (GST)-fused Cdc42Q61L incubated with Par complex and/or Par-3 PDZ1-APM, PDZ2, or BR-PDZ2. Shaded regions indicate the fraction applied to the gel (soluble-phase or solid-phase components after mixing with soluble-phase components and washing). Cumming estimation plot of normalized Cdc42-bound Par complex (Par-6 or aPKC) band intensity in the absence and presence of Par-3 variants. The result of each replicate (filled circles) along with the mean and standard deviation (gap and bars next to circles) are plotted on the left and the mean differences are plotted on the right as a bootstrap sampling distribution (shaded region) with a 95% confidence interval (black error bar). B, Effect of Cdc42 on the interaction between Par-3 PDZ3 and the Par complex. GST-fused Par-3 PDZ3 incubated with Par complex and/or Cdc42Q61L. Labeling as described in (A). Gardner-Altman estimation plot of normalized Par-3-bound Par complex (Par-6 or aPKC) band intensity in the absence and presence of Cdc42Q61L. The results of each replicate (filled circles) are plotted on the left and the mean difference is plotted on the right as a bootstrap sampling distribution (shaded region) with a 95% confidence interval (black error bar). C, Summary of Cdc42, Par-3, Par-6/aPKC elements that are sufficient for negative cooperativity between Par-3 and Cdc42 for the Par complex.



Our results indicate that neither Par-3 PDZ1 or PDZ3 are required for negative cooperativity with Cdc42 for the Par complex and that displacement of Cdc42 from the Par complex by Par-3 is dependent on the PDZ2 domain.

We recently discovered that Par-3 PDZ2 and PDZ3 interact with aPKC Kinase Domain-PBM (KD-PBM) module (Penkert et al., 2022). Given that Par-3 PDZ2 is required to displace Cdc42 from the Par complex, we examined whether the aPKC PBM was also required for this activity. We found that removing the aPKC PBM (Par-6/aPKC Δ PBM) prevented Par-3 from displacing Cdc42 from the Par complex (Fig. 18B). Our results indicate that Par-3 PDZ2 and aPKC PBM are necessary for Par-3 to disrupt the Cdc42–Par complex interaction (Fig. 18C).

Par-3 BR-PDZ2 and PDZ3 displace Cdc42 from the Par complex

Given the requirement of the aPKC KD-PBM for Par-3's ability to displace Cdc42 from the Par complex, we examined whether the Par-3 domains that bind the KD-PBM (PDZ2 and PDZ3) were each sufficient for this activity. We recently discovered a conserved basic region (BR) at the N-terminal end of Par-3 PDZ2 that increases PDZ2's affinity for the Par complex, so we also examined the effect of Par-3 BR-PDZ2 (Penkert et al., 2022). We found that PDZ2 alone was sufficient to displace Cdc42 from the Par complex but was not as effective as PDZ1-APM such that some Par complex remained bound to solid phase Cdc42 (Fig. 19A). In contrast, BR-PDZ2 displaced Cdc42 to a similar extent as PDZ1-APM and resulted in little to no Par complex associated with solid phase Cdc42 (Fig. 19A). We conclude that Par-3 BR-PDZ2 can sufficiently displace Cdc42 from the Par complex.

Like Par-3 PDZ2, Par-3 PDZ3 was found to interact with the Par complex utilizing a similar binding mode. Thus, we also tested the ability of Par-3 PDZ3 to displace Cdc42 from the Par complex. Given that Par-3 PDZ3 has a weak binding affinity for the Par complex (K_d of 78.9 μ M) (Penkert et al., 2022), we were unable to detect any significant change in the amount of Par complex bound to solid phase Cdc42 (data not shown). Therefore, we instead formed a Par-3 PDZ3-bound Par complex utilizing GST-Par-3 PDZ3 on the solid phase and soluble Par complex and examined the effect of Cdc42Q61L. We observed that addition of Cdc42 resulted in a reduction in the amount of Par complex bound to solid phase Par-3 PDZ3 indicating that Cdc42 is sufficient to displace PDZ3 from the Par complex (Fig. 19B). Thus, our finding that Par-3 PDZ1-APM Δ PDZ2 cannot displace Cdc42 (Fig. 18A) likely arises from the low binding affinity of PDZ3 for the Par complex compared to BR-PDZ2. Altogether, our results indicate that the

Par-3 BR-PDZ2 and PDZ3—aPKC kinase domain-PBM (predominantly through BR-PDZ2) interactions negatively cooperate with the Cdc42—Par-6 CRIB-PDZ interaction (Fig. 19C, 20A).

DISCUSSION

We examined how the Par complex transitions from Par-3- to Cdc42-bound states, a step that is thought to be critical for forming the Par cortical domain. In this model, the large size of oligomerized Par-3 couples the Par complex to actomyosin-driven directional cortical flows that transport the complex to its active domain (Dickinson et al., 2017; Rodriguez et al., 2017; Wang et al., 2017). Once in this membrane region, the complex dissociates from Par-3 and binds Cdc42, allowing it to remain on the cortex and become activated. While the transition from Par-3

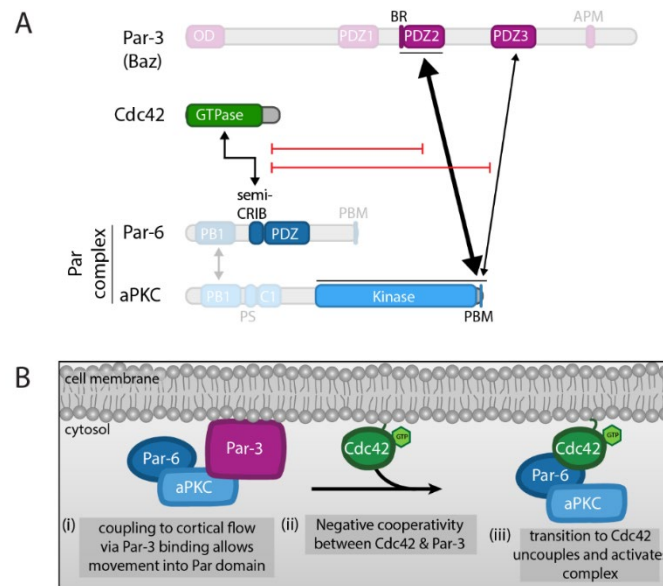


Figure 20. Model for transition from Par-3- to Cdc42-bound Par complex. A, Domain architecture demonstrating the interactions between Par-3, Cdc42, and the Par complex that are sufficient for regulating the transition between a Par-3- and Cdc42-bound Par complex. B, Model for polarization of the Par complex through the formation of distinct Par-3- and Cdc42-bound complexes. (i) Par-3-bound Par complex is coupled to cortical flow, allowing it to move towards the Par domain, (ii) active Cdc42 binds to Par-6 and inhibits the Par-3 BR-PDZ2/PDZ3—aPKC kinase-PBM interaction, resulting in the displacement of Par-3 from the Par complex and the formation of a Cdc42-bound Par complex, (iii) Cdc42-bound Par complex is polarized and active.

to Cdc42 is central to this model, little has been known about how switching between binding of each regulator occurs. We used a biochemical reconstitution approach to understand the mechanism of regulator switching, with the goal of identifying the minimal set of components required for the transition. A previous study that used co-immunoprecipitation from cultured cell extracts concluded that Cdc42 and Par-3 can bind simultaneously to the Par complex, suggesting that other cellular components are required (Joberty et al., 2000). For example, mechanical separation of the complexes by actomyosin-generated contraction has been proposed as one possibility (Dickinson et al., 2017; Rodriguez et al., 2017; Wang et al., 2017). Using purified components, we found that external factors are not required as Cdc42 and Par-3 bind to the Par complex with strong negative cooperativity (Fig. 20B). In this section, we examine the implications of our findings and speculate on key outstanding issues that remain in understanding this critical step in Par-mediated polarity.

How can the strong negative cooperativity between Cdc42 and Par-3 binding to the Par complex that we observed be reconciled with the previous observation of a quaternary complex? There are several possible explanations. First, it does not appear that ATP was included in the previous binding experiment, perhaps because it was not clear that Par-3 is an aPKC substrate at the time. We have found that the phosphorylation site on Par-3 can form a stalled complex with the aPKC kinase domain when ATP is not present (Holly et al., 2020; Holly and Prehoda, 2019). Alternately, since the experiment was performed in extracts, it's possible that additional factors were present that inhibit negative cooperativity, allowing Cdc42 and Par-3 to bind simultaneously. Finally, the presence of negative cooperativity does not necessarily preclude formation of a quaternary complex, albeit at reduced levels.

The nature of the Par complex interaction with Par-3 has been enigmatic because many distinct interactions have been reported (Garrard et al., 2003; Holly et al., 2020; Izumi et al., 1998; Joberty et al., 2000; J. Li et al., 2010; Lin et al., 2000; Noda et al., 2001; Penkert et al., 2022; Qiu et al., 2000; Renschler et al., 2018; Wodarz et al., 2000). We examined which Par-3 interactions are coupled to Cdc42 binding and found that only one involving the aPKC kinase domain and PDZ binding motif (KD-PBM) is affected by Cdc42. This site binds with highest affinity to Par-3's BR-PDZ2 domain but with weaker affinity to PDZ3 (Penkert et al., 2022). Our results are consistent with the reported relative affinities – BR-PDZ2 most effectively reduces Cdc42 binding to the Par complex. We found that binding to the aPKC KD-PBM is both necessary and sufficient to displace Cdc42, and that Cdc42 can nearly completely displace Par-3 PDZ1-APM from the Par complex. These results indicate that the other reported interactions of Par-3 with the Par complex are not likely to be relevant to this step of Par-mediated cell polarity.

A central consequence of our findings for Par complex function is that the transition from Par-3-bound to Cdc42-bound Par complex does not require additional factors. Thus, the presence of Cdc42 alone could be sufficient for the transition to take place. However, our results do not preclude the possibility that other factors assist in complex switching. As we found that the affinity of Cdc42 for the Par complex may be lower than that of Par-3, a higher concentration of Cdc42 could be required to achieve the same amount of Cdc42-bound complex. It is possible that the amount of Cdc42-bound complex does not need to be in excess of Par-3-bound complex, or that the concentration of active Cdc42 is higher than Par-3. Alternately, other factors could influence the affinity of Cdc42 with the Par complex – ligands of the Par-6 PDZ domain have been found to be coupled to Cdc42 binding, for example (Peterson et al., 2004; Whitney et al., 2016).

How might the Cdc42 and Par-3 binding sites be coupled? The strongest negative cooperativity arises from a steric mechanism, where the binding sites would require steric overlap for Cdc42 and Par-3 to bind simultaneously. Alternately, in an allosteric mechanism binding is coupled to changes in structure or dynamics that reduce the affinity for the other regulator. While the binding site for Cdc42 is on Par-6 (semi-CRIB) and Par-3's binding site is on aPKC (KD-PBM), little is known about the structural arrangement of the domains within the Par complex. Thus, it is formally possible that the semi-CRIB and KD-PBM are near one another, and it has been speculated that the PDZ domain adjacent to the semi-CRIB interacts with the KD-PBM (Dong et al., 2020). However, it is also clear that the Par complex is highly allosteric, as aPKC is autoinhibited from an intramolecular interaction between its pseudosubstrate and the kinase domain, and that Par-6 partially disrupts this interaction (Graybill et al., 2012). Additional biochemical and structural information will be required to uncover the mechanism of energetic coupling between Cdc42 and Par-3 binding to the Par complex.

EXPERIMENTAL PROCEDURES

Protein Expression

Bacterial cells

Plasmids were transformed into BL21-DE3 cells, aliquoted onto LB + AMP plates, and grown at 37°C for 18 hours. Colonies were picked to inoculate 100 mL LB + AMP starter cultures and grown at 37°C for 2-3 hours until an OD600 of 0.4-1.0 was reached. Starter cultures were then diluted into 2 L LB + AMP, grown at 37°C to an OD600 of 0.8-1.0, and induced with 500 μ M IPTG for 3 hours. Cultures were centrifuged at 5,000 RPM for 15-20 minutes and pellets were resuspended in nickel lysis buffer (50 mM NaH₃PO₄, 300 mM NaCl, 10 mM

Imidazole, pH 8.0), GST lysis buffer (IX PBS, 1 mM DTT, pH 7.5), or maltose lysis buffer (20 mM Tris, 200 mM NaCl, 1 mM EDTA, 1 mM DTT, pH 7.5). Resuspended pellets were then frozen in liquid N₂ and stored at -80°C.

Mammalian Cells

Par-6 and aPKC plasmids were co-expressed in FreeStyle 293-F cells as previously described (Graybill et al., 2012; Holly et al., 2020; Penkert et al., 2022). Briefly, cells were grown in FreeStyle 293 expression media in shaker flasks at 37°C with 8% CO₂ and transfected with either 293fectin or ExpiFectamine (see Manufacturer's protocol for more details). After 48 hours, cells were centrifuged 1-2x at 500 g for 3 minutes and cell pellets were resuspended in nickel lysis buffer (50 mM NaH₃PO₄, 300 mM NaCl, 10 mM Imidazole, pH 8.0). Resuspended pellets were then frozen in liquid N₂ and stored at -80°C.

Protein Purification

Bacterial cells

Resuspended pellets were thawed and then lysed by probe sonication at 70% amplitude, 0.3 seconds/0.7 seconds on/off pulse rate, 3x 1 minute. To pellet cellular debris, lysates were centrifuged at 15,000 RPM for 20 minutes. Lysates for GST-Cdc42Q61L and GST-Par-3 PDZ3 were aliquoted, frozen in liquid N₂ and stored at -80°C. For all other proteins, lysates were incubated with resin (amylose for most MBP-fused proteins and cobalt or nickel resin for His-fused proteins; MBP-Par-3 PDZ1-APM-His was His-purified) for 30-60 minutes at 4°C with mixing. Protein-bound resin was washed 3x with nickel lysis buffer (50 mM NaH₃PO₄, 300 mM NaCl, 10 mM Imidazole, pH 8.0) or maltose lysis buffer (20 mM Tris, 200 mM NaCl, 1 mM

EDTA, 1 mM DTT, pH 7.5) and then eluted in 0.5-1.8 mL fractions with nickel elution buffer (50 mM NH₃PO₄, 300 mM NaCl, 300 mM Imidazole, pH 8.0) or maltose elution buffer (maltose lysis buffer, 10 mM Maltose). Protein-containing fractions were pooled and buffer exchanged into 20 mM HEPES, pH 7.5, 100 mM NaCl, and 1 mM DTT using a PD10 desalting column. Protein was then concentrated using a Vivaspin 20 centrifugal concentrator, aliquoted, frozen in liquid N₂, and stored at -80°C.

Mammalian cells

Resuspended 293F pellets were thawed, lysed by probe sonication at 70% amplitude, 0.3 seconds/0.7 seconds on/off pulse rate, 4x 1 minute, and centrifuged at 15,000 RPM for 20 minutes. Lysates were incubated with resin (cobalt or nickel resin) for 30-60 minutes at 4°C with mixing. Protein-bound resin was washed 3x with nickel lysis buffer (50 mM NaH₃PO₄, 300 mM NaCl, 10 mM Imidazole, pH 8.0), with the first and second washes containing 100 μM ATP and 5 mM MgCl₂. Protein was eluted in 0.5-0.6 mL fractions with nickel elution buffer (50 mM NH₃PO₄, 300 mM NaCl, 300 mM Imidazole, pH 8.0) and protein-containing fractions were then pooled together. Protein was buffer exchanged into 20 mM Tris, pH 7.5, 100 mM NaCl, 1 mM DTT, 100 μM ATP, and 5 mM MgCl₂ using a PD10 desalting column and then purified by anion exchange chromatography using an AKTA FPLC protein purification system. Protein was filtered, injected into a Source Q column, and eluted with a salt gradient of 100-500 mM NaCl. Par complex-containing fractions were pooled and buffer exchanged into 20 mM HEPES, pH 7.5, 100 mM NaCl, 1 mM DTT, 100 μM ATP, and 5 mM MgCl₂ using a PD10 desalting column. Protein was then concentrated using a Vivaspin 20 centrifugal concentrator, aliquoted, frozen in liquid N₂, and stored at -80°C.

Qualitative Binding Assay (Affinity Chromatography)

Bacterial lysates were incubated with resin (glutathione or amylose) for 30 minutes at 4°C and washed 4x with binding buffer (20 mM HEPES pH 7.5, 100 mM NaCl, 5 mM MgCl₂, 0.5% Tween-20, 1 mM DTT, and 200 μM ATP). Soluble proteins were added to protein-labeled resin and incubated at room temperature with rotational mixing (incubation times of 10 minutes for MBP-Par-3 PDZ1-APM and 60 minutes for GST-fused proteins). Resin was washed 2-3x with binding buffer and proteins were eluted with 4X LDS sample buffer. Samples were run on a 12% Bis-Tris gel and stained with Coomassie Brilliant Blue R-250. Band intensities were quantified using ImageJ (v1.53a). The normalized band intensity was determined by first obtaining the mean of Par complex (either Par-6 or aPKC) band intensities (in the presence of no other soluble protein) and then dividing each band intensity value by that mean. All data was analyzed using Microsoft Excel (v16.53), GraphPad Prism (v9.2), and DABEST (Ho et al., 2019).

Quantitative Binding Assay (Supernatant Depletion)

Bacterial lysates were incubated with resin (glutathione or amylose) for 30 minutes at 4°C and washed 6x (3x quick washes, 3x 5 minutes washes) with binding buffer (20 mM HEPES pH 7.5, 100 mM NaCl, 5 mM MgCl₂, 0.5% Tween-20, 1 mM DTT, and 200 μM ATP). Two-fold serial dilutions of protein-bound resin were prepared with unlabeled resin as previously described (Holly et al., 2020; Penkert et al., 2022). Soluble protein (“receptor” or R) was added to protein-bound resin (“ligand” or L) and incubated at room temperature with rotational mixing (incubation times of 10 minutes for MBP-Par-3 PDZ1-APM and 60 minutes for GST-

Cdc42^{Q61L}). Samples containing only unlabeled resin and soluble protein were used as a negative control for binding. After incubation, samples were centrifuged, and an aliquot of the supernatant was collected and diluted in 4X LDS sample buffer. Samples were then run on a 12% Bis-Tris gel and stained with Coomassie Brilliant Blue R-250. Solid phase protein concentration was verified using a standard curve generated with known concentrations of a protein standard. All band intensities were quantified using ImageJ (v1.53a). The fraction of soluble phase protein (R) bound to solid phase protein (L) at a specific concentration of L ([L] = x) was determined with the following equation:

$$\text{Fraction bound } (F_b)_{[L]=x} = 1 - \frac{R \text{ band intensity}_{[L]=x}}{R \text{ band intensity}_{[L]=0}}$$

We then determined the dilution at which L resulted in 30-60% depletion ($F_b = 0.3-0.6$) and repeated the assay at this dilution in sextuplicate. Using F_b , we determined the binding equilibrium dissociation constant (K_d) with the following equation:

$$K_d = \frac{[L][R]}{[LR]}$$

where [L] and [R] are the concentrations of free L and R at equilibrium and [LR] is the concentration of L bound to R.

$$K_d = \frac{([L]_{total} - [LR])([R]_{total} - [LR])}{[LR]}$$

$$K_d = \frac{([L]_{total} - F_b[R]_{total})([R]_{total} - F_b[R]_{total})}{F_b[R]_{total}}$$

We also used the equation for the standard Gibbs free energy exchange to determine the binding energy of these interactions:

$$\Delta G^\circ = -RT \ln [K_d]$$

All data was analyzed using Microsoft Excel (v16.53), GraphPad Prism (v9.2), and DABEST (Ho et al., 2019).

Key Resources Table 3

Reagent or Resource type	Reagent or Resource	Source	Identifier	Additional Information
Recombinant Protein	MBP-Par-3 PDZ1-APM	PMID: 32084408		Expressed in BL21 cells from pMAL Par-3 309-987-His; His-purified; <i>Drosophila melanogaster</i> protein
Recombinant Protein	MBP-Par-3 PDZ1-APM Δ PDZ1	This paper		Cloned by Q5 site-directed mutagenesis; expressed in BL21 cells from pMAL Par-3 393-987-His; His-purified; <i>Drosophila melanogaster</i> protein
Recombinant Protein	MBP-Par-3 PDZ1-APM Δ PDZ2	PMID: 35787373		Expressed in BL21 cells from pMAL Par-3 309-987 Δ 437-533-His; His-purified; <i>Drosophila melanogaster</i> protein
Recombinant Protein	MBP-Par-3 PDZ1-APM Δ PDZ3	This paper		Cloned by Q5 site-directed mutagenesis; expressed in BL21 cells from pMAL Par-3 309-987 Δ 616-741-His; His-purified; <i>Drosophila melanogaster</i> protein
Recombinant Protein	His-Par-3 PDZ2	PMID: 35787373		Expressed in BL21 cells from pET19 Par-3 444-533; His-purified; <i>Drosophila melanogaster</i> protein

Recombinant Protein	His-Par-3 BR-PDZ2	PMID: 35787373		Expressed in BL21 cells from pET19 Par-3 426-533; His-purified; <i>Drosophila melanogaster</i> protein
Recombinant Protein	GST-Par-3 PDZ3	PMID: 35787373		Expressed in BL21 cells from pGEX Par-3 616-741; <i>Drosophila melanogaster</i> protein
Recombinant Protein	His-Cdc42 ^{Q61L}	This paper		Cloned by traditional methods; expressed in BL21 cells from pBH Cdc42 1-191 Q61L; His-purified; <i>Drosophila melanogaster</i> protein
Recombinant Protein	GST-Cdc42 ^{Q61L}	This paper		Cloned by traditional methods; expressed in BL21 cells from pGEX Cdc42 1-191 Q61L; <i>Drosophila melanogaster</i> protein
Recombinant Protein	Par complex	PMID: 32084408		Expressed in 293F cells from pCMV His Par-6 1-351 and pCMV aPKC 1-606; His-purified; <i>Drosophila melanogaster</i> proteins
Recombinant Protein	Par complex Δ aPKC PBM	PMID: 32084408		Expressed in 293F cells from pCMV His Par-6 1-351 and pCMV aPKC 1-600; His-purified; <i>Drosophila melanogaster</i> proteins
Recombinant Protein	GST-Par-6 CRIB-PDZ	This paper		Cloned by Gibson assembly; expressed in BL21 cells from pGEX Par-6 130-256; <i>Drosophila melanogaster</i> protein

Recombinant Protein	His-Par-6 CRIB-PDZ	This paper		Cloned by traditional methods; expressed in BL21 cells from pBH Par-6 130-255; His-purified; <i>Drosophila melanogaster</i> protein
Recombinant DNA	pCMV (mammalian expression plasmid)	ThermoFisher	10586014	
Recombinant DNA	pMAL c4X (bacterial expression plasmid)	Addgene	75288	
Recombinant DNA	pGEX 4T1 (bacterial expression plasmid)	Amersham	27458001	
Recombinant DNA	pBH (bacterial expression plasmid)	PMID: 15023337		
Recombinant DNA	pET19 (bacterial expression plasmid)	Millipore Sigma (Novagen)	69677	
Bacterial Strain	TG1			Molecular cloning
Bacterial Strain	BL21-DE3			Protein expression
Cell Line	FreeStyle 293-F	ThermoFisher	R79007	
Chemical	293fectin Transfection Reagent	ThermoFisher	12347019	
Chemical	ExpiFectamine 293 Transfection Kit	ThermoFisher	A14524	

Chemical	Freestyle 293 Expression Medium	ThermoFisher	12338018	
Chemical	Expi293 Expression Medium	ThermoFisher	A1435101	
Chemical	Opti-MEM	ThermoFisher	3198588	
Chemical	HisPur Cobalt Resin	ThermoFisher	89965	
Chemical	HisPur NiNTA Resin	ThermoFisher	88222	
Chemical	Amylose Resin	NEB	E8021L	
Chemical	Glutathione Resin	GoldBio	G250-100	
Chemical	Source 30Q Anion Exchange Resin	GE Healthcare	17-1275-01	
Chemical	4X BOLT LDS Sample Buffer	ThermoFisher	B0007	
Chemical	PageRuler Plus Prestained Protein Ladder, 10-250 kDa	ThermoFisher	26619	
Chemical	20X BOLT MES SDS Running Buffer	ThermoFisher	B0002	
Chemical	Coomassie Brilliant Blue R-250	GoldBio	C-461-5	
Chemical	Q5 Site-Directed Mutagenesis Kit	NEB	E0552S	

Chemical	Gibson Assembly Cloning Kit	NEB	E5510S	
Other	125 mL Erlenmeyer Flasks	VWR	89095-258	
Other	250 mL Erlenmeyer Flasks	VWR	89095-266	
Other	Bolt 12% Bis-Tris Gels	ThermoFisher	NW00125B OX	
Other	PD-10 Desalting Columns	VWR	95017-001	
Other	VivaSpin 20 MWCO 5kDa	Cytiva	28932359	
Other	VivaSpin 20 MWCO 10kDa	Cytiva	28932360	
Other	VivaSpin 20 MWCO 30kDa	Cytiva	28932361	
Software	ImageJ	NIH		https://imagej.nih.gov/ij/
Software	Prism	GraphPad Software		https://www.graphpad.com/
Software	Estimation Statistics BETA	PMID: 31217592		www.estimatedstats.com

BRIDGE TO CHAPTER V

In this chapter, we argue that Par-3 and Cdc42 compete for binding to the Par complex and that no other cellular components are required. Using qualitative binding assays and purified components, we argue that Par-3 and Cdc42 cannot bind to the Par complex simultaneously to form a quaternary complex. Through further analysis, we demonstrate that the Par-3 PDZ2 and

PDZ3—aPKC KD-PBM interactions negatively cooperate with the Cdc42—Par-6 CRIB-PDZ interaction. Our findings support the model that Par-3 and Cdc42 form mutually exclusive complexes with the Par complex to regulate cell polarity. In the following chapter, I summarize our key findings and discuss the implications of our work. Additionally, I discuss the outstanding questions that remain. Together, our findings have advanced the cell polarity field by identifying the molecular mechanisms by which aPKC is regulated.

CHAPTER V

SUMMARY AND DISCUSSION

SUMMARY

In Chapter I, I introduced the concept of animal cell polarity in numerous cellular processes that allow for proper animal development and homeostasis. I focused on polarity proteins, which have been well studied for over 30 years, and their role in various cell processes such as asymmetric cell division or cell migration. The key mediator of cell polarity is the kinase aPKC, which phosphorylates downstream proteins resulting in their displacement from the same domain and in their polarized localization (Bailey and Prehoda, 2015). As aPKC drives cell polarity, its localization and activity need to be tightly regulated in a spatially and temporally defined manner. aPKC is not only regulated through an autoinhibition mechanism, but through protein-protein interactions and protein-lipid interactions (Hong, 2018). I focused on the models that have been proposed on aPKC's regulation by Par-6, Par-3, and Cdc42. During polarity establishment, aPKC and Par-6 bind to form the Par complex (Joberty et al., 2000; Suzuki et al., 2001). Whether Par-6 activates or represses aPKC remains in question. However, Par-3 can now bind and recruit the Par complex. Although the exact interactions between Par-3 and the Par complex that contribute to the formation of this complex are unknown, Par-3 is required for Par complex membrane recruitment while maintaining aPKC in an inactive state (Dickinson et al., 2017; Rodriguez et al., 2017; Wang et al., 2017)). Prenylated Cdc42-GTP can also recruit the Par complex through binding to Par-6 (Garrard et al., 2003; Joberty et al., 2000; Lin et al., 2000; Noda et al., 2001; Qiu et al., 2000). It remains unclear whether the Par complex forms two ternary complexes: one bound to Par-3 and another bound to Cdc42, or whether they can form a

quaternary complex. However, unlike Par-3, the Cdc42-bound Par complex induces catalytic activity and allows aPKC to phosphorylate its substrate and regulate cell polarity (Atwood et al., 2007; Yamanaka et al., 2001). Although the information above points towards a defined model for Par-mediated polarity, conflicting observations have made it challenging to understand how aPKC is regulated through autoinhibition and through its intermolecular interactions with Par-6, Cdc42, and Par-3. It is clear that these four proteins significantly contribute to animal cell polarity, but current models lack the molecular details to understand the mechanism of regulation.

Chapter II was centered around Par-6's regulation of aPKC. While the interaction between the Par-6 and aPKC PB1 domains is well documented (Hirano et al., 2005; Noda et al., 2003), the effect that Par-6 has on aPKC activity is not well understood. One model suggests that Par-6 activates aPKC, removing autoinhibition by displacing the PS from the substrate binding pocket (Graybill et al., 2012). However, other evidence suggests that Par-6 represses aPKC (Dong et al., 2020; Yamanaka et al., 2001). Recently, it was reported that Par-6 binding displaces the PS from the substrate binding pocket, but the Par-6 CRIB-PDZ domains inhibit kinase domain and prevent activation (Dong et al., 2020). While both models agree that Par-6 displaces the PS, the effect of CRIB-PDZ is unknown. This chapter sought to resolve the effect of Par-6 on aPKC. Using a biochemical reconstitution approach with purified proteins, we determined that Par-6 CRIB-PDZ interacts with aPKC KD-PBM. We found that Par-6 CRIB-PDZ negatively cooperates with aPKC PB1-C1, suggesting that the CRIB-PDZ is necessary for relieving autoinhibition. Additionally, the CRIB-PDZ—aPKC KD-PBM interaction is regulated by Par-6 regulators, such as Cdc42, Crumbs, and Stardust. While this work does not touch on the activity

of aPKC when binding to Par-6, these findings provide us with a strong foundation to better grasp how Par-6 regulates aPKC activity.

Chapter III focused on the interaction between Par-3 and the Par complex. Numerous interactions have been reported between Par-3 and the Par complex, making it difficult to understand exactly how Par-3 regulates the Par complex (Holly et al., 2020; Izumi et al., 1998; Joberty et al., 2000; Lin et al., 2000; Penkert et al., 2022; Renschler et al., 2018; Wodarz et al., 2000). Not only that, but many of these interactions were examined without the intact Par complex and in a qualitative rather than quantitative manner. This chapter addressed which domains within Par-3, Par-6, and aPKC contribute to their overall binding energy. Utilizing a quantitative supernatant depletion assay with purified components, we determined that the strongest interaction contributing to the overall binding energy was between Par-3 BR-PDZ2 and PDZ3 and aPKC KD-PBM. These interactions almost fully recapitulated the binding affinity observed when using Par-3 PDZ1-APM and the full-length Par complex proteins. Our results indicated that Par-3 could potentially interact with two Par complexes at a time to efficiently recruit the Par complex to the membrane during cell polarity establishment. These findings provide new perspectives on the energetic determinants and the structural conformation of the Par-3-bound Par complex.

In Chapter IV, I discussed the mechanism of Par complex polarity and focused on the formation of Par-3- and Cdc42-bound Par complexes. While *in vivo* evidence supported a model in which the Par complex transitions from a Par-3 to Cdc42 bound Par complex, an *in vitro* study showed that Par-3 and Cdc42 could bind to the Par complex simultaneously to form a quaternary complex leading to a model whereby other cellular components would be required to displace Par-3 (Joberty et al., 2000). This chapter sought to determine the molecular details concerning

the transition from Par-3 to Cdc42 as this is a key step in Par-mediated polarity. Using a biochemical approach with purified components, we found that Par-3 and Cdc42 negatively cooperate for binding to the Par complex and that no other cellular components are required for this transition to occur. We further determined that the Par-3 BR-PDZ2 and PDZ3—aPKC KD-PBM interactions compete with the Cdc42—Par-6 CRIB-PDZ interaction. This work contributes to the mechanistic framework for understanding a key step in Par complex polarization and activity.

DISCUSSION

Throughout this dissertation, we addressed the current understanding for how aPKC is regulated by intermolecular interactions. Specifically, we utilized biochemical approaches and purified proteins to understand the molecular mechanisms that control aPKC. While this work provides new insights into aPKC regulation and closes some of the knowledge gaps, many questions remain.

Although we identified a new interaction between Par-6 CRIB-PDZ and aPKC KD-PBM, we have yet to understand how it regulates aPKC activity. There is evidence supporting the idea that Par-6 activates aPKC activity. While it appears that Par-6 PB1 slightly activates the autoinhibited full-length aPKC, the presence of the CRIB-PDZ domains further activated aPKC (Graybill et al., 2012). However, it is important to note that the full-length intact Par complex was not as active as the aPKC KD-PBM alone, suggesting that a mechanism of inhibition is still at work in this system. While aPKC KD-PBM may be more active than the Par complex, the “level” of activation that is required for aPKC’s ability to phosphorylate substrates is unclear. There is additional evidence that suggests the opposite form of regulation: Par-6 is an inhibitor of

aPKC activity. This model proposed Par-6 displaced the PS but that the C-terminal domains of Par-6 inhibited aPKC activity (Dong et al., 2020; Yamanaka et al., 2001). Furthermore, one of these studies concluded this inhibition was alleviated through binding of Crumbs to Par-6 (Dong et al., 2020). Although this study did not find that Cdc42, unlike Crumbs, activated Par-6, our result that the Par-6 CRIB-PDZ—aPKC KD-PBM interaction is regulated by Cdc42, Crumbs, and Stardust suggest that these Par-6 regulators aid in activating aPKC. However, it also remains possible that these Par-6 regulators displace Par-6 CRIB-PDZ from aPKC KD-PBM and subsequently give aPKC PS access to the substrate binding pocket to once again autoinhibit aPKC. It is clear that figuring out where exactly the PS is localized in the context of the Par complex and the Cdc42-bound Par complex is critical for establishing aPKC's activity when bound to these proteins.

While we identified the relative contributions of each of the reported interactions to the overall binding affinity between Par-3 and the Par complex, how these interactions regulate aPKC activity is unclear. Par-3 was largely considered to be an inhibitor of aPKC activity because the Par-3 APM (aPKC phosphorylation motif) was shown to prevent aPKC substrates from accessing the substrate binding pocket (Soriano et al., 2016). However, the experiment lacked ATP and therefore made a transient interaction appear as a persistent interaction. Further work demonstrated that in the presence of ATP, substrates were able to compete with Par-3 APM for the substrate binding pocket (Holly and Prehoda, 2019). The Par-3 APM—aPKC KD interaction has confused the field and made it difficult to understand exactly how Par-3 regulates aPKC localization and activity. Further analysis of Par-3 and the Par complex demonstrated that their binding is dependent on Par-3 PDZ2 and a newly identified PBM at the C-terminus of aPKC (Holly et al., 2020). Our result that Par-3 BR-PDZ2 and PDZ3 interact with aPKC PBM

with additional binding energy from aPKC KD support this finding. The observation that these Par-3 PDZ domains interact with aPKC KD-PBM brings up the question of whether these interactions are regulating aPKC's catalytic activity. In this case, the Par-3 PDZ domains would be blocking access to the substrate binding site. Details about the structure of the intact Par complex or the full-length proteins would significantly impact our comprehension of the conformation of these protein complexes.

Our finding that Par-3 and Cdc42 negatively cooperate for binding to the Par complex raises the question of what the exact mechanism of competition entails. It could be steric occlusion, where the Cdc42 and Par-3 binding sites overlap and make it impossible for them to bind simultaneously. On the other hand, it could be an allosteric mechanism where the Cdc42 and Par-3 binding sites are coupled to structural changes that reduce the binding affinity of the other regulator when one is bound. Structural studies are necessary to understand the conformational changes that occur to regulate the formation of these complexes. One of findings indicated that Cdc42 had a lower binding affinity for the Par complex than Par-3. This could suggest that other factors may be involved to aid Cdc42 in displacing Par-3 from the Par complex. It's well known that the Par-6 CRIB and PDZ domains are coupled, thus binding of Par-6 PDZ ligands could increase the affinity of Cdc42 for the Par complex, making it a better competitor (Peterson et al., 2004; Whitney et al., 2016, 2011).

CLOSING REMARKS

Prior to my contributions to the cell polarity field, current models lacked the molecular details to understand the mechanisms of aPKC regulation. I set out to address how aPKC is regulated through protein-protein interactions by specifically focusing on aPKC's well known

regulators: Par-6, Par-3, and Cdc42. I identified a novel interaction between aPKC KD-PBM and Par-6 CRIB-PDZ that may play a significant role in regulation of aPKC activity. Furthermore, I assisted in the determination of the energetic contributions of all of the reported Par-3 and Par complex interactions and found that most of the binding energy was contributed by binding of Par-3 BR-PDZ2 and PDZ3 to aPKC KD-PBM. Lastly, I found that Par-3 and Cdc42 negatively cooperate for binding to the Par complex. Overall, my dissertation provides essential mechanistic insights that enhance our comprehension of how aPKC is regulated for proper animal cell polarity.

APPENDIX

APPENDIX A: SUPPLEMENTAL MATERIAL FOR CHAPTER III

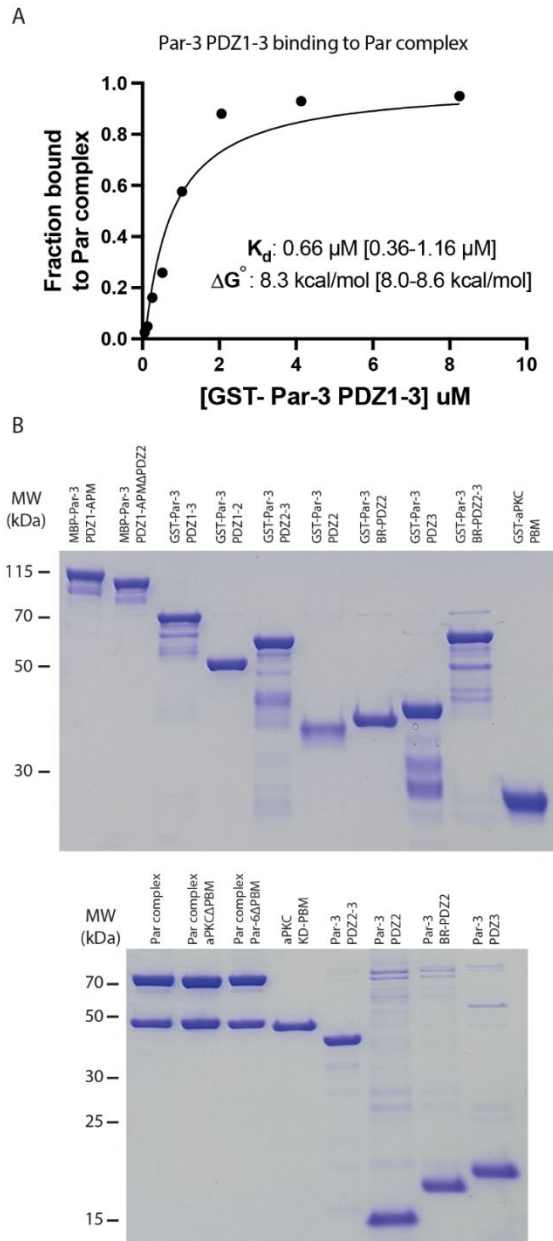


Figure S1 Supernatant depletion binding assay. (A) Dose response curve for binding of Par-3 PDZ1-3 to the Par complex. 95% confidence intervals are shown for best fit values. (B) Protein reagents used in this study.

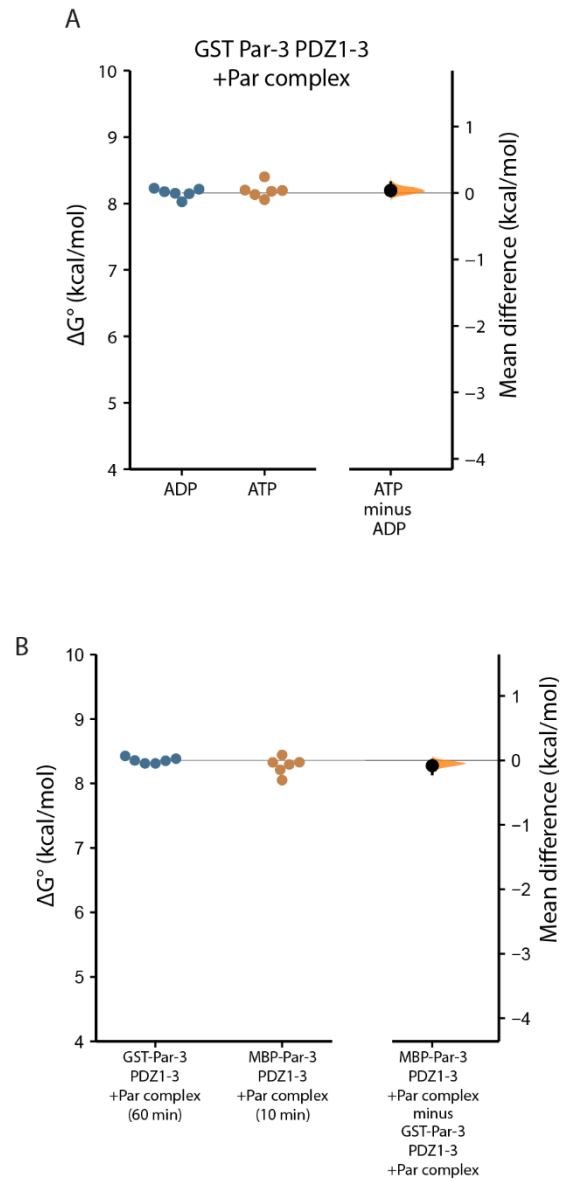


Figure S2 Supernatant depletion binding assay. (A) Effect of nucleotide state on binding of Par-3 PDZ1-3 to the Par complex. (B) Time dependence of binding energy measurement for Par-3 PDZ1-3 binding to the Par complex.

APPENDIX

APPENDIX B: SUPPLEMENTAL MATERIAL FOR CHAPTER IV

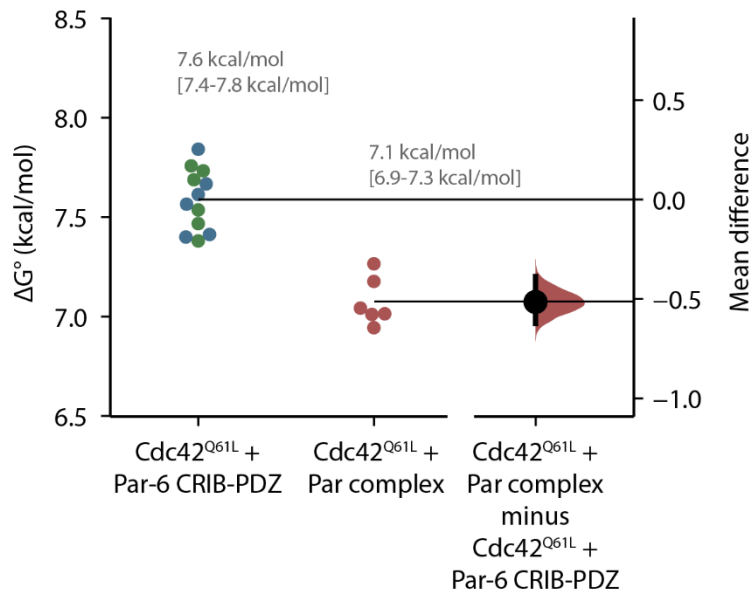


Figure S1 Cdc42Q61L binds with higher affinity to Par-6 CRIB-PDZ than to the Par complex in a supernatant depletion assay. Gardner-Altman estimation plot comparing the binding affinity of Cdc42Q61L/Par-6 CRIB-PDZ to the affinity of Cdc42Q61L/Par complex measured using a supernatant depletion assay. Each replicate (filled circles) along with the mean and standard deviation (gap and bars next to circles) are plotted on the left and the mean difference is plotted on the right as a bootstrap sampling distribution (shaded region) with a 95% confidence interval (black error bar). Different colored circles for Cdc42Q61L + Par-6 represent two assays using either solid phase Cdc42Q61L + soluble Par-6 or soluble Cdc42Q61L + solid phase Par-6.

REFERENCES CITED

- Aceto, D., Beers, M., Kemphues, K.J., 2006. Interaction of PAR-6 with CDC-42 is required for maintenance but not establishment of PAR asymmetry in *C. elegans*. *Dev. Biol.* 299, 386–397.
- Atwood, S.X., Chabu, C., Penkert, R.R., Doe, C.Q., Prehoda, K.E., 2007. Cdc42 acts downstream of Bazooka to regulate neuroblast polarity through Par-6 aPKC. *J. Cell Sci.* 120,
- Atwood, S.X., Prehoda, K.E., 2009. aPKC Phosphorylates Miranda to Polarize Fate Determinants during Neuroblast Asymmetric Cell Division. *Curr. Biol.* 19, 723–729.
- Bailey, M.J., Prehoda, K.E., 2015. Establishment of Par-Polarized Cortical Domains via Phosphoregulated Membrane Motifs. *Dev. Cell* 35, 199–210.
- Beers, M., 2006. Depletion of the co-chaperone CDC-37 reveals two modes of PAR-6 cortical association in *C. elegans* embryos. *Development* 133, 3745–3754.
- Buckley, C.E., St Johnston, D., 2022. Apical–basal polarity and the control of epithelial form and function. *Nat. Rev. Mol. Cell Biol.*
- Campanale, J.P., Sun, T.Y., Montell, D.J., 2017. Development and dynamics of cell polarity at a glance. *J. Cell Sci.* 130, 1201–1207.
- Chang, Y., Dickinson, D.J., 2022. A particle size threshold governs diffusion and segregation of PAR-3 during cell polarization. *Cell Rep.* 39, 110652.
- Chia, W., Somers, W.G., Wang, H., 2008. *Drosophila* neuroblast asymmetric divisions: cell cycle regulators, asymmetric protein localization, and tumorigenesis. *J. Cell Biol.* 180, 267–272.
- Dickinson, D.J., Schwager, F., Pintard, L., Gotta, M., Goldstein, B., 2017. A Single-Cell Biochemistry Approach Reveals PAR Complex Dynamics during Cell Polarization. *Dev. Cell* 42, 416-434.e11.
- Dong, W., Lu, J., Zhang, X., Wu, Y., Lettieri, K., Hammond, G.R., Hong, Y., 2020. A polybasic domain in aPKC mediates Par6-dependent control of membrane targeting and kinase activity. *J. Cell Biol.* 219, e201903031.
- Drummond, M.L., Prehoda, K.E., 2016. Molecular Control of Atypical Protein Kinase C: Tipping the Balance between Self-Renewal and Differentiation. *J. Mol. Biol.* 428, 1455–1464.
- Garg, R., Benedetti, L.G., Abera, M.B., Wang, H., Abba, M., Kazanietz, M.G., 2014. Protein kinase C and cancer: what we know and what we do not. *Oncogene* 33, 5225–5237.

- Garrard, S.M., Capaldo, C.T., Gao, L., Rosen, M.K., Macara, I.G., Tomchick, D.R., 2003. Structure of Cdc42 in a complex with the GTPase-binding domain of the cell polarity protein, Par6. *EMBO J.* 22, 1125–1133.
- Goldstein, B., Macara, I.G., 2007. The PAR Proteins: Fundamental Players in Animal Cell Polarization. *Dev. Cell* 13, 609–622.
- Gotta, M., Abraham, M.C., Ahringer, J., 2001. CDC-42 controls early cell polarity and spindle orientation in *C. elegans*. *Curr. Biol.* 11, 482–488.
- Graybill, C., Wee, B., Atwood, S.X., Prehoda, K.E., 2012. Partitioning-defective Protein 6 (Par-6) Activates Atypical Protein Kinase C (aPKC) by Pseudosubstrate Displacement. *J. Biol. Chem.* 287, 21003–21011.
- Hirano, Y., Yoshinaga, S., Takeya, R., Suzuki, N.N., Horiuchi, M., Kohjima, M., Sumimoto, H., Inagaki, F., 2005. Structure of a Cell Polarity Regulator, a Complex between Atypical PKC and Par6 PB1 Domains. *J. Biol. Chem.* 280, 9653–9661.
- Ho, J., Tumkaya, T., Aryal, S., Choi, H., Claridge-Chang, A., 2019. Moving beyond P values: data analysis with estimation graphics. *Nat. Methods* 16, 565–566.
- Holly, R.W., Jones, K., Prehoda, K.E., 2020. A Conserved PDZ-Binding Motif in aPKC Interacts with Par-3 and Mediates Cortical Polarity. *Curr. Biol.* 30, 893–898.e5.
- Holly, R.W., Prehoda, K.E., 2019. Phosphorylation of Par-3 by Atypical Protein Kinase C and Competition between Its Substrates. *Dev. Cell* 49, 678–679.
- Hong, Y., 2018. aPKC: the Kinase that Phosphorylates Cell Polarity. *F1000Research* 7, 903.
- House, C., Kemp, B.E., 1987. Protein Kinase C Contains a Pseudosubstrate Prototope in Its Regulatory Domain. *Science* 238, 1726–1728.
- Hung, T.-J., Kemphues, K.K., 1999. Molecular cloning and characterization of PAR-6. *Development* 126, 127–135.
- Hutterer, A., Betschinger, J., Petronczki, M., Knoblich, J.A., 2004. Sequential Roles of Cdc42, Par-6, aPKC, and Lgl in the Establishment of Epithelial Polarity during *Drosophila* Embryogenesis. *Dev. Cell* 6, 845–854.
- Izumi, Y., Hirose, T., Tamai, Y., Hirai, S., Nagashima, Y., Fujimoto, T., Tabuse, Y., Kemphues, K.J., Ohno, S., 1998. An Atypical PKC Directly Associates and Colocalizes at the Epithelial Tight Junction with ASIP, a Mammalian Homologue of *Caenorhabditis elegans* Polarity Protein PAR-3. *J. Cell Biol.* 143, 95–106.
- Joberty, G., Petersen, C., Gao, L., Macara, I.G., 2000. The cell-polarity protein Par6 links Par3 and atypical protein kinase C to Cdc42. *Nat. Cell Biol.* 2, 531–539.

- Jones, K.A., Drummond, M.L., Penkert, R.R., Prehoda, K.E., 2023. Cooperative regulation of C1-domain membrane recruitment polarizes atypical protein kinase C. *J. Cell Biol.* 222, e202112143.
- Lang, C.F., Munro, E., 2017. The PAR proteins: from molecular circuits to dynamic self-stabilizing cell polarity. *Development* 144, 3405–3416.
- Leroux, A.E., Biondi, R.M., 2020. Renaissance of Allosteric to Disrupt Protein Kinase Interactions. *Trends Biochem. Sci.* 45, 27–41.
- Li, B., Kim, H., Beers, M., Kemphues, K., 2010. Different domains of *C. elegans* PAR-3 are required at different times in development. *Dev. Biol.* 344, 745–757.
- Li, J., Kim, H., Aceto, D.G., Hung, J., Aono, S., Kemphues, K.J., 2010. Binding to PKC-3, but not to PAR-3 or to a conventional PDZ domain ligand, is required for PAR-6 function in *C. elegans*. *Dev. Biol.* 340, 88–98.
- Lin, D., Edwards, A.S., Fawcett, J.P., Mbamalu, G., Scott, J.D., Pawson, T., 2000. A mammalian PAR-3–PAR-6 complex implicated in Cdc42/Rac1 and aPKC signalling and cell polarity. *Nat. Cell Biol.* 2, 540–547.
- Lipp, P., Reither, G., 2011. Protein Kinase C: The “Masters” of Calcium and Lipid. *Cold Spring Harb. Perspect. Biol.* 3, a004556–a004556.
- Lopez-Garcia, L.A., Schulze, J.O., Fröhner, W., Zhang, H., Süß, E., Weber, N., Navratil, J., Amon, S., Hindie, V., Zeuzem, S., Jørgensen, T.J.D., Alzari, P.M., Neimanis, S., Engel, M., Biondi, R.M., 2011. Allosteric Regulation of Protein Kinase PKC ζ by the N-Terminal C1 Domain and Small Compounds to the PIF-Pocket. *Chem. Biol.* 18, 1463–1473.
- Loyer, N., Januschke, J., 2020. Where does asymmetry come from? Illustrating principles of polarity and asymmetry establishment in *Drosophila* neuroblasts. *Curr. Opin. Cell Biol.* 62, 70–77.
- Martin, E., Girardello, R., Dittmar, G., Ludwig, A., 2021. New insights into the organization and regulation of the apical polarity network in mammalian epithelial cells. *FEBS J.* 288, 7073–7095.
- Mazel, T., 2017. Crosstalk of cell polarity signaling pathways. *Protoplasma* 254, 1241–1258.
- Morais-de-Sá, E., Mirouse, V., St Johnston, D., 2010. aPKC phosphorylation of Bazooka defines the apical/lateral border in *Drosophila* epithelial cells. *Cell* 141, 509–523.
- Munro, E., Nance, J., Priess, J.R., 2004. Cortical Flows Powered by Asymmetrical Contraction Transport PAR Proteins to Establish and Maintain Anterior-Posterior Polarity in the Early *C. elegans* Embryo. *Dev. Cell* 7, 413–424.

- Nelson, W.J., 2003. Adaptation of core mechanisms to generate cell polarity. *Nature* 422, 766–774.
- Newton, A.C., 2018. Protein kinase C: perfectly balanced. *Crit. Rev. Biochem. Mol. Biol.* 53, 208–230.
- Noda, Y., Kohjima, M., Izaki, T., Ota, K., Yoshinaga, S., Inagaki, F., Ito, T., Sumimoto, H., 2003. Molecular Recognition in Dimerization between PB1 Domains. *J. Biol. Chem.* 278, 43516–43524.
- Noda, Y., Takeya, R., Ohno, S., Naito, S., Ito, T., Sumimoto, H., 2001. Human homologues of the *Caenorhabditis elegans* cell polarity protein PAR6 as an adaptor that links the small GTPases Rac and Cdc42 to atypical protein kinase C: Human PAR6s link Rac and Cdc42 to aPKC. *Genes Cells* 6, 107–119.
- Nunes de Almeida, F., Walther, R.F., Pressé, M.T., Vlassaks, E., Pichaud, F., 2019. Cdc42 defines apical identity and regulates epithelial morphogenesis by promoting apical recruitment of Par6-aPKC and Crumbs. *Development* 146, dev175497.
- Oon, C.H., Prehoda, K.E., 2021. Phases of cortical actomyosin dynamics coupled to the neuroblast polarity cycle. *eLife* 10, e66574.
- Oon, C.H., Prehoda, K.E., 2019. Asymmetric recruitment and actin-dependent cortical flows drive the neuroblast polarity cycle. *eLife* 8, e45815.
- Penkert, R.R., DiVittorio, H.M., Prehoda, K.E., 2004. Internal recognition through PDZ domain plasticity in the Par-6–Pals1 complex. *Nat. Struct. Mol. Biol.* 11, 1122–1127.
- Penkert, R.R., Vargas, E., Prehoda, K.E., 2022. Energetic determinants of animal cell polarity regulator Par-3 interaction with the Par complex. *J. Biol. Chem.* 298, 102223.
- Peterson, F.C., Penkert, R.R., Volkman, B.F., Prehoda, K.E., 2004. Cdc42 Regulates the Par-6 PDZ Domain through an Allosteric CRIB-PDZ Transition. *Mol. Cell* 13, 665–676.
- Pollard, T.D., 2010. A Guide to Simple and Informative Binding Assays. *Mol. Biol. Cell* 21, 4061–4067.
- Prehoda, K.E., 2009. Polarization of *Drosophila* Neuroblasts During Asymmetric Division. *Cold Spring Harb. Perspect. Biol.* 1, a001388–a001388.
- Qiu, R.-G., Abo, A., Martin, G.S., 2000. A human homolog of the *C. elegans* polarity determinant Par-6 links Rac and Cdc42 to PKC ζ signaling and cell transformation. *Curr. Biol.* 10, 697–707.
- Reményi, A., Good, M.C., Lim, W.A., 2006. Docking interactions in protein kinase and phosphatase networks. *Curr. Opin. Struct. Biol.* 16, 676–685.

- Renschler, F.A., Bruekner, S.R., Salomon, P.L., Mukherjee, A., Kullmann, L., Schütz-Stoffregen, M.C., Henzler, C., Pawson, T., Krahn, M.P., Wiesner, S., 2018. Structural basis for the interaction between the cell polarity proteins Par3 and Par6. *Sci. Signal.* 11, eaam9899.
- Riga, A., Castiglioni, V.G., Boxem, M., 2020. New insights into apical-basal polarization in epithelia. *Curr. Opin. Cell Biol.* 62, 1–8.
- Rodriguez, J., Peglion, F., Martin, J., Hubatsch, L., Reich, J., Hirani, N., Gubieda, A.G., Roffey, J., Fernandes, A.R., St Johnston, D., Ahringer, J., Goehring, N.W., 2017. aPKC Cycles between Functionally Distinct PAR Protein Assemblies to Drive Cell Polarity. *Dev. Cell* 42, 400–415.e9.
- Rosse, C., Linch, M., Kermorgant, S., Cameron, A.J.M., Boeckeler, K., Parker, P.J., 2010. PKC and the control of localized signal dynamics. *Nat. Rev. Mol. Cell Biol.* 11, 103–112.
- Sommese, R.F., Ritt, M., Swanson, C.J., Sivaramakrishnan, S., 2017. The Role of Regulatory Domains in Maintaining Autoinhibition in the Multidomain Kinase PKC α . *J. Biol. Chem.* 292, 2873–2880.
- Soriano, E.V., Ivanova, M.E., Fletcher, G., Riou, P., Knowles, P.P., Barnouin, K., Purkiss, A., Kostecky, B., Saiu, P., Linch, M., Elbediwy, A., Kjær, S., O'Reilly, N., Snijders, A.P., Parker, P.J., Thompson, B.J., McDonald, N.Q., 2016. aPKC Inhibition by Par3 CR3 Flanking Regions Controls Substrate Access and Underpins Apical-Junctional Polarization. *Dev. Cell* 38, 384–398.
- Sulston, J.E., Schierenberg, E., White, J.G., Thomson, J.N., 1983. The embryonic cell lineage of the nematode *Caenorhabditis elegans*. *Dev. Biol.* 100, 64–119.
- Sunchu, B., Cabernard, C., 2020. Principles and mechanisms of asymmetric cell division. *Development* 147, dev167650.
- Suzuki, A., Yamanaka, T., Hirose, T., Manabe, N., Mizuno, K., Shimizu, M., Akimoto, K., Izumi, Y., Ohnishi, T., Ohno, S., 2001. Atypical Protein Kinase C Is Involved in the Evolutionarily Conserved Par Protein Complex and Plays a Critical Role in Establishing Epithelia-Specific Junctional Structures. *J. Cell Biol.* 152, 1183–1196.
- Thompson, B.J., 2021. Par-3 family proteins in cell polarity & adhesion. *FEBS J.* febs.15754.
- Walther, R.F., Pichaud, F., 2010. Crumbs/DaPKC-Dependent Apical Exclusion of Bazooka Promotes Photoreceptor Polarity Remodeling. *Curr. Biol.* 20, 1065–1074.
- Wang, S.-C., Low, T.Y.F., Nishimura, Y., Gole, L., Yu, W., Motegi, F., 2017. Cortical forces and CDC-42 control clustering of PAR proteins for *Caenorhabditis elegans* embryonic polarization. *Nat. Cell Biol.* 19, 988–995.

- Watts, J.L., Etemad-Moghadam, B., Guo, S., Boyd, L., Draper, B.W., Mello, C.C., Priess, J.R., Kempfues, K.J., 1996. *par-6*, a gene involved in the establishment of asymmetry in early *C. elegans* embryos, mediates the asymmetric localization of PAR-3. *Development* 122, 3133–3140.
- Whitney, D.S., Peterson, F.C., Kittell, A.W., Egner, J.M., Prehoda, K.E., Volkman, B.F., 2016. Binding of Crumbs to the Par-6 CRIB-PDZ Module Is Regulated by Cdc42. *Biochemistry* 55, 1455–1461.
- Whitney, D.S., Peterson, F.C., Volkman, B.F., 2011. A Conformational Switch in the CRIB-PDZ Module of Par-6. *Structure* 19, 1711–1722.
- Wieschaus, E., Nusslein-Volhard, C., Jurgens, G., 1984. Mutations affecting the pattern of the larval cuticle in *Drosophila melanogaster*: III. Zygotic loci on the X-chromosome and fourth chromosome. *Wilhelm Roux Arch. Dev. Biol.* 193, 296–307.
- Wirtz-Peitz, F., Nishimura, T., Knoblich, J.A., 2008. Linking Cell Cycle to Asymmetric Division: Aurora-A Phosphorylates the Par Complex to Regulate Numb Localization. *Cell* 135, 161–173.
- Wodarz, A., Ramrath, A., Grimm, A., Knust, E., 2000. *Drosophila* Atypical Protein Kinase C Associates with Bazooka and Controls Polarity of Epithelia and Neuroblasts. *J. Cell Biol.* 150, 1361–1374.
- Wu, X., Cai, Q., Feng, Z., Zhang, M., 2020. Liquid-Liquid Phase Separation in Neuronal Development and Synaptic Signaling. *Dev. Cell* 55, 18–29.
- Yamanaka, T., Horikoshi, Y., Suzuki, A., Sugiyama, Y., Kitamura, K., Maniwa, R., Nagai, Y., Yamashita, A., Hirose, T., Ishikawa, H., Ohno, S., 2001. PAR-6 regulates aPKC activity in a novel way and mediates cell-cell contact-induced formation of the epithelial junctional complex: PAR-6 regulates aPKC in cell polarization. *Genes Cells* 6, 721–731.
- Zhou, Y., Johnson, J.L., Cerione, R.A., Erickson, J.W., 2013. Prenylation and Membrane Localization of Cdc42 Are Essential for Activation by DOCK7. *Biochemistry* 52, 4354–4363.